

**MODELING AND ANALYSIS OF CHILLED WATER SYSTEMS**

A Thesis

Presented to

The Academic Faculty

by

Shawn Eric Klawunder

In Partial Fulfillment

of the Requirements for the Degree

Master of Science in Mechanical Engineering

GEORGIA INSTITUTE OF TECHNOLOGY

APRIL 2000

**DISTRIBUTION STATEMENT A**

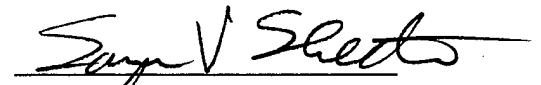
Approved for Public Release  
Distribution Unlimited

DTIC QUALITY INSPECTED 2

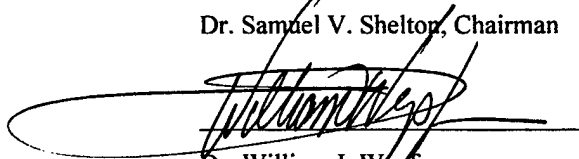
20000417 038

**MODELING AND ANALYSIS OF CHILLED WATER SYSTEMS**

Approved:



Dr. Samuel V. Shelton, Chairman



Dr. William J. Wepper



Dr. Sheldon M. Jeter

Date Approved \_\_\_\_\_

## **ACKNOWLEDGEMENT**

I wish to thank Dr. Sam Shelton for his constant advice and support over the past two years. This study has been an invaluable learning experience that would not have been possible without his counsel. I would also like to thank my wife and children for their support and patience during the course of this study. Finally, a great thanks goes to God for giving me the opportunity and determination to complete this work.

## TABLE OF CONTENTS

TABLE OF CONTENTS .....	1
LIST OF TABLES .....	3
LIST OF FIGURES .....	5
INTRODUCTION .....	13
Background .....	13
1. System Descriptions .....	13
2. Low chiller $\Delta T$ issues .....	17
Objective .....	19
MODELING .....	23
Air Handler .....	24
1. Model .....	24
2. Air Handler Performance Characteristics .....	38
Chiller .....	42
1. Manufacturer's data .....	42
2. Compressor Model .....	43
3. Evaporator Heat Exchanger Model .....	48
4. Condenser Heat Exchanger Model .....	54
5. Chiller Comparison .....	57
6. Performance Characteristics .....	61
Pump Model .....	64
1. Constant Speed Pumping .....	64
2. Variable Speed Pumping .....	66
Cooling Tower Model .....	72
1. Cooling Tower NTU Calculation .....	75
2. Cooling Tower Fan Model .....	76
Piping Model .....	78
OPERATIONAL STRATEGIES .....	80
Chilled Water Reset .....	80
Tower minimum set point .....	84
Free Cooling .....	85
Multiple Chiller Scheduling .....	86
Chilled Water Set Point Reduction .....	89
DESIGN OPTIONS .....	91
Increasing Air Handler Capacity .....	91
Check Valve .....	91
Single Loop, Variable Flow Rate .....	92
LOAD PROFILES AND WEATHER DATA .....	94
Atlanta .....	96
Phoenix .....	97
Chicago .....	98

Air Conditioning & Refrigeration Institute.....	99
<b>PERFORMANCE STUDIES .....</b>	<b>100</b>
Annual efficiency .....	101
1. Base Case.....	101
2. Constant Speed Pumping Design.....	105
3. Other Load Profiles.....	105
4. Effects of Air Handler Degradation.....	107
5. Increased Air Handler Capacity.....	108
6. Low Efficiency Chiller Analysis .....	109
7. Multiple Chiller Plant Analysis .....	110
Over-design Load Operation .....	111
1. Base Case.....	111
2. Reducing Chilled Water Set Point.....	117
3. Effects of Air Handler Degradation on System Capacity .....	119
4. Increasing Air Handler Capacity .....	120
<b>CONCLUSIONS .....</b>	<b>122</b>
Part Load efficiency.....	122
Greater Capacity .....	122
Adapts to Load Problems.....	123
Minimum Evaporator Water Flow Rate .....	123
Control Strategy.....	123
Summary.....	124
<b>RECOMMENDATIONS.....</b>	<b>125</b>
Appendix A .....	126
Single Loop, Base Case Code.....	126
Appendix B.....	139
Primary-Secondary, Base Case Code .....	139
References .....	154

## LIST OF TABLES

Table 1. Base case comparison.....	19
Table 2. Constant speed pumping comparison.....	20
Table 3. Multiple chiller system comparison.....	20
Table 4. Low efficiency chiller comparison.....	21
Table 5. Increased air handler capacity comparison.....	21
Table 6. Fouled air handler comparison.....	22
Table 7. Present Day Chiller Data.....	42
Table 8. Compressor constants.....	47
Table 9. Liu's High Efficiency Chiller (B).....	58
Table 10. Liu's Low Efficiency Chiller (C).....	58
Table 11. Single loop, constant speed, primary pump.....	65
Table 12. Primary-secondary system, constant speed, secondary pump.....	66
Table 13. Single loop, variable speed, primary pump.....	69
Table 14. Primary-secondary system, variable speed, secondary pump.....	69
Table 15. Tower box geometry.....	76
Table 16. Atlanta weather data.....	96
Table 17. Phoenix weather data.....	97
Table 18. Chicago weather data.....	98
Table 19. ARI conditions.....	99
Table 20. Base case IER analysis.....	104
Table 21. Constant speed pumping IER analysis.....	105
Table 22. Phoenix IER analysis.....	106
Table 23. Chicago IER analysis.....	106
Table 24. ARI Load analysis.....	107

Table 25. Fouled system IER analysis.....	108
Table 26. Increased air handler capacity IER analysis .....	108
Table 27. Low efficiency chiller analysis.....	109
Table 28. Multiple chiller plant IER analysis .....	110

## LIST OF FIGURES

Figure 1. Constant-volume primary system.....	14
Figure 2. Primary-secondary system .....	15
Figure 3. Single loop system .....	16
Figure 4. Simplified variable volume air handler .....	24
Figure 5. Air Handler Load Profile.....	25
Figure 6. Chilled Water Coil .....	31
Figure 7. Accuracy of UA calculation.....	32
Figure 8. Friction Factor for Arrays of Staggered Tubes.....	34
Figure 9. Accuracy of Calculated Water-side Head .....	36
Figure 10. Accuracy of Calculated Air-side Pressure Drop.....	37
Figure 11. Chilled Water $\Delta T$ versus Load .....	38
Figure 12. System flow rate versus load.....	39
Figure 13. Fouled air handler water-side T versus load.....	40
Figure 14. Fouled air handler flow rate versus load .....	41
Figure 15. Weber's compressor model accuracy.....	44
Figure 16. Liu's Compressor Model Accuracy .....	45
Figure 17. Compressor Power Actual versus Carnot.....	46
Figure 18. Revised Compressor Model Accuracy .....	47
Figure 19. Evaporator UA versus Flow Rate.....	48
Figure 20. Cross-section of a Single Tube in the Evaporator Tube Bundle.....	49
Figure 21. Evaporator UA versus Reynolds Number .....	50
Figure 22. Accuracy Results for Evaporator UA Calculation.....	52
Figure 23. Accuracy Results for Evaporator Pressure Drop.....	53
Figure 24. Condenser UA versus Load.....	54

Figure 25. Condenser UA versus Condensing Temperature.....	55
Figure 26. Accuracy Results For Condenser UA Calculation .....	56
Figure 27. Accuracy of condenser head model.....	57
Figure 28. Compressor Performance Comparison.....	59
Figure 29. Evaporator Performance Comparison .....	60
Figure 30. Condenser Performance Comparison.....	60
Figure 31. Chiller efficiency versus load.....	61
Figure 32. Effect of variable flow on chiller performance .....	62
Figure 33. Efficiency versus set point .....	63
Figure 34. Centrifugal Pump and System Curves.....	65
Figure 35. Effects of Changing Speed on the Pump Curve .....	67
Figure 36. Design efficiency curve.....	68
Figure 37. Motor and Variable Speed Drive Efficiency versus Pump Speed .....	71
Figure 38. Defining a Linear Saturation Enthalpy.....	74
Figure 39. Chilled water reset.....	81
Figure 40. Flow rate variation with reset.....	82
Figure 41. System $\Delta T$ response to reset.....	82
Figure 42. Energy savings resulting from reset .....	83
Figure 43. ARI efficiency curve .....	87
Figure 44. Chiller efficiency curve with constant condenser inlet temperature.....	88
Figure 45. Chiller scheduling .....	89
Figure 46. Effect of reducing chiller set point .....	90
Figure 47. Primary-secondary system with check valve.....	92
Figure 48. Previous load profile .....	95
Figure 49. Atlanta Load Profile.....	96
Figure 50. Phoenix Load Profile.....	97
Figure 51. Chicago Load Profile .....	98

Figure 52. ARI Load Profile.....	99
Figure 53. Load profile.....	100
Figure 54. Base case designs .....	102
Figure 55. Base case pump power .....	103
Figure 56. Base case compressor power .....	104
Figure 57. Mixing on over-design primary-secondary system .....	112
Figure 58. Over-loaded primary-secondary system.....	113
Figure 59. System capacity versus water flow rate.....	114
Figure 60. System capacity versus air flow rate .....	115
Figure 61. Air handler LMTD .....	116
Figure 62. System capacity.....	117
Figure 63. Adjusting the chiller set point .....	118
Figure 64. Chiller efficiency with reduced set point.....	119
Figure 65. Effect of fouling on system capacity .....	120
Figure 66. Increased design $\Delta T$ system capacity .....	121

## LIST OF SYMBOLS

A	area
$A_v$	surface area of water droplets per volume of tower
C	heat capacity
C	specific heat of incompressible liquid
C <sub>fm</sub>	air flow rate
C <sub>p</sub>	specific heat
C <sub>r</sub>	ratio of heat capacities (minimum to maximum)
D	diameter
f	friction factor
g	gravitational constant
G <sub>c</sub>	mass velocity through the minimum free-flow area
h	heat transfer coefficient
hA	heat conductance
h <sub>a</sub>	enthalpy of air
h <sub>d</sub>	diffusion mass transfer coefficient
h <sub>ref,w</sub>	enthalpy of water above reference state of liquid water
IER	integral efficiency rating
k	thermal conductivity
L	length
LMTD	logarithmic mean temperature difference
$\dot{m}$	mass flow rate
N	speed
n <sub>t</sub>	number of tubes

$P$	pressure
$\dot{Q}$	Heat transfer rate
$R_f$	fouling factor
$T$	Temperature
$UA$	overall heat conductance
$V$	velocity
$V_{max}$	velocity through the minimum free flow area
$V$	volume
$V_t$	total tower volume
$\dot{W}$	power
$Z$	elevation
$\Delta$	change
$\epsilon$	roughness
$\epsilon_a$	heat transfer effectiveness based with respect to the air-side
$\epsilon_{min}$	heat transfer effectiveness based with respect to the side with the smallest heat capacity
$\eta$	efficiency
$\xi$	ratio of inner to outer heat conductance
$\rho$	density
$\sigma$	ratio of minimum free-flow to frontal area
$\omega$	humidity ratio

Additional subscripts:

$A$	air
$ah$	air handler

ave	average
b	tube spacing in the direction of flow
cond	condenser
DPC	design pump curve
Eff	effective
evap	evaporator
f	fin
frict	friction
i	inner
in	inlet state conditions
isent	isentropic
m	mean
motor/vsd	combination of motor and variable speed drive
o	outer
out	outlet state conditions
ref	reference value
rev	reversible process
s	saturated
t	tube
tot	total
w	water

## SUMMARY

The most popular large commercial building chilled water system today is the primary-secondary design. This system separates the generation zone (chiller/evaporator) of a chilled water system from the distribution zone (air handlers). The generation (primary) loop maintains a constant chilled water flow rate. The distribution (secondary) loop varies flow rate in response to cooling load fluctuations. This variable flow rate in the secondary loop permits energy savings over older, constant flow, single loop systems (Rishel, 1996). Recently, new chiller controls have been implemented that allow variable chilled water flow rate in chillers. As a result, a new chilled water system design has become available. This design is a single loop system with a single set of pumps. Like the primary-secondary system the single loop design has two-way valves in air handlers. This variable flow rate, primary system also eliminates the primary-secondary bypass loop. Existing primary-secondary systems can be converted to this design by simply valving off the bypass leg.

The purpose of this study was to compare the performance characteristics of the primary-secondary system with the single loop, variable flow rate design. To accomplish this, individual system components were modeled. These component models were compared with manufacturer's data in order to validate their accuracy. The modeled components include; air handler, chiller, pump and cooling tower. These component models were combined to form primary-secondary and single loop system models.

Comparisons of these two systems were made to determine relative system efficiency and cooling capacity. Different designs and cooling load conditions were applied to the primary-secondary and single loop systems. These situations include:

- 1) Single and multiple chiller systems
- 2) Constant and variable speed pumping schemes
- 3) Various load profiles
- 4) Under and oversized air handlers
- 5) Chilled water coil fouling

Each comparison showed the single loop system to have greater efficiency and cooling capacity than the primary-secondary design.

Different control strategies and designs were employed in an effort to improve primary-secondary system performance. None of these changes allowed the primary-secondary system performance to rise to that of the single loop, variable flow rate design. As a result, this investigation concludes that the variable flow rate, primary (single loop), chilled water design is advantageous compared to the popular primary-secondary system.

# CHAPTER I

## INTRODUCTION

### Background

In the recent past, due to rising energy costs, manufacturers have invested great time and money to increase HVAC component efficiency. However, it is impossible to predict entire system effects by studying only a single component. Certainly, increasing a component's efficiency will affect overall system performance. For example, a chiller's efficiency is increased by adding heat transfer surface area or augmentation to the condenser and evaporator. This raises the chiller efficiency by increasing heat exchanger UA. However, the addition of area or augmentation can increase the heat exchanger pressure drop, and with it the pump power requirement. Without analyzing the entire system, it is impossible to determine the effect that this change has on system performance. This study compares the system performance of two basic chilled water piping schemes in order to determine their individual advantages and disadvantages.

### 1. System Descriptions

In the early 1970's, variable speed pumping was rarely used in HVAC applications. Constant speed pumps were used throughout chilled water loops. This resulted in inefficient part load operation, because the constant speed pumping scheme maintains a large flow rate and pressure drop at all loads. In the late 1970's, the primary-secondary chilled water system was developed to take advantage of variable speed pumping. This system maintains constant flow rate in the primary loop. It has a bypass loop that uncouples the primary loop from the distribution loop. This allows for variable speed in a distribution (secondary) loop. These changes resulted from increased energy costs, making the larger first cost of a more efficient system worth while. Over the past 20 years, numerous problems with the primary-secondary arrangement have been discovered. These problems have prompted the study of different chilled water arrangements. One of the proposed arrangements is a system that varies the water flow rate through

chillers as well as the load. It uses variable speed primary pumps on chillers and two way valves in all air handlers. These three systems are described in greater detail below.

a) Constant-flow rate primary systems

The constant-flow rate primary chilled water system maintains constant flow throughout the entire system. All air handlers have three-way modulating valves that provide constant flow. The temperature difference across the water-side of an air handler changes with load. This design was common when energy was relatively cheap. At that time, variable speed drives were not used in HVAC applications and thus constant flow rate was necessary. Figure 1 shows the layout of the constant-flow rate primary system.

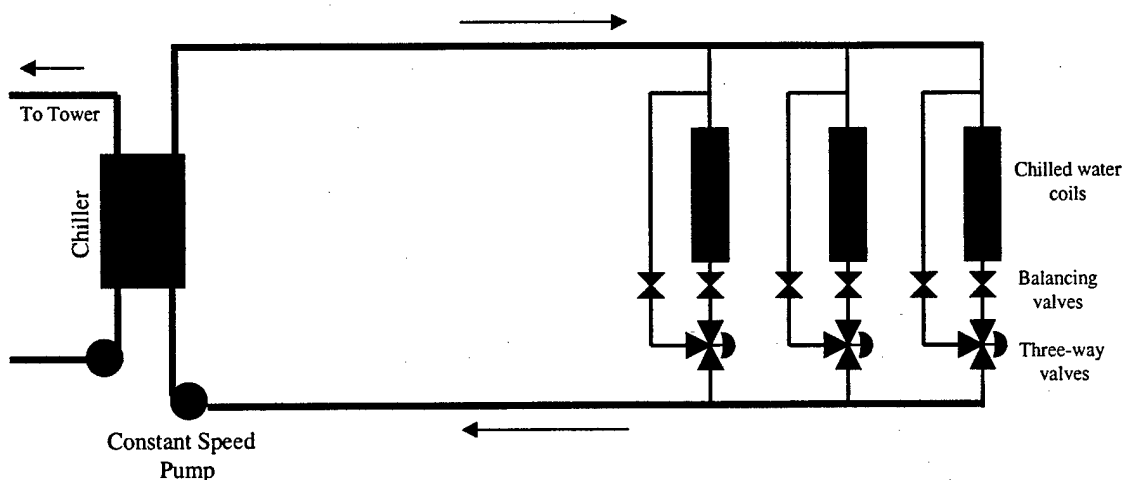


**Figure 1. Constant-volume primary system**

The primary constant-volume system had several wasteful conditions that are no longer acceptable (Rishel 1996). For example,

- 1) Constant flow means the system maintains the same head in all situations. This translates to identical pump power requirements on the hottest and coolest days.
- 2) Balancing valves were used to increase the head in coils near the chiller in order to maintain adequate flow in distant coils.
- 3) As the system load decreases the  $\Delta T$  across each chiller is reduced, but the chillers must remain on-line to maintain system flow.

b) Primary-secondary systems

Currently, the most popular chilled water design is the primary-secondary system. It separates the chiller zone from distribution zone, thus taking advantage of variable speed pumping. It uses two-way valves in the air handlers that modulate secondary loop flow rate with load requirements. A bypass line is included between the chilled water supply and return to permit constant flow through the chillers (Rishel, 1996).

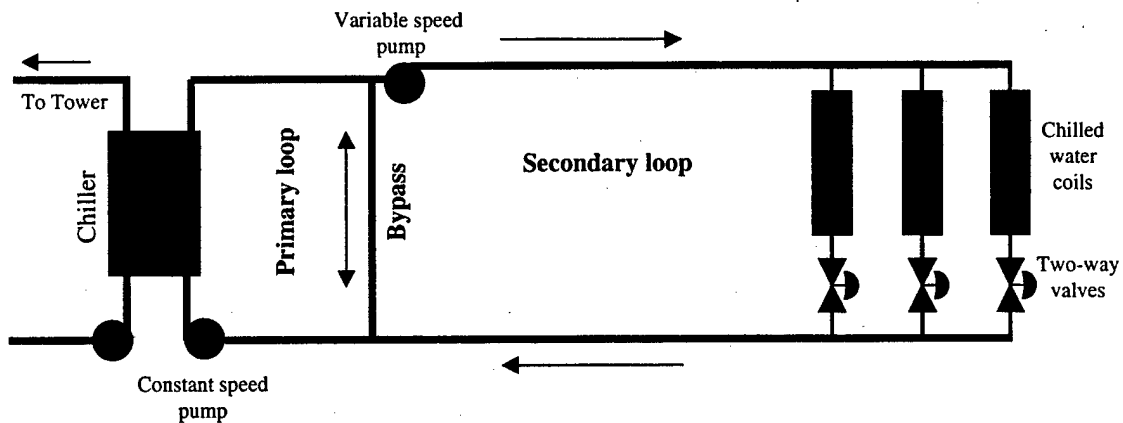


**Figure 2. Primary-secondary system**

While the primary-secondary system takes advantage of the reduced pumping cost offered by variable speed secondary loop pumping, it still has drawbacks.

- 1) The increased first cost of acquiring primary and secondary pumps.
  - 2) Constant evaporator water-side pressure drop.
  - 3) Mixing from supply to return across the bypass in part load situations. This creates a low temperature differential in the primary loop.
  - 4) Mixing from the return to supply while operating above design conditions. This raises the coil's chilled water inlet temperature.
  - 5) Chillers need to stay on-line in order to prevent detrimental mixing when low system  $\Delta T$  problem exists. These problems can be caused by air handler fouling, poorly controlled air handler set points and a variety of other causes.
- c) Variable-flow rate primary (Single loop) systems

Variable-flow rate primary systems take advantage of modern control systems which allow variable chilled water flow through the chiller's evaporator. This is done by removing the bypass and using variable speed drives with primary pumps. Two-way valves modulate the entire system flow. This variable flow allows for reduced pumping power due to a smaller evaporator head at part load. The system also prevents mixing between the chilled water supply and return lines. Despite these advantages this system is not widely accepted primarily because it presents two problems.

- 1) The possibility of laminar water flow in the evaporator at small loads and low flow rates.

This situation is possible in single chiller facilities where one chiller is required to meet all loads. Laminar evaporator flow is far less likely in multiple chiller plants.

- 2) Difficulty starting up lag chillers.

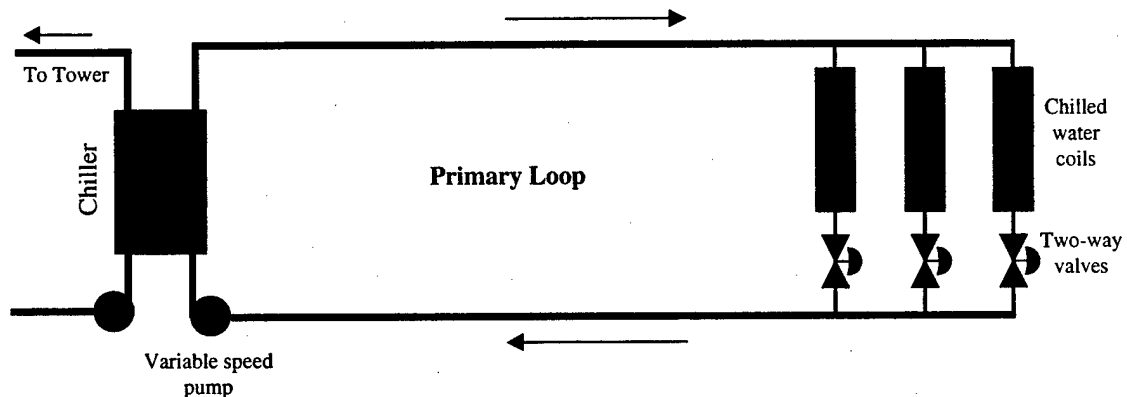


**Figure 3. Single loop system**

Control strategies are available to rectify these problems. Chilled water reset is an option which prevents laminar flow in the evaporator. At low system loads the chiller set point is raised. This change has two results. First, the system flow is increased. Air handlers require more flow to increase the UA, because the logarithmic mean temperature difference (LMTD) between the air and water-sides is smaller. Secondly, the chiller's power requirement is reduced due to a smaller compressor lift. One can see that this technique is a trade-off. Its use increases pumping while reducing chiller power requirements. Under most situations this strategy increases efficiency and as such it is common practice by the HVAC community (Erth, 1987). Therefore, not only does it prevent laminar flow but saves energy as well.

Some facilities require a constant chilled water supply temperatures. In this case chilled water reset is not an option. Although variable flow may be attained by placing a control valve in the bypass line that opens to prevent laminar evaporator flow (Coad, 1998).

Centrifugal chillers are protected from harm by a number of safeties. One such device is an evaporator limit safety that takes a chiller off line if the refrigerant temperature falls below 30°F. This situation often occurs as a result of an abrupt chiller load variation. For example, a multiple-chiller, single loop system may be operating with a single chiller at a relatively large load. The load increases until the lag chiller is brought on line. The lead chiller flow rate and load are rapidly reduced as the lag chiller is energized. The refrigerant temperature in the evaporator falls below 30°F because the compressor hasn't had time to respond to the reduced load. The lead chiller drops off line (Eppelheimer, 1996). In older chillers the evaporator limit safety is a mechanical thermostat that senses the instantaneous refrigerant temperature. Modern low evaporator temperature control uses more sophisticated, solid-state technology. Modern chillers have a microprocessor based control that averages over a 50 second interval. This control allows the refrigerant temperature to momentarily fall below the minimum set point without tripping the chiller off line. The delay gives the compressor time to adjust to abrupt load variations that accompany chiller scheduling (Kirsner, 1996)

## 2. Low chiller $\Delta T$ issues

Kirsner (1996) describes a problem afflicting most primary-secondary chilled water systems in service today. He describes a situation where the chilled water temperature difference between the supply and return habitually runs at half the design value. This creates three problems. First, at a fixed load, the secondary loop requires twice the flow rate. This flow rate requires the use of additional chillers to prevent return to supply mixing. This mixing is a detrimental situation because it increases the air handler water supply temperature, reducing heat transfer. These chillers are then running at or below 50% load. As a result, the system capacity is diminished to half of its designed level. Furthermore, the system is operating inefficiently, chillers are not optimally loaded and increased pump power is required. Kirsner states " To

my knowledge, every chilled water plant serving distributed loads is afflicted with it to some degree.”

Sauer (1989) describes a number of the causes.

Poorly controlled or calibrated air handler controls are often the culprit. Air handler water flow rate is controlled by the cold deck temperature. If this temperature is adjusted too low the system will attempt to meet the set point by increasing water flow. Typically, the valves are forced wide open. The result is a primary-secondary system with constant flow in both loops.

When valves are not properly calibrated, hot and cold water coils may be in use simultaneously. In some air handlers, these coils share the same deck. The reheat here directly increases the cold deck temperature. This again leads to an increased chilled water flow.

Poor chilled water coil selection, also, leads to low temperature differential. Since it is difficult to determine a particular zone's precise cooling requirement the load may be underestimated. The engineer selects a coil that is too small to handle the load. Later, in the air handler performance analysis, it will be shown that an overloaded air handler delivers a reduced temperature differential.

Fouling is another culprit. Over time dirt builds on the air-side of a chilled water coil. This buildup impedes heat transfer through the tube wall. The air handler compensates by increasing the water flow rate attempting to raise the UA. Poor water treatment causes water-side fouling which has a similar effect on air handler performance.

A major design issue with the primary-secondary system, as Kirsner (1996) points out, is that it is “blinded” by low temperature differential. In some primary-secondary systems chillers are scheduled as a function of bypass flow. When secondary flow rate exceeds primary flow rate another chiller is energized. When primary flow rate exceeds secondary flow rate by one chiller's flow rate a chiller is turned off. This strategy assumes system flow rate varies appropriately with the load. When a facility is afflicted with low  $\Delta T$  chillers are required to stay in use to handle the flow rather than the cooling load. At times all chillers may be energized at a 40% to 50% load in order to prevent secondary from exceeding primary flow.

Engineers have developed a number of methods to deal with low chiller  $\Delta T$ . These methods include; over-sizing air handlers, inserting a check valve in the bypass loop and closing the bypass altogether. These design options will be discussed in greater detail in the body of this text.

### **Objective**

The purpose of this study is to investigate bypass loop effects on the total chilled water system performance. This is accomplished by modeling each system component and combining them into comprehensive system models. The components include air handler, chiller, pump and cooling tower models. Combination of these models allows the study of system performance effects due to changing a single component.

Single loop and primary-secondary systems are compared under different situations to determine their individual strengths and weaknesses. Comparisons were made using the following system pairs:

System Design	Single loop	Primary-secondary
Plant type	Single chiller	Single chiller
Primary Pumps	Variable speed	Constant speed
Secondary pumps	N/A	Variable speed
Air handler design capacity	100 tons	100 tons
Air handler quantity	10	10
Air handler status	Unfouled	Unfouled

**Table 1. Base case comparison**

System Design	Single loop	Primary-secondary
Plant type	Single chiller	Single chiller
Primary Pumps	Constant speed	Constant speed
Secondary pumps	N/A	Constant speed
Air handler design capacity	100 tons	100 tons
Air handler quantity	10	10
Air handler status	Unfouled	Unfouled

**Table 2. Constant speed pumping comparison**

System Design	Single loop	Primary-secondary
Plant type	Two chillers	Two chillers
Primary Pumps	Variable speed	Constant speed
Secondary pumps	N/A	Variable speed
Air handler design capacity	100 tons	100 tons
Air handler quantity	10	10
Air handler status	Unfouled	Unfouled

**Table 3. Multiple chiller system comparison**

System Design	Single loop	Primary-secondary
Plant type	Single low efficiency chiller	Single low efficiency chiller
Primary Pumps	Variable speed	Constant speed
Secondary pumps	N/A	Variable speed
Air handler design capacity	100 tons	100 tons
Air handler quantity	10	10
Air handler status	Unfouled	Unfouled

**Table 4. Low efficiency chiller comparison**

System Design	Single loop	Primary-secondary
Plant type	Single chiller	Single chiller
Primary Pumps	Variable speed	Constant speed
Secondary pumps	N/A	Variable speed
Air handler design capacity	145 tons	145 tons
Air handler quantity	10	10
Air handler status	Unfouled	Unfouled

**Table 5. Increased air handler capacity comparison**

System Design	Single loop	Primary-secondary
Plant type	Single chiller	Single chiller
Primary Pumps	Variable speed	Constant speed
Secondary pumps	N/A	Variable speed
Air handler design capacity	100 tons	100 tons
Air handler quantity	10	10
Air handler status	Fouled	Fouled

**Table 6. Fouled air handler comparison**

Additionally, a variety of load profiles were tested on each pair to ensure consistent results. Each system pair's performance is compared by two methods. The first compares the system relative efficiencies when the actual load is smaller than the design value. The second compares the system capacities when the actual load exceeds the design value.

It is assumed that each system is fully instrumented and calibrated. This instrumentation allows the operator precise temperature, pressure and flow rate readings throughout the system. Furthermore, it is assumed that the operator executes the chosen control strategy perfectly. In reality, this detailed instrumentation and precise control is not possible. However, the primary-secondary system is more prone to mismanagement. As stated before the bypass loop blinds the plant to the actual load conditions. As a result optimal chiller scheduling is more difficult. Ideal operation is assumed in this study in order to obtain an objective comparison of system performance.

## CHAPTER II

### MODELING

Component models were developed using fundamental principles and equations found in literature. These equations were compiled using the Engineering Equation Solver software package (EES) (Klein, 1999). Engineering Equation Solver was chosen for this research due to its ability to call a variety of thermodynamic functions. For example, with the enthalpy and pressure of water known, all other thermodynamic quantities are readily available for use. Additionally, psychrometric functions of air-water mixtures are available and used in air handler and cooling tower models. Furthermore, EES is able to iterate large numbers of transcendental equations, an ability essential to the system models.

The outputs from component models have been compared with actual manufacturer's data to verify model accuracy. The system models were manipulated with different conditions and compared to determine trends in system performance.

## Air Handler

### 1. Model

The air handler chosen for this study is a variable air volume system shown in Figure 4 (Lorsch 1993). This air handler has only a cold deck. The bypass and hot deck were not considered for simplicity, as they would have no effect on the chilled water system. The air handler operates by modulating both air and water flow in response to temperature change.

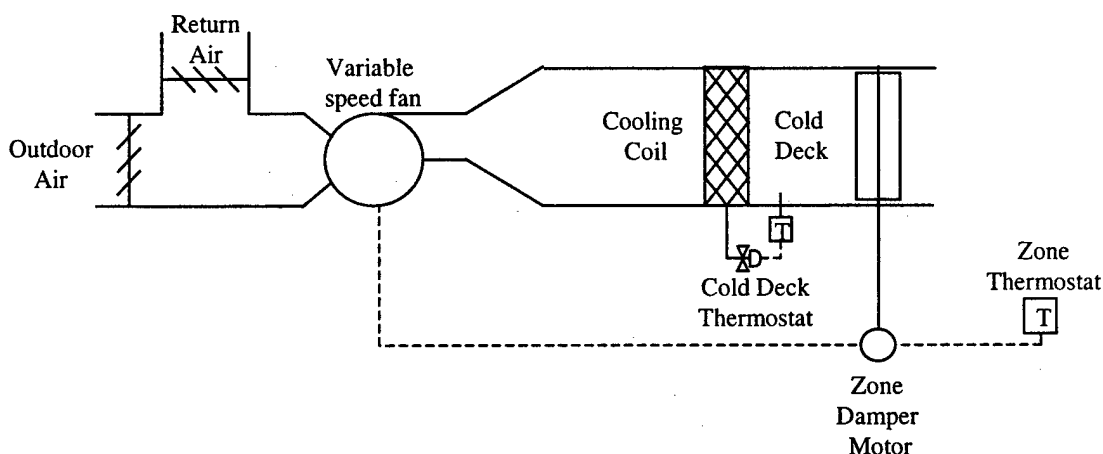


**Figure 4. Simplified variable volume air handler**

The inlet water temperature is essentially set by the chiller evaporator exit temperature. The pipe flow from the chiller to the air handler is assumed to be a constant enthalpy process. Since the air handler water inlet pressure is smaller than the evaporator exit pressure, the air handler inlet temperature is elevated by a fraction of a degree. A mixture of 15% outdoor to 85% return air is maintained. Therefore, the inlet air temperature is fixed by the room and ambient temperature. A constant 75°F room temperature and 55% maximum relative humidity are used to ensure thermal comfort (Lorsch 1993). In order to maintain this condition the cold deck is set to a constant 58°F. The air handler varies air flow by changing fan speed and altering damper positions to different zones in order to maintain a constant room temperature. If a room starts to overheat, more cold air is directed into that area. The chilled water flow rate adjusts to ensure the

cold deck remains 58°F. If the cold deck temperature increases, the air handler's two-way valve compensates by opening to allow more chilled water into the coil. The two-way valves, controlled by cold deck temperatures, dictate the entire system's chilled water flow rate.

The air handler is modeled using NTU-effectiveness relations. Air handler load is assumed to be a function of outdoor dry bulb temperature. This assumption results from Shabo (1992), where a similar load profile was developed using data from a commercial building in Atlanta. The assumed load function for an Atlanta office building is shown below. Notice that at 95°F the system is at 100% load. This corresponds to the design conditions for Atlanta, 95°F dry bulb and 78°F wet bulb. The load decreases linearly until it reaches 20% at 60°F. The load then stays constant until the ambient temperature reaches 45°F when the facility is assumed to switch to a water-side economizer.

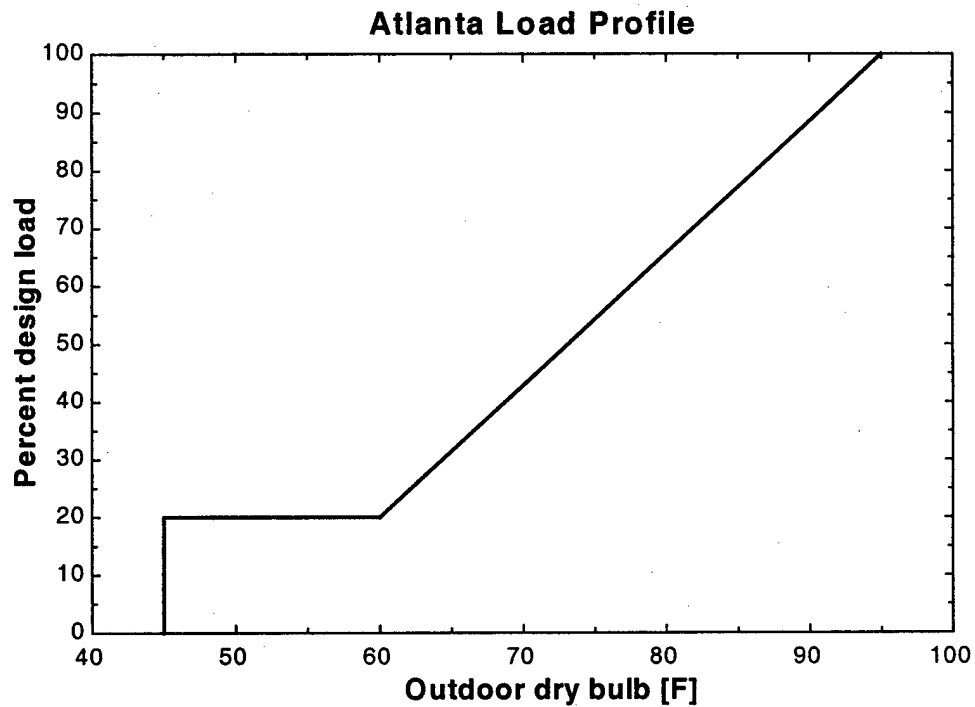


**Figure 5. Air Handler Load Profile**

The air handler is modeled using three heat transfer equations (Incropera and Dewitt 1985).

$$\dot{Q}_{ah} = \dot{m}_w C_w (T_{w,out} - T_{w,in}) \quad \text{Equation 1}$$

$$\dot{Q}_{ah} = \dot{m}_w C_{p,eff} (T_{a,in} - T_{a,out}) \quad \text{Equation 2}$$

$$\dot{Q}_{ah} = \epsilon_{min} C_{min} (T_{a,in} - T_{w,in}) \quad \text{Equation 3}$$

Here  $C_{p,eff}$  is the effective specific heat of the air-water vapor in the coil. This specific heat accounts for the latent as well as sensible heat. Its value is given by:

$$C_{p,eff} = \frac{h_{a,in} - h_{a,out}}{T_{a,in} - T_{a,out}} \quad \text{Equation 4}$$

The enthalpies are evaluated by use of the psychrometric charts in EES. The value  $C_{min}$  is determined by comparing the relative heat capacities of the air-side and water-side. The heat exchanger effectiveness is determined using two NTU relations for cross-flow heat exchangers (Incropera and Dewitt, 1985). Here it is assumed that the water is mixed and the air is unmixed. Equation 5 is used when the water heat capacity exceeds that of the air. Equation 6 is used when the heat capacity of air is largest.

$$\varepsilon = \left( \frac{1}{C_r} \right) \left\{ 1 - \exp \left[ -C_r (1 - \exp(-NTU)) \right] \right\} \quad \text{Equation 5}$$

$$\varepsilon = 1 - \exp \left\{ \left( -\frac{1}{C_r} \right) \left[ 1 - \exp(-C_r \cdot NTU) \right] \right\} \quad \text{Equation 6}$$

where:

$$C_r = \frac{C_{\min}}{C_{\max}} \quad \text{Equation 7}$$

The number of heat transfer units is given by:

$$NTU = \frac{UA}{C_{\min}} \quad \text{Equation 8}$$

Therefore, the remaining unknowns in the initial three heat transfer equations are water exit temperature, water and air mass flow rates and the overall heat transfer conductance (UA). In order to solve this set of equations, the overall heat transfer conductance is needed. The development is described below.

a) Heat Transfer Calculations

1) Overall Heat Transfer Conductance

The chilled water coil UA is a function of the tube material, geometry and the individual heat transfer coefficients. It is given by (Oskarsson, 1990):

$$UA = \frac{1}{\left[ \left( \frac{1}{h_i A_i} \right) + \left( \frac{\ln \left( \frac{D_o}{D_i} \right)}{2\pi \cdot k_t \cdot L \cdot n_t} \right) + \left( \frac{1}{h_o A_o \eta_o} \right) \right]} \quad \text{Equation 9}$$

In this equation  $h_i$  and  $h_o$ , represent the inner and outer heat transfer coefficients respectively.  $A_o$  and  $A_i$  are the total inner and outer surface area.  $D_o$  and  $D_i$  are the tube inner and outer diameters,  $k_t$  is the thermal conductivity of the tube,  $L$  is the length of one pass, and  $\eta_o$  is the overall outside air handler effectiveness. This outer effectiveness is related to the fin efficiency and the air handler geometry using the expression.

$$\eta_o = \frac{A_e}{A_o} \quad \text{Equation 10}$$

where:

$$A_e = A_t + \eta_f \cdot A_f \quad \text{Equation 11}$$

$$A_o = A_t + A_f \quad \text{Equation 12}$$

where,  $A_t$  and  $A_f$  are the tube and fin surface areas and  $\eta_f$  is the fin efficiency.

## 2) Air-side Heat transfer coefficient

Two methods were used to model the air-side heat transfer coefficient. These developments result from the work of McQuiston (1981) and Rich (1973). Each formulation is described below as well as comparisons with manufacturer's data.

### 3) McQuiston's Method

McQuiston finds the airside heat transfer coefficient by determining a factor,  $JP$ , which is a function of the air handler geometry as well as flow characteristics (McQuiston 1981).

$$JP = \text{Re}_{D_o}^{-0.4} \left[ \frac{A_o}{A_t} \right]^{-0.15} \quad \text{Equation 13}$$

In this equation  $\text{Re}_{D_o}$  is the Reynolds number based on the tube outer diameter,  $A_o$  is the outer surface area (fins and tubes), and  $A_t$  is the outer surface area of tubes alone.

The factor  $JP$  is related to a  $j_4$  factor which determines a four-row coil's heat transfer performance.

$$j_4 = 0.0014 + 0.2618(JP) \quad \text{Equation 14}$$

The variable,  $j_n$  for a coil with other than four rows is found by,

$$\frac{j_n}{j_4} = \frac{1 - 1280 \cdot n \cdot \text{Re}_b^{-1.2}}{1 - 1280 \cdot 4 \cdot \text{Re}_b^{-1.2}} \quad \text{Equation 15}$$

where  $n$  is the number of tube rows and  $\text{Re}_b$  is the Reynolds number based on the tube spacing in the flow direction. The  $j_n$  factor is then related to the heat transfer coefficient by,

$$h = \frac{j_n \cdot G_c \cdot Cp}{\text{Pr}^{2/3}} \quad \text{Equation 16}$$

where  $G_c$  is the mass velocity through the minimum flow area,  $Cp$  is the specific heat of the air and  $\text{Pr}$  is the Prantl number of the air.

### 4) Rich's Method

Rich's method differs in that it assumes the coil's heat transfer coefficient is relatively uniform from the first to the last row. Rich used a four row coil to obtain experimental data. One then expects

fairly consistent results when modeling a four row coil. Rich uses a j factor that is a function of the Reynolds number based on the longitudinal tube spacing. This j factor is given by (Rich 1973):

$$j = 0.195 \cdot Re_b^{-0.35} \quad \text{Equation 17}$$

Here the j factor is related to the outer heat transfer coefficient in the same manner as McQuiston gives.

#### 5) Water-side Heat transfer coefficient

The water-side heat transfer coefficient is a function of fluid and flow properties. If the flow in the tubes is laminar then the heat transfer coefficient is given by (Bejan, 1995):

$$Nu = 4.36 \quad \text{Equation 18}$$

Here, Nu is the Nusselt number and is related to the inner heat transfer coefficient by:

$$Nu = \frac{h_i \cdot D_i}{k_w} \quad \text{Equation 19}$$

where,  $h_i$  is the inner heat transfer coefficient,  $D_i$  is the tube inner diameter, and  $k_w$  is the water's thermal conductivity. When flow is turbulent, the heat transfer coefficient is determined by the relation (Bejan 1997):

$$Nu = 0.023 \cdot Re_{D_i}^{0.8} Pr^{0.4} \quad \text{Equation 20}$$

where the Reynolds number here is based on tube inner diameter.

#### 6) Manufacturer's data

The two methods presented above have been compared with manufacturer's data to evaluate their merit. The selected chilled water coil is shown in Figure 6 (Colmac Coil Inc., 1993).

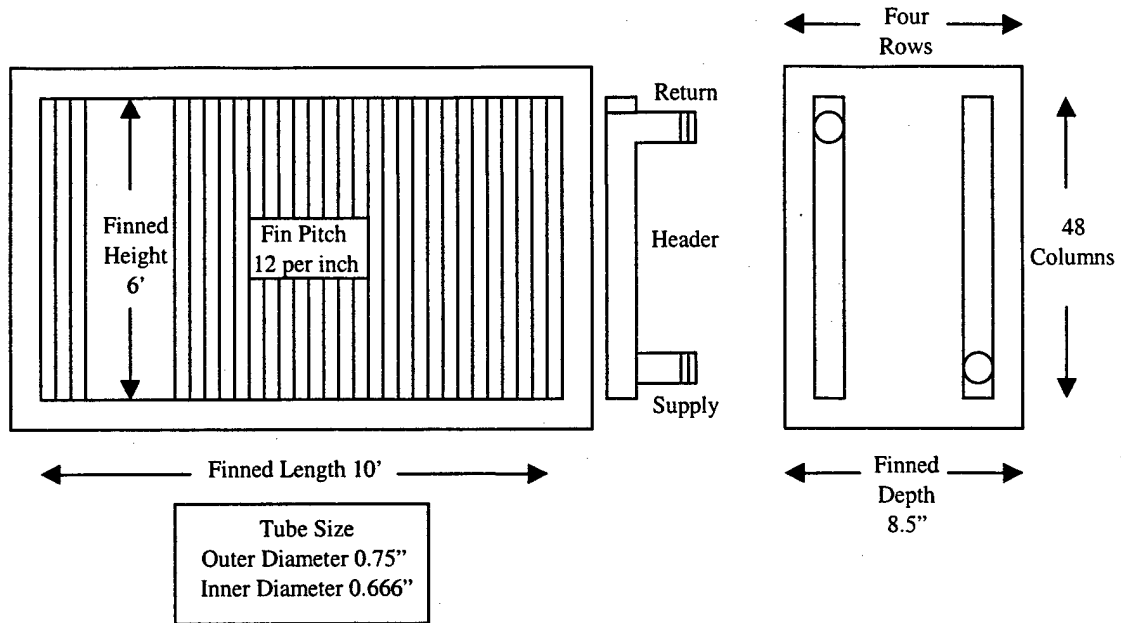


**Figure 6. Chilled Water Coil**

The following figure shows how well the calculated overall heat transfer coefficients compare with the manufacturer's results for the coil shown above. The plot depicts the UA with air velocities from 400 to 700 ft/min and water velocities of two to eight ft/sec.

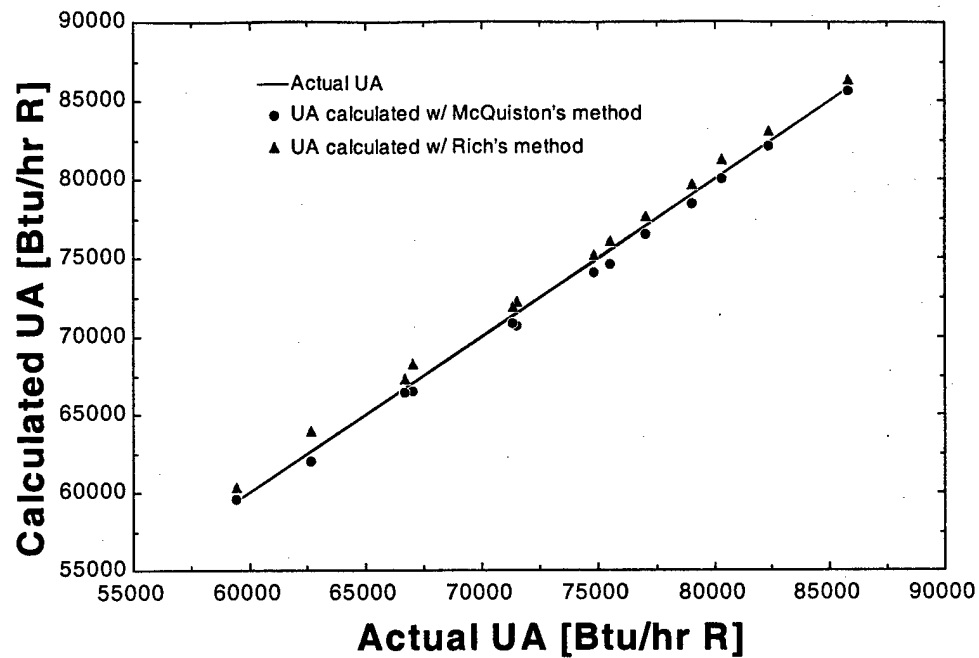


Figure 7. Accuracy of UA calculation

It is evident from these figures that both formulations model the heat transfer well. In fact, the maximum disparity between McQuiston's method and the manufacturer's data was 1% and the average difference was 0.6%. Rich's model delivered a maximum difference of 2% and a average of 1%. McQuiston's model was chosen because it provides more design flexibility by accounting for the number of tube rows.

b) Pressure Drop Calculation

1) Air-side Pressure Drop

The airside pressure drop model used was developed by Donald Rich. It assumes that the pressure drop across the airside of the coil can be broken into two components. The first portion is the pressure drop due to the presence of the tubes alone, the other part is due to the fins alone. Rich relates a fin friction factor to the pressure drop using (Rich, 1973):

$$\Delta P_{fin} = f_f \frac{G_c^2}{2 \rho_m} \sigma \quad \text{Equation 21}$$

where,  $f_f$  is the fin friction factor and  $\rho_m$  is the mean air density. Additionally,  $\sigma$  is the ratio of minimum air-flow to frontal area and  $G_c$  is the mass velocity through the minimum air-flow area. The fin friction factor is related to the Reynolds number based on the longitudinal spacing by:

$$f_f = \frac{1.7}{Re_b^{1/2}} \quad \text{Equation 22}$$

The pressure drop due through a staggered array of tubes is determined by a relation developed by Kakac and Zukauskas (Bejan, 1995).

$$\Delta P_t = n_t \cdot f_t \cdot \chi \left( \frac{\rho_a V_{a,max}^2}{2} \right) \quad \text{Equation 23}$$

Here,  $n_t$  is the number of rows in the flow direction,  $\rho_a$  is the air density, and  $V_{a,max}$  is the air velocity in the minimum free-flow area. The two terms  $f_t$  and  $\chi$  are determined using the Figure 8 (Bejan, 1995).

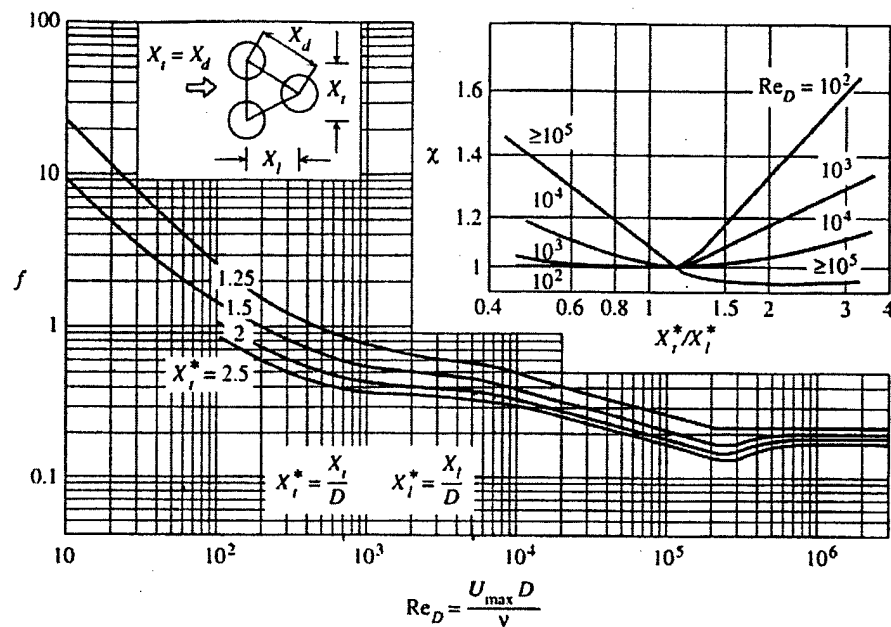


Figure 8. Friction Factor for Arrays of Staggered Tubes

Finally the total pressure drop is found by summing the pressure drop due to the fins with that due to the tubes.

$$\Delta P_{tot} = \Delta P_t + \Delta P_f \quad \text{Equation 24}$$

## 2) Water-side Pressure Drop

The pressure drop across the inside of the air handler is assumed to be a function of flow, tube roughness and coil geometry. First, the pressure drop attributed to the straight tube walls is determined. Then the pressure drop due to the tube bends and the header are found. In this calculation, the pressure drop due to tube bends is a relatively large value and thus cannot be neglected. In some situations the pressure drop resulting from the tube bends and header can equal or even surpass the pressure drop from tubes. The friction factor for tubes is found using (White, 1986):

$$\frac{1}{f^{1/2}} = -1.8 \cdot \log_{10} \left[ \frac{6.9}{\text{Re}_{D_i}} + \left( \frac{\varepsilon}{3.7 \cdot D_i} \right)^{1.11} \right] \quad \text{Equation 25}$$

The pressure drop from the tube walls alone is found using:

$$\Delta P_t = \frac{f_t \cdot L_t}{D_i} \left( \frac{\rho_w V_w^2}{2} \right) \quad \text{Equation 26}$$

The pressure drop is then converted into a head using a common relation:

$$\text{Head}_t = \frac{\Delta P_t}{\rho_w \cdot g} \quad \text{Equation 27}$$

In this formula, the term  $\Delta P_t$  is the pressure drop from tubes,  $\rho_w$  is the density of the water inside the tubes and  $g$  is the gravitational constant. To find the pressure drop due to tube bends and header, it is assumed that each header contains two 90° bends or one 180° bend. A single air handler has two headers. So an air handler with four passes has five 180° bends. Three of these bends connect the air handler's four passes and the last two bends result from inlet and outlet headers. The head due to these bends is found using the relation (White, 1986).

$$\text{Head}_{bend} = \frac{K_{bend} \cdot V_w^2}{2g} \quad \text{Equation 28}$$

where  $K_{bend}$  is a constant that depends on tube diameter and bend geometry.

### 3) Manufacturer's data

Both air and water-side pressure drop formulations have been verified using manufacturer's data. The coil used in this analysis is shown in Figure 6. Figure 9 shows the correlation between the calculated

and actual water-side head. The maximum deviation between the calculated and actual results is less than 8% with an average difference of 4%.

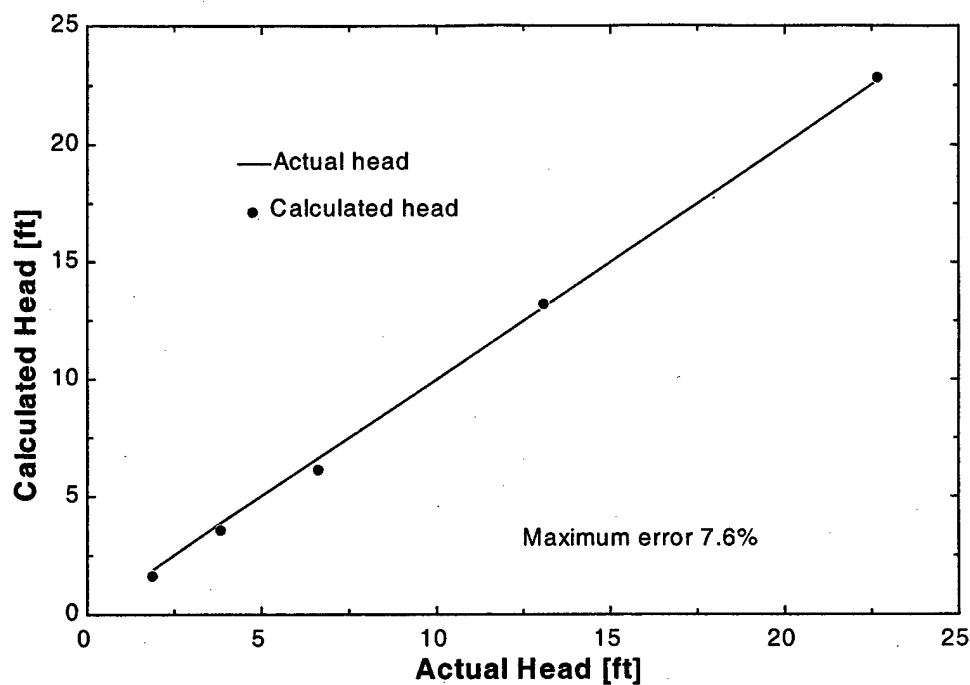


**Figure 9. Accuracy of Calculated Water-side Head**

The air-side pressure drop results are less agreeable. The model predicts the pressure drop fairly well at high flow rates but does not perform as well at low flow rates. Figure 10 shows the model's agreement. The disagreement between the manufacturer's data and calculated values does not exceed 5% when the air flow rate is between 800 and 400 ft/min. However, the disparity grows to nearly 21% when the flow rate decreases to 300 ft/min.

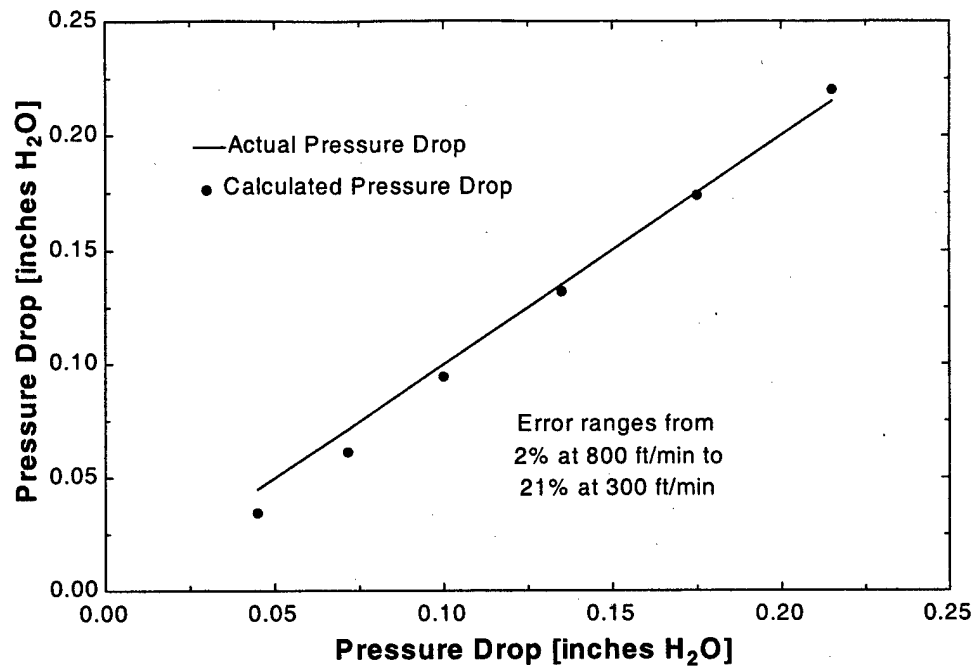


**Figure 10. Accuracy of Calculated Air-side Pressure Drop**

These differences do not affect this study's conclusions. First, the airside pressure drop is only used to determine the air handler fan power requirement, which accounts for less than 4% of the annual energy consumption. Secondly, the air handler fans are operated similarly in each case. Thus, this small error exists in every case to an equal degree.

#### 4) Fan model

The air handler fan is modeled similar to a pump. The isentropic efficiency is equal to the ratio of the enthalpy change of an isentropic fan to that of the actual fan. Assuming a constant isentropic efficiency allows for calculation of the exit enthalpy using,

$$h_{a,out} = \left( \frac{h_{a,out,rev} - h_{a,in}}{\eta_{fan}} \right) + h_{a,in} \quad \text{Equation 29}$$

where  $h_{a,out,rev}$  is the exit enthalpy of the air if the fan operated reversibly. This reversible exit enthalpy may be determined because three independent properties of the air-water vapor mixture are known. The exit

pressure is taken as the ambient pressure plus the pressure drop that must be overcome through the chilled water coil. The humidity ratio and the entropy are taken to equal the fan's inlet condition.

Once the exit enthalpy is known the fan power requirement is determined using:

$$\dot{W}_{fan} = \dot{m}_a (h_{a,in} - h_{a,out}) \quad \text{Equation 30}$$

## 2. Air Handler Performance Characteristics

In order to properly analyze a chilled water system it is necessary to understand the dynamics of the air handler. The air handler dictates the flow rate of the entire system, and determines the maximum chilled water  $\Delta T$ . This air handler is designed to have a 10°F water-side temperature change under design conditions.

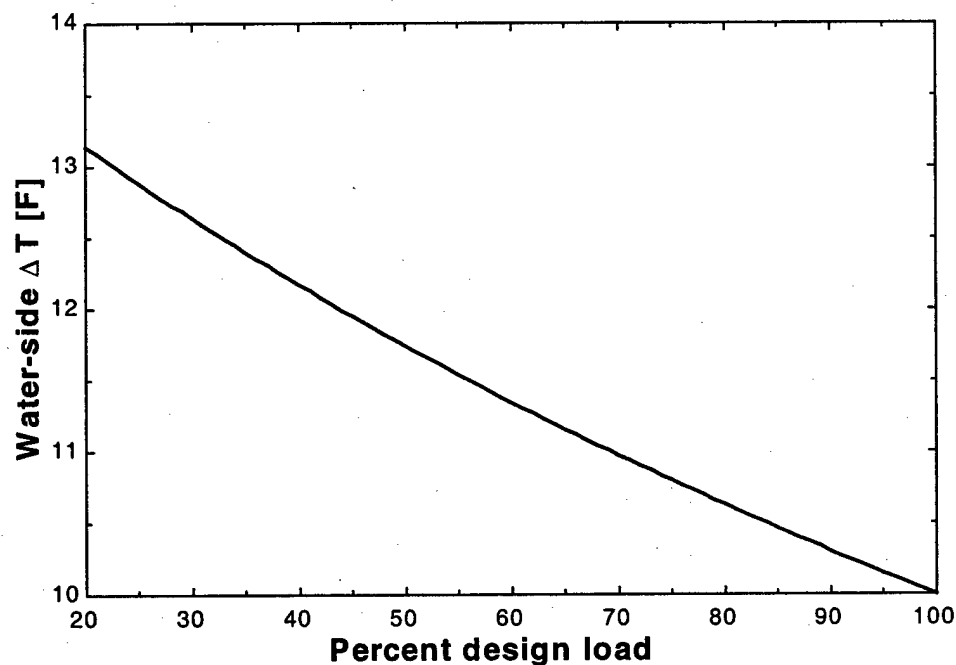


Figure 11. Chilled Water  $\Delta T$  versus Load

Figure 11 shows how the chilled water  $\Delta T$  increases as air handler load is reduced. This trend is verified by research conducted by Sauer (1989). Furthermore, he discovered that a number of factors may affect the trend. Some of these include improper air flow, improperly adjusted set points and fouled coils.

Since the waterside temperature difference increases inversely with load the water-side flow rate has more than a linear decrease.

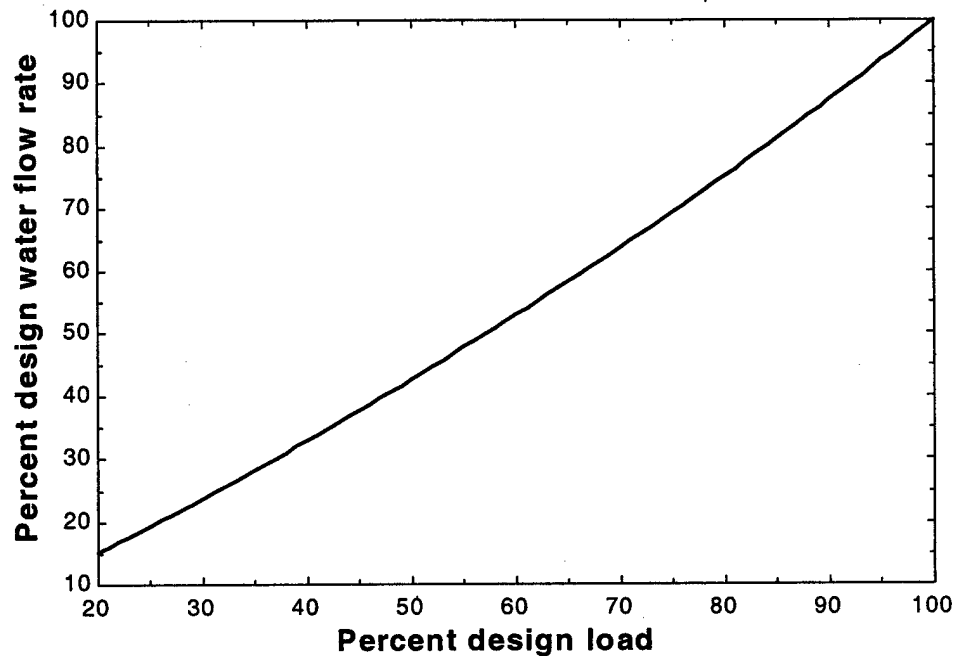


Figure 12. System flow rate versus load

This sharp decrease in flow rate has a significant effect on the part load pumping requirements.

Another aspect of air handler performance is the effect of fouling. Air handlers get fouled on the air-side and, to a lesser degree, on the water-side. The air-side fouling is a result of small particles that build up on the coil's outer surfaces. Periodic cleaning can minimize this problem. Water-side fouling results from water contaminants being deposited on tube walls. Most systems add chemical treatment to chilled water to minimize this build up. Fouling is added to the air handler model by including a fouling factor into the overall heat transfer equation. With the addition of fouling the equation becomes (Icropera and Dewitt, 1985):

$$UA = \frac{1}{\left[ \left( \frac{1}{h_i A_i} \right) + \left( \frac{R_{f,i}}{A_i} \right) + \left( \frac{\ln(D_o/D_i)}{2\pi k_t L_t n_t} \right) + \left( \frac{R_{f,o}}{A_o} \right) + \left( \frac{1}{h_o A_o \eta_o} \right) \right]} \quad \text{Equation 31}$$

Figure 13 shows the effect of fouling on air handler performance. This air handler is assumed to be fouled to the point that it has a 7°F waterside temperature difference at design load, rather than the intended 10°F.

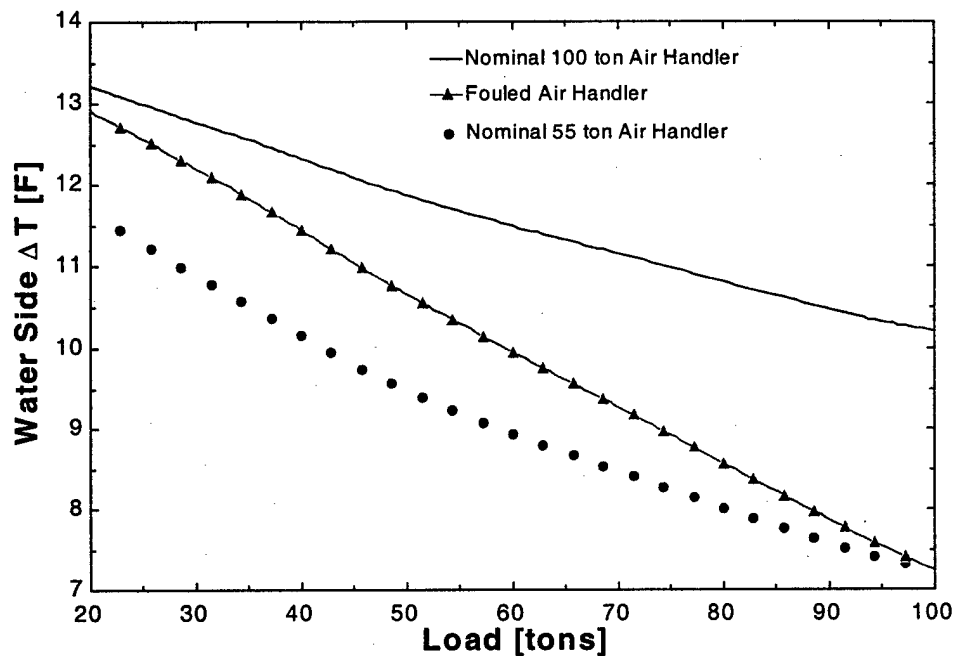


Figure 13. Fouled air handler water-side T versus load

Notice that the fouled air handler operates as if it were a 55 ton capacity air handler at design conditions, rather than 100 tons. The fouling effect becomes less evident as load decreases. This means at design conditions a system with fouled air handlers requires a much larger water flow rate. The increase in flow rate is seen in Figure 14.

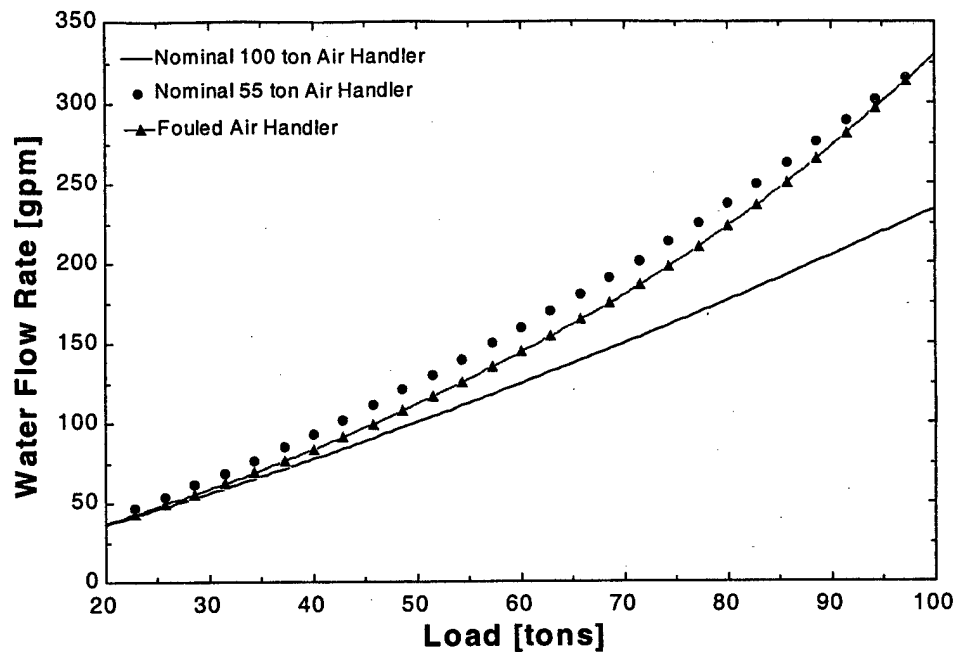


Figure 14. Fouled air handler flow rate versus load

This change in flow rate has a significant impact on pumping power. System analysis will show that this affects chiller scheduling as well.

Finally it is important to understand how the system load relates to other system variables. This analysis is especially important when operating above design conditions. Consider the equation:

$$\dot{Q} = UA \cdot LMTD$$

Equation 32

where LMTD is the log mean temperature difference between the air and water-sides. The UA is predominantly a function of water and air flow rates. Consider four variables: the flow rates and coil inlet temperatures of the water and air streams. Holding the other three constant, if either the air or water flow is increased the heat transfer rate rises. If the flow rates and air inlet temperature are held constant reducing the chiller set point will increase the heat transfer. Finally, raising the air inlet temperature, in effect, the outdoor dry bulb temperature also increases the heat transfer.

## Chiller

### 1. Manufacturer's data

The chiller components that were modeled include the compressor, evaporator and condenser.

Manufacturer's performance data was used to verify each model's accuracy. For proprietary reasons, any reference to manufacturer or equipment has been excluded.

Compressor				Evaporator					Condenser				
Tons	% Load	KW	KW/Ton	LWT	GPM	EWT	Ref. Temp	PD (ft)	EWT	GPM	LWT	Ref. Temp	PD (ft.)
1000	100	520	0.520	44	3300	51.27	41.12	36.37	85	3000	94.27	95.60	25.71
1000	100	522	0.522	44	2400	54.00	41.49	19.73	85	3000	94.25	95.60	25.71
1000	100	523	0.523	44	1130	65.24	42.38	4.63	85	3000	94.23	95.60	25.71
660	66	308	0.467	44	3300	48.80	41.60	36.43	85	3000	91.40	91.87	25.80
660	66	310	0.470	44	2400	50.60	41.87	19.77	85	3000	91.03	91.87	25.80
660	66	313	0.474	44	1130	58.02	42.54	4.62	85	3000	91.02	91.85	25.80
330	33	170	0.515	44	3300	46.40	42.03	36.49	85	3000	88.07	88.46	25.89
330	33	173	0.524	44	2400	47.30	42.20	19.81	85	3000	88.07	88.46	25.89
330	33	177	0.536	44	1130	51.01	42.66	4.62	85	3000	88.07	88.46	25.89
1000	100	445	0.445	44	3430	51.00	41.08	39.17	75	3000	84.10	85.45	26.32
1000	100	444	0.444	44	2400	54.00	41.49	19.81	75	3000	84.06	85.44	26.32
1000	100	442	0.442	44	1130	65.24	42.38	4.63	75	3000	84.04	85.41	26.32
660	66	259	0.392	44	3940	48.02	41.47	51.19	75	3000	80.92	81.77	26.42
660	66	262	0.397	44	2400	50.60	41.87	19.77	75	3000	80.91	81.77	26.42
660	66	266	0.403	44	1080	58.67	42.58	3.89	75	3000	80.91	81.76	26.42
330	33	141	0.427	44	3940	46.01	41.95	51.06	75	3000	78.00	78.40	26.52
330	33	145	0.439	44	2400	47.30	42.20	19.81	75	3000	78.00	78.40	26.52
330	33	148	0.448	44	1250	50.34	42.60	5.67	75	3000	78.00	78.40	26.52
1000	100	398	0.398	44	3940	50.09	40.95	51.12	65	3000	73.97	75.39	27.00
1000	100	400	0.400	44	2400	54.00	41.49	19.73	65	3000	73.96	75.38	27.00
1000	100	402	0.402	44	1130	65.20	42.27	4.63	65	3000	73.94	75.37	27.00
660	66	230	0.348	44	3940	48.02	41.47	51.19	65	3000	70.85	71.74	27.11
660	66	233	0.353	44	2400	50.60	41.87	19.77	65	3000	70.84	71.73	27.11
660	66	237	0.359	44	1080	58.67	42.58	3.89	65	3000	70.84	71.73	27.11
330	33	120	0.364	44	3940	46.01	41.95	51.25	65	3000	67.95	68.36	27.22
330	33	123	0.373	44	2400	47.30	42.20	19.81	65	3000	67.94	68.36	27.22
330	33	126	0.382	44	1250	50.34	42.60	5.67	65	3000	67.94	68.36	27.22

**Table 7. Present Day Chiller Data**

The data used in this study is that of a modern, 1000 ton capacity, electrical chiller. The data depicts 27 different operating conditions, with varying evaporator flow rates, loads and condenser inlet temperatures.

## 2. Compressor Model

### a) Weber's Compressor Model

An earlier compressor model developed by Weber (1988) and used by Joyce (1990) utilized the ideal, Carnot efficiency multiplied by a constant isentropic compressor efficiency and a part load efficiency factor. The reader should consult Weber for the complete model development.

The model's purpose is to predict the compressor power required at various loads, condenser pressures and evaporator pressures. Weber initially assumes an isentropic compressor that compresses refrigerant from the evaporator pressure to the higher condenser pressure. The model then determines the power needed by this reversed Carnot cycle using the relation:

$$\dot{W}_{carnot} = \dot{Q}_{evap} \left[ \frac{T_{cond}}{T_{evap}} - 1 \right] \quad \text{Equation 33}$$

The manufacturer's power requirement is then related to that of the reversed Carnot cycle using an isentropic compressor efficiency,  $\eta_{isent}$ , at design load. This factor takes into account the electric motor efficiency as well as internal compressor irreversibility. Finally, Weber includes an efficiency load factor,  $\eta_{ton}$ , that decreases with increasing load. The final relationship is given as:

$$\frac{\dot{W}_{actual}}{\dot{Q}_{evap}} = \frac{\left( \frac{\dot{W}_{carnot}}{\dot{Q}_{evap}} \right)}{(\eta_{isent} \cdot \eta_{ton})} \quad \text{Equation 34}$$

Figure 15 shows present day chiller data modeled using Weber's formulation. The greatest error encountered using this model is 9% while the average error is 3%.

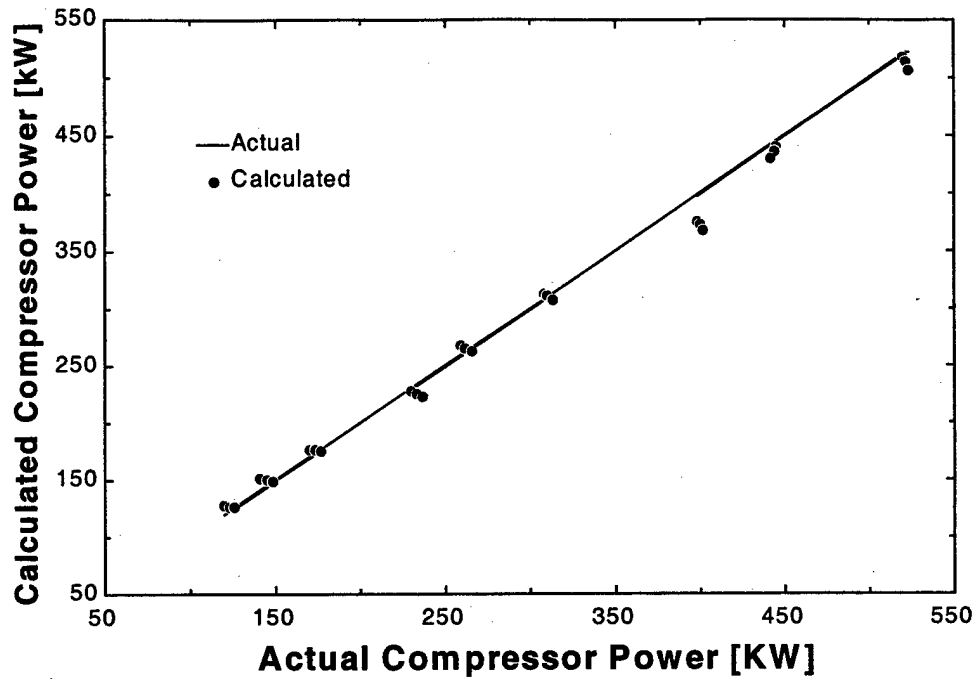


Figure 15. Weber's compressor model accuracy

b) Liu's Compressor Model

Liu (1997) revised Weber's compressor model by assuming a certain amount of the compressor power is used to overcome constant frictional power. The remainder of the power corresponds to the Carnot efficiency.

$$\dot{W}_{actual} = A \cdot \dot{W}_{carnot} + \dot{W}_{frict} \quad \text{Equation 35}$$

Figure 16 shows the present day chiller data modeled using Liu's formulation. The largest error using this approach is 14% and the average error is 5%.

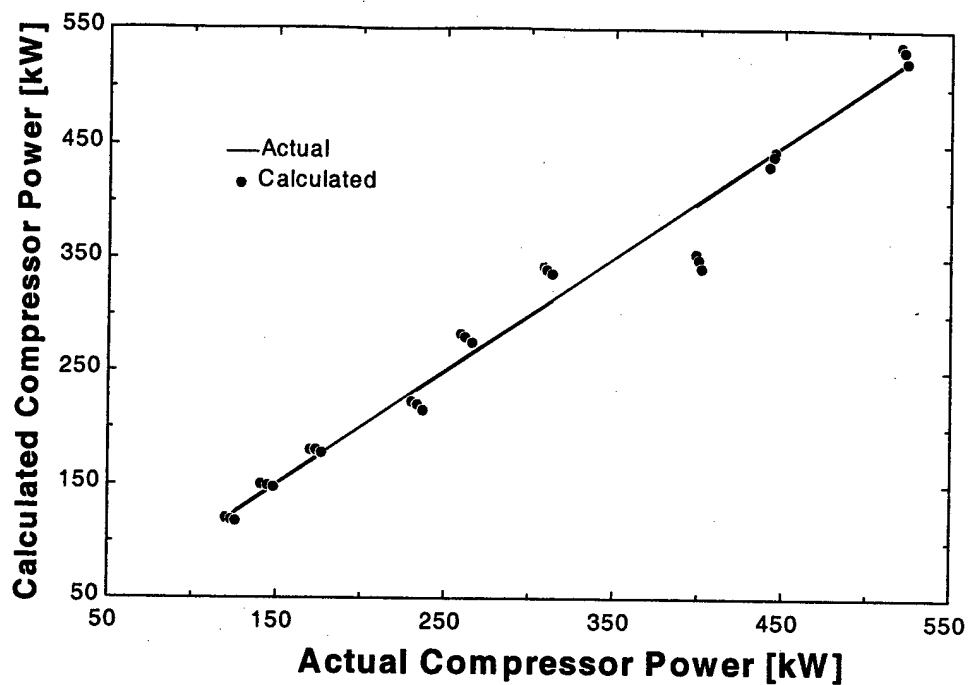


Figure 16. Liu's Compressor Model Accuracy

c) Revised Compressor Model

In order to improve the chiller model's ability to replicate present day chiller performance, a new compressor model was designed. Like Liu's model, it is assumed that a portion of the power input to the compressor is needed to overcome frictional power. This frictional power, however, are assumed to be a function of chiller load. The remaining compressor power corresponds to the Carnot power requirement, although this is also taken to be a function of load.

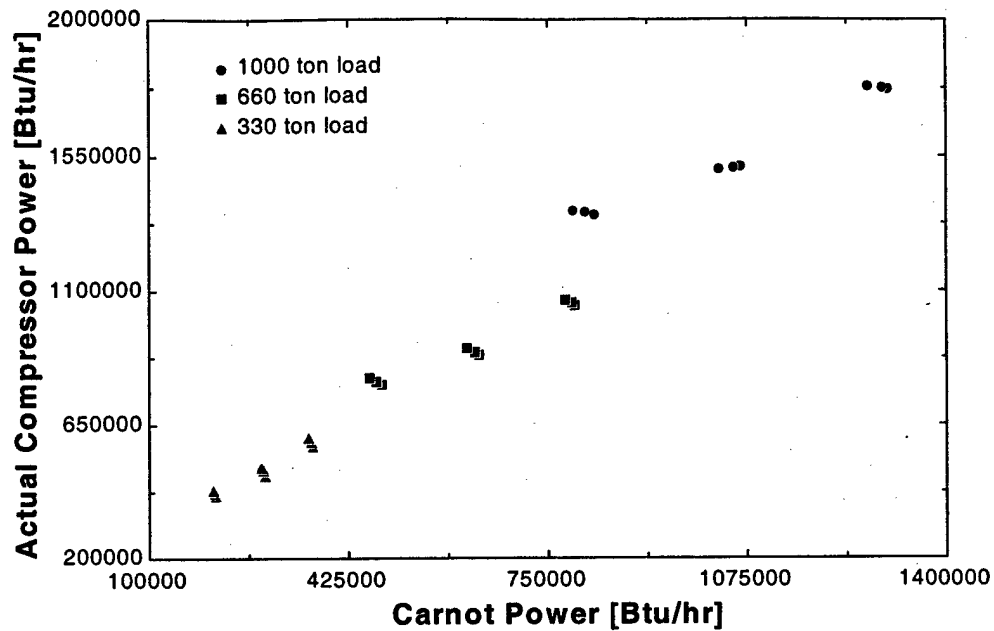


Figure 17. Compressor Power Actual versus Carnot

Figure 17 shows that compressor power is not purely a function of the Carnot efficiency, but a function of load as well. As a compressor proceeds from a large to a smaller load, inlet vanes in the compressor are turned adding swirl to the refrigerant entering the compressor. This allows the compressor to run at a constant speed, while controlling the refrigerant flow rate. However, adding this swirl increases frictional losses. The compressor motor efficiency is also a function of load. A chiller is normally designed for its highest efficiency at part load, because it operates there most of its life. As a result, the compressor motor appears to operate optimally between 75% and 85% of full load. As the load increases or decreases the compressor's efficiency decreases. The relation used for finding compressor power is given by:

$$\dot{W}_{actual} = \dot{W}_{carnot}^2 \cdot fn_1(\dot{Q}_{evap}) + \dot{W}_{carnot} \cdot fn_2(\dot{Q}_{evap}) + \dot{W}_{frict} \cdot fn_3(\dot{Q}_{evap}) \quad \text{Equation 36}$$

These individual functions are:

$$fn_n = A_n \cdot \dot{Q}_{evap}^2 + B_n \cdot \dot{Q}_{evap} + C_n \quad \text{Equation 37}$$

Where the heat transfer rate is in units of tons and the constants are given in the table below.

	1	2	3
A	1.31E-12	2.03E-06	0.952
B	3.15E-09	4.39E-03	705
C	2.79E-06	1.23	3040

**Table 8 . Compressor constants**

Figure 18 shows the revised model's accuracy. The largest error is 3% and the average is 1.5%.

The revised model appears to replicate the present day compressor's performance somewhat better than Weber's formulation and much better than Liu's technique.

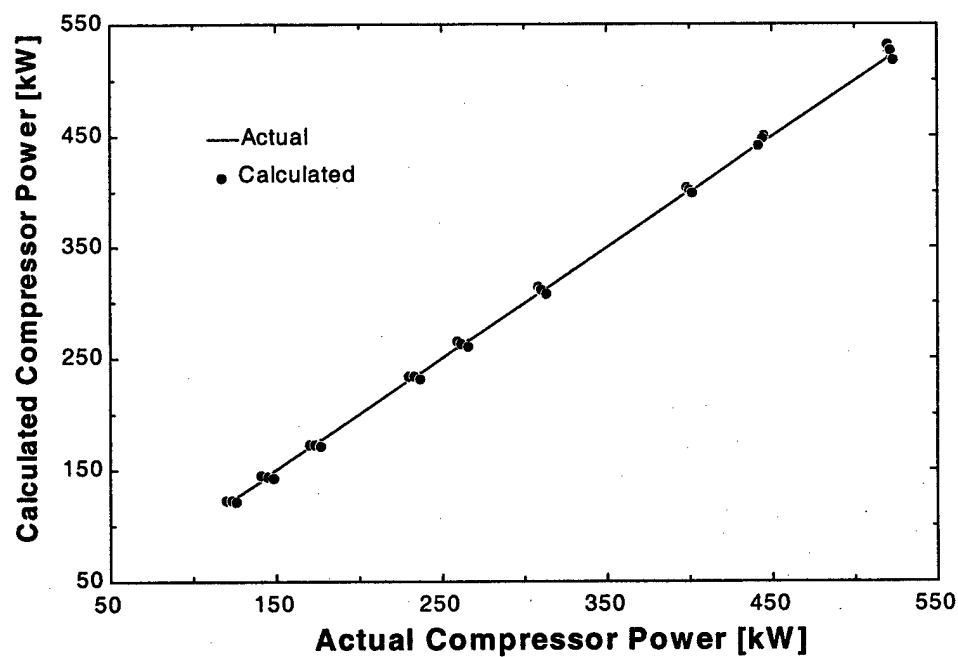


**Figure 18. Revised Compressor Model Accuracy**

### 3. Evaporator Heat Exchanger Model

#### a) Heat transfer calculation

In a previous study Weber (1988) modeled the affect that varying condenser water flow rate has on condenser heat exchanger UA. Weber assumed that at a fixed load, the UA is only a function of flow rate. He determined a relationship between UA and condenser flow rate at a constant load. He assumed that at a fixed flow rate the overall UA is only a function of load. Thus, Weber simply shifts the UA versus GPM curve up and down to accommodate different loads. This development seems logical, however, Weber had only two data points at a loads below the design load. As a result, it was impossible for him to validate his assumptions. This study attempts a similar approach to model variable evaporator flow.

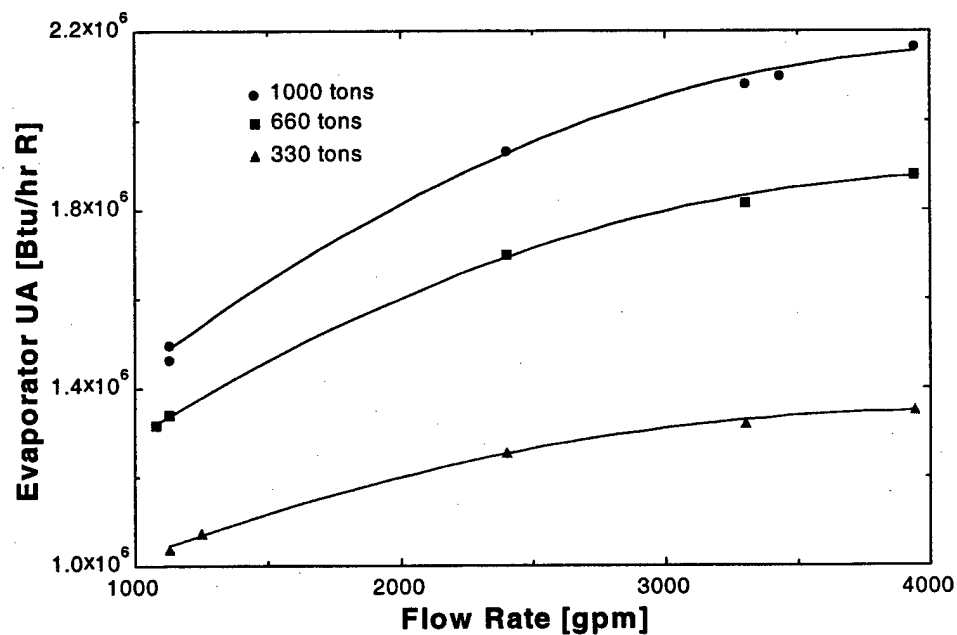


**Figure 19. Evaporator UA versus Flow Rate**

Figure 19 represents the relationship between evaporator UA and water flow rate for three different load conditions. This figure clearly shows that at lower flow rates the curves approach each other, while they separate at the flow rate increases.

The inner, water-side, heat transfer coefficient is a function of flow and fluid properties, namely the Reynolds and Prantl numbers. The outer, refrigerant side, heat transfer coefficient is a function of load,

or rate of boiling. In the evaporator refrigerant is boiling on the outside of tubes. At very small loads natural convection starts around the tube bundle. As the load increases, nucleate boiling begins. Initially, there is only isolated bubbles. As load increases the boiling refrigerant forms slugs and columns of vapor. While boiling transitions from isolated bubbles to rapid boiling the refrigerant becomes more agitated, increasing the outer heat transfer coefficient. This explains why the refrigerant side heat transfer coefficient is tied to load.

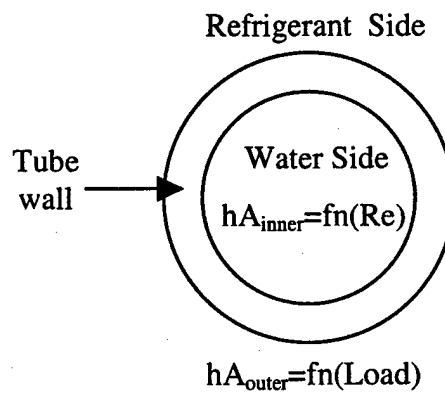


**Figure 20. Cross-section of a Single Tube in the Evaporator Tube Bundle**

For the given chiller, the inner tube diameter as well as water velocity at a specified flow rate were known. With this knowledge, the Reynolds number was found as a function of water flow rate. Evaporator UA was determined directly from the manufacturer's data. Using these values a relationship was developed for evaporator UA as a function of Reynolds number at a fixed load. This function was then evaluated as the Reynolds number approached zero. It was assumed that the UA below the intercept of this function and the Y-axis is due to refrigerant side conditions. While the portion of UA above the intercept is due to water-side conditions.

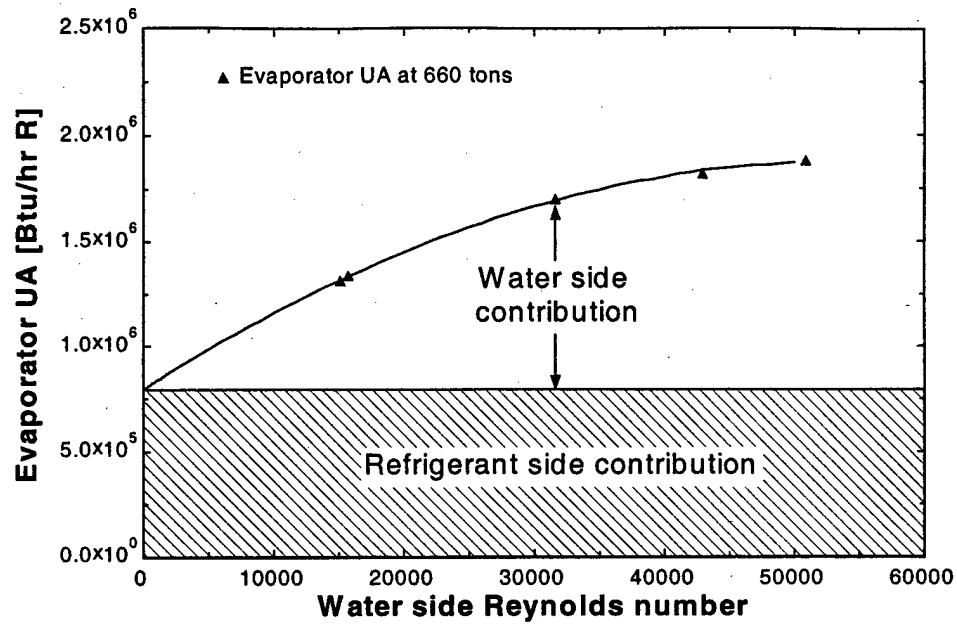


Figure 21. Evaporator UA versus Reynolds Number

A ratio of these components,  $\xi_{evap}$ , was used to reduce the number of unknowns in the overall heat transfer coefficient calculation.

$$\xi_{evap} = \frac{hA_i}{hA_o} \quad \text{Equation 38}$$

then

$$UA_{evap} = \frac{1}{\left[ \frac{1}{\xi_{evap} \cdot hA_o} + \frac{1}{hA_o} \right]} \quad \text{Equation 39}$$

It was assumed the refrigerant side  $hA$  remains constant with fixed load. Since the  $UA$  is known, as well as the refrigerant side  $hA$  at the specified load, it was possible to solve for the water-side  $hA$  as a function of Reynolds number. This function takes the form,

$$hA_i = K \cdot \text{Re}^a \quad \text{Equation 40}$$

where K and a are constants. This relationship was refined knowing the heat transfer coefficient is also a function of fluid properties. The heat transfer coefficient for a fluid losing heat is proportional to  $\text{Pr}^{0.3}$ .

Thus, the equation becomes,

$$hA_i = D \cdot \text{Pr}^{0.3} \cdot \text{Re}^a \quad \text{Equation 41}$$

where the constant D depends on the geometry of the tube bundle. The constants D and a were determined from experimental data and take the values 6210 and 0.533 respectively. This value for the constant, a, is relatively close to the expected value, 0.8. The difference is assumed to result from heat transfer augmentation.

With the water-side hA known the refrigerant side hA was found as a function of load, taking the form of a quadratic.

$$hA_o = A \cdot \dot{Q}_{evap}^2 + B \cdot \dot{Q}_{evap} + C \quad \text{Equation 42}$$

Here the values A, B and C were found to be 1.47, 9,240 and 181,000 respectively.

The method described above models the evaporator heat transfer very well as seen in Figure 22.

The maximum error using this method is 2%.

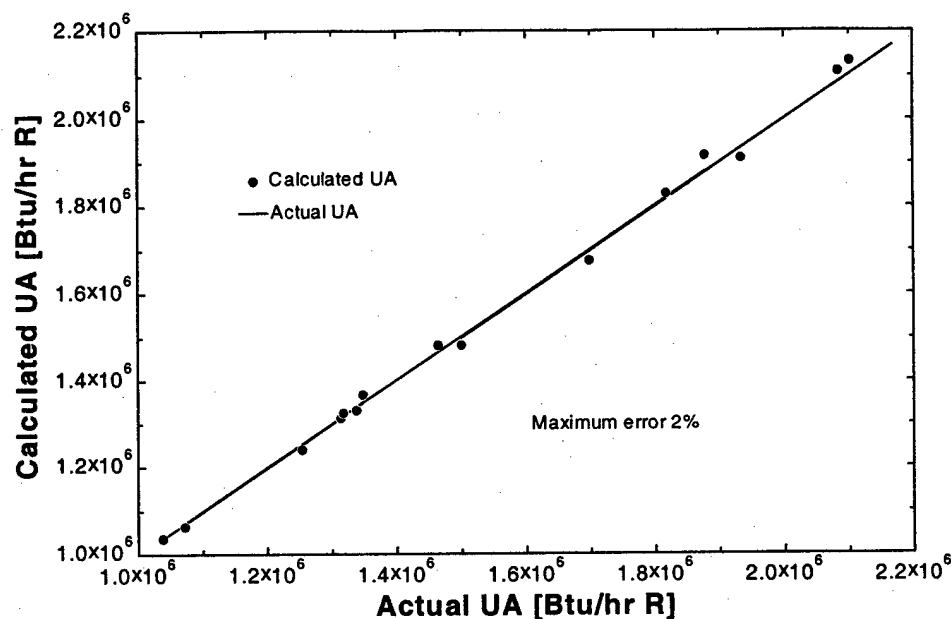


Figure 22. Accuracy Results for Evaporator UA Calculation

b) Pressure drop calculation

The evaporator heat exchanger water-side pressure drop calculation is critical to this study because the evaporator makes a major contribution to the chilled water system's pressure drop. Decreasing water flow rate through the evaporator at part load reduces the pressure drop and with it the pump power. Since a primary-secondary system keeps a constant flow rate through the evaporator, this savings is not available. Bypass loop removal, however, permits this savings.

Due to proprietary reasons the manufacturer was unwilling to release any information pertaining to tube bundle inner surfaces. It is expected that there is augmentation on the tubes inner surfaces which increases heat transfer between the chilled water and tube wall. This augmentation affects evaporator pressure drop. In order to model the evaporator pressure drop, an effective length and roughness were determined. In actuality, the evaporator is much shorter and rougher than this effective length and roughness indicate. Also, much of the evaporator pressure drop results from tube bends and header losses.

However, since the actual geometry is not available, effective values were used. The following relations were used in this calculation (White 1985):

$$\frac{1}{f_{t,i}^{1/2}} = -1.8 \cdot \log_{10} \left[ \frac{6.9}{\text{Re}_{D_i}} + \left( \frac{\epsilon_{\text{eff}}}{3.7 \cdot D_i} \right)^{1.11} \right] \quad \text{Equation 43}$$

$$\Delta P_{\text{evap}} = \frac{f_{t,i} \cdot L_{\text{eff}}}{D_i} \left( \frac{\rho_w V_w^2}{2} \right) \quad \text{Equation 44}$$

In order to solve for  $L_{\text{eff}}$  and  $\epsilon_{\text{eff}}$  two data points are used, one was chosen at maximum evaporator flow and another at minimum flow. These points, with the equations above, were used to solve for two unknowns,  $L_{\text{eff}}$  and  $\epsilon_{\text{eff}}$ . It is apparent from Figure 23 that the model replicates the manufacturer's data very well throughout the range of flow rates.

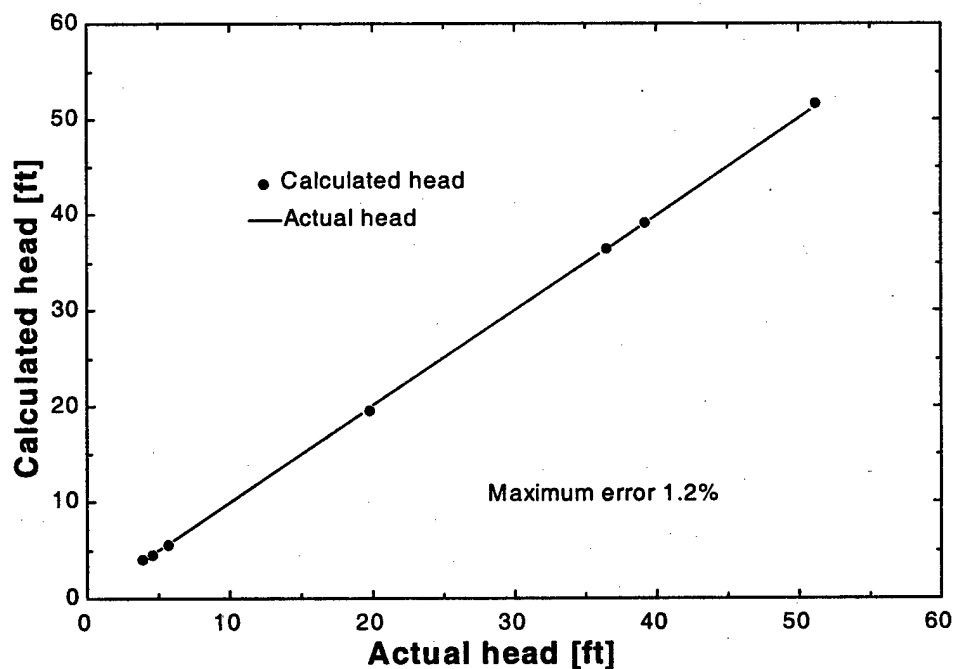


Figure 23. Accuracy Results for Evaporator Pressure Drop

#### 4. Condenser Heat Exchanger Model

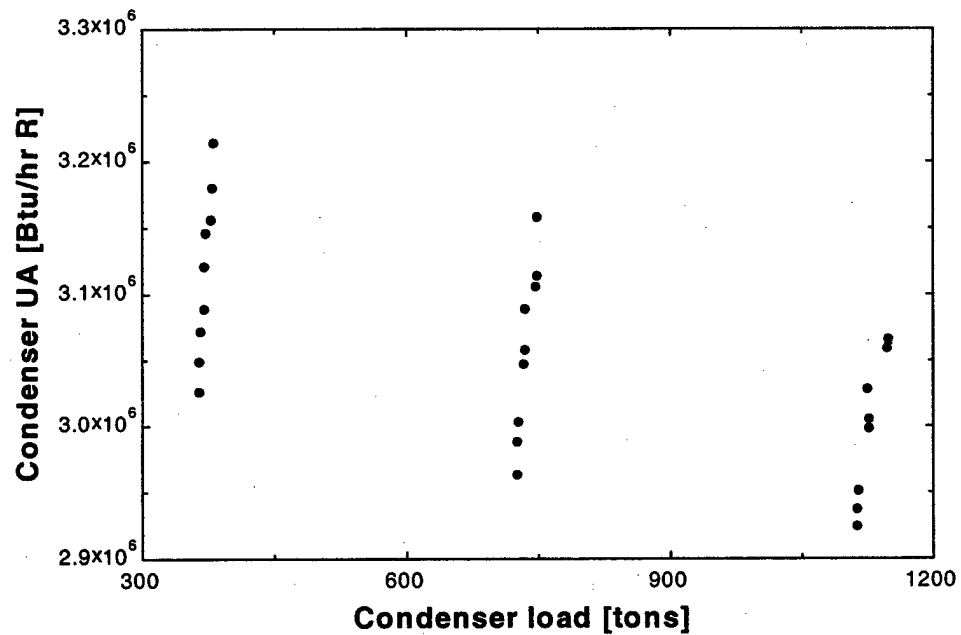
##### a) Heat transfer calculation

The following equations were used to determine the condenser's heat transfer performance:

$$\dot{Q}_{cond} = \dot{m}_{w,cond} C_{w,cond} (T_{w,out} - T_{w,in}) \quad \text{Equation 45}$$

$$\dot{Q}_{cond} = UA_{cond} LMTD_{cond} \quad \text{Equation 46}$$

$$LMTD = \frac{T_{w,out} - T_{w,in}}{\ln \left( \frac{T_{cond} - T_{w,in}}{T_{cond} - T_{w,out}} \right)} \quad \text{Equation 47}$$



more condensate builds on the tube walls. As a result, the liquid film layer tends to insulate the refrigerant from the tube wall. When load continues to increase this film grows thicker, hampering heat transfer.

Therefore, the condenser UA has an inverse relation with load.

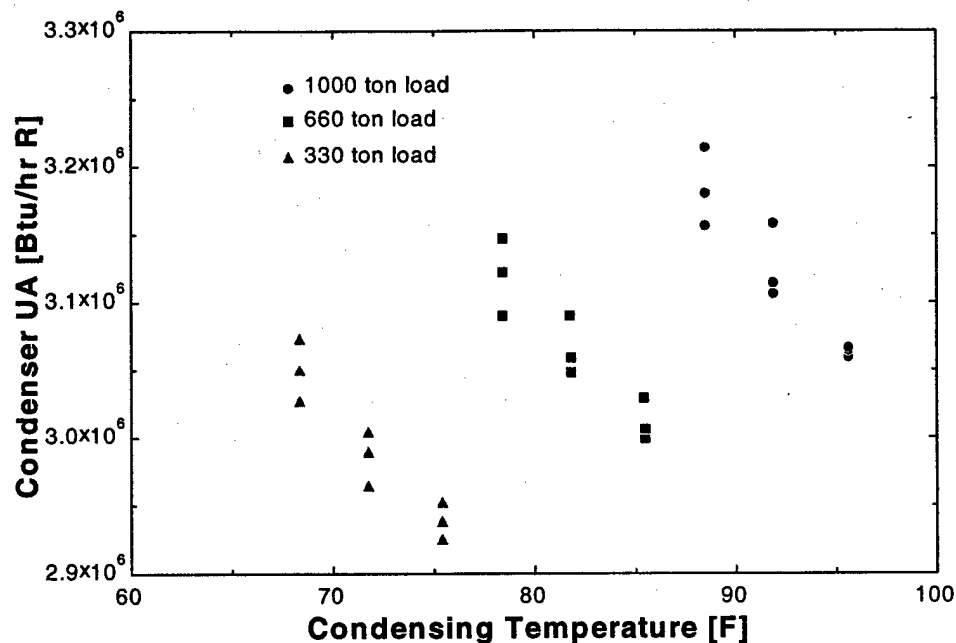


Figure 25. Condenser UA versus Condensing Temperature

Figure 25 shows that the condenser UA is a function of condensing temperature. This is because the refrigerant film thickness is affected by the condensing temperature. When the refrigerant is condensing at a high temperature, it is less viscous and does not cling to the tube walls well. So it is not able to build a thick film. When the condensing temperature decreases, the refrigerant becomes more viscous and is able to develop a thicker layer. This thick film impairs heat transfer, so the condenser UA decreases with condensing temperature. Taking the chiller load and condensing temperature into account the following relation was developed.

$$UA_{cond} = f(\text{Load}) \cdot f(T_{cond}) \quad \text{Equation 48}$$

The two functions were determined from curve fits of manufacturers data. The load function is a linear function, and the temperature factor is assumed to be second order. These functions are:

$$f(T_{cond}) = 185000 + 22800 \cdot \dot{Q}_{cond} - 96.2 \cdot \dot{Q}_{cond}^2 \quad \text{Equation 49}$$

$$f(load) = 1.06 - 9.23 \cdot 10^{-5} \cdot \dot{Q}_{cond} \quad \text{Equation 50}$$

Figure 26 shows the model's accuracy. The maximum error was 1.3% and the average error was 0.6%.

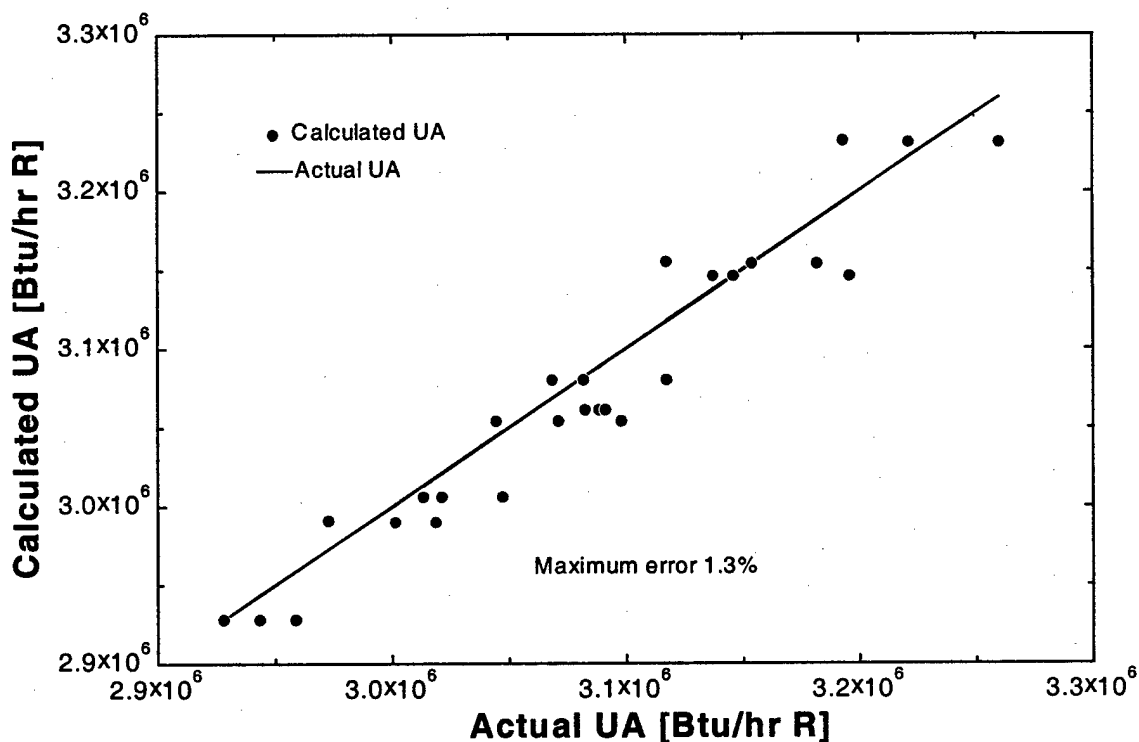


Figure 26. Accuracy Results For Condenser UA Calculation

b) Pressure drop calculation

The chilled water system considered in this study assumes a constant condenser water flow rate of 3 gpm per ton capacity. For example, a single chiller plant with a 1000 ton capacity chiller has a constant 3000 gpm condenser flow rate. As a result, the condenser pressure drop is almost constant. Since the condenser flow rate is constant, the condenser water temperature is the only variable that affects condenser head. At cooler condenser water temperatures the water will become more viscous, causing a greater head. These variations are small; about a 10% change from the maximum to minimum head over the range of

temperatures considered. Since the head varies indirectly with condenser temperature, the head is modeled using the relation.

$$Head_{cond} = A(T_{w,cond,ave})^{-B} \quad \text{Equation 51}$$

Where the constants A and B are 60.6 and 0.191 respectively. This model results in maximum errors of less than 0.06% when compared with manufacturer's data.

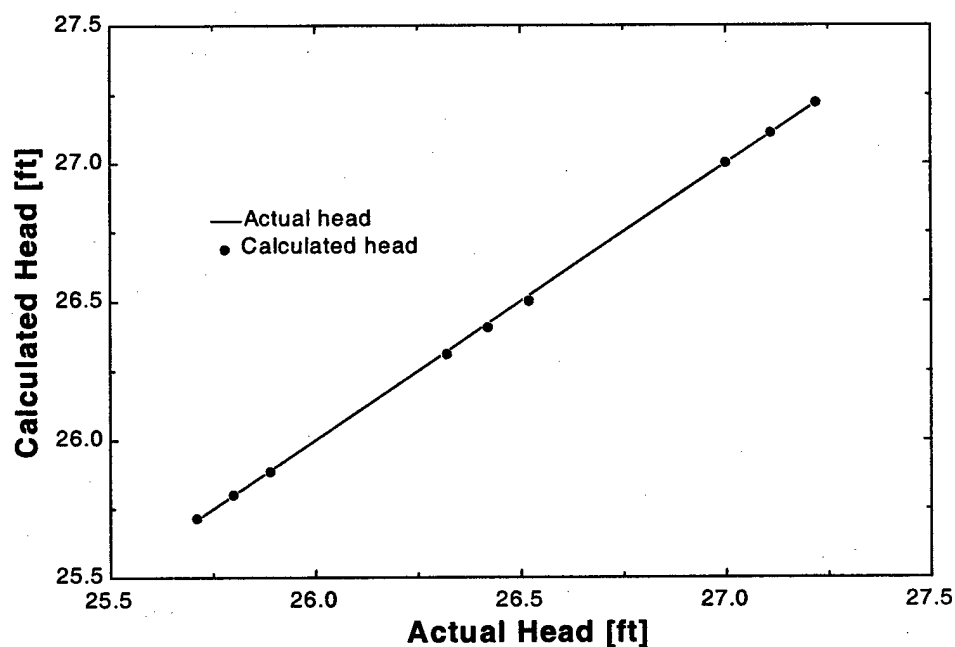


Figure 27. Accuracy of condenser head model

## 5. Chiller Comparison

Data from three chillers has been compared in order to examine the differences in chiller performance. The three chillers studied are all 1000 ton electric chillers. One is the current high efficiency chiller shown in Table 7. For the purpose of this discussion this chiller is labeled chiller A. The other two include a high efficiency chiller and a lower efficiency chiller, both available and popular in 1995. These chillers are labeled as chillers B and C respectively. Data from these older chillers is presented below.

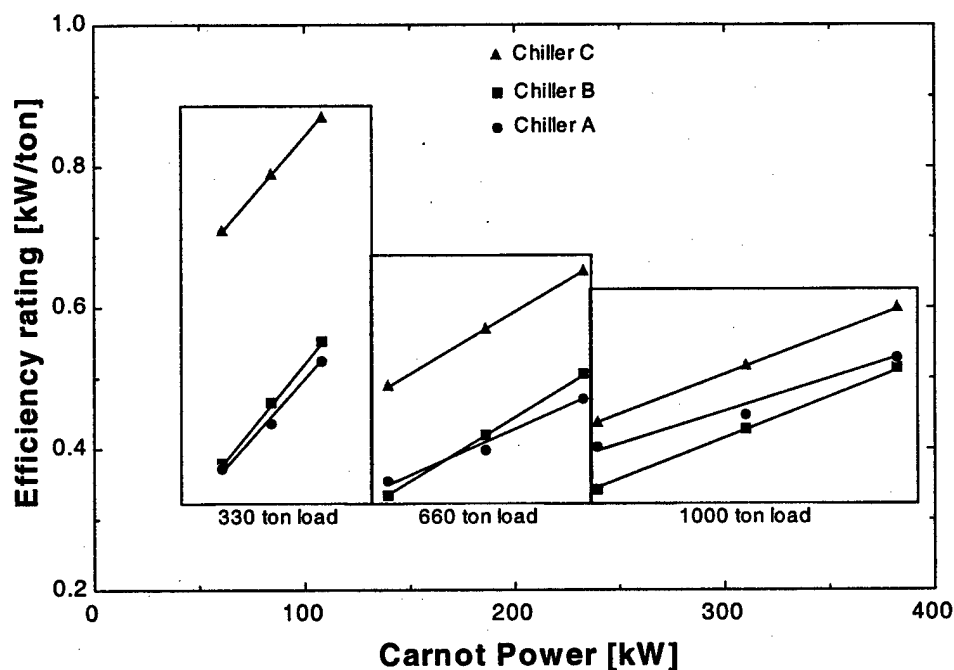
Load	T <sub>cond,in</sub>	T <sub>evap,out</sub>	GPM <sub>cond</sub>	GPM <sub>evap</sub>	KW	T <sub>cond</sub>	T <sub>evap</sub>
1000	85	44	3000	2400	538	96.95	40.99
900	85	44	3000	2400	463	95.67	41.15
800	85	44	3000	2400	406	94.45	41.3
700	85	44	3000	2400	352	93.23	41.46
600	85	44	3000	2400	302	92.04	41.61
500	85	44	3000	2400	259	90.87	41.76
1000	75	44	3000	2400	455	86.077	40.99
900	75	44	3000	2400	402	85.55	41.15
800	75	44	3000	2400	350	84.33	41.3
700	75	44	3000	2400	304	83.14	41.46
600	75	44	3000	2400	261	91.96	41.61
500	75	44	3000	2400	222	80.79	41.76
400	75	44	3000	2400	185	79.65	41.91

Table 9. Liu's High Efficiency Chiller (B)

Load	T <sub>cond,in</sub>	T <sub>evap,out</sub>	GPM <sub>cond</sub>	GPM <sub>evap</sub>	KW	T <sub>cond</sub>	T <sub>evap</sub>
1000	85	44	3000	2400	612	97.15	40.91
900	85	44	3000	2400	555	95.93	41.14
800	85	44	3000	2400	503	94.76	41.35
700	85	44	3000	2400	453	93.57	41.55
600	85	44	3000	2400	406	92.37	41.75
500	85	44	3000	2400	362	91.19	41.93
400	85	44	3000	2400	318	90	42.11
300	85	44	3000	2400	273	88.81	42.27
200	85	44	3000	2400	220	87.65	42.42
1000	75	44	3000	2400	536	86.95	40.9
900	75	44	3000	2400	483	85.75	41.14
800	75	44	3000	2400	436	84.54	41.35
700	75	44	3000	2400	395	83.41	41.56
600	75	44	3000	2400	356	82.24	41.75
500	75	44	3000	2400	319	81.07	41.93
400	75	44	3000	2400	281	79.9	42.11
300	75	44	3000	2400	243	78.73	42.27
1000	65	44	3000	2400	478	76.83	40.9
900	65	44	3000	2400	437	75.65	41.14
800	65	44	3000	2400	396	74.51	41.35
700	65	44	3000	2400	361	73.35	41.56
600	65	44	3000	2400	328	72.19	41.75
500	65	44	3000	2400	296	71.04	41.93
400	65	44	3000	2400	260	69.86	42.11
300	65	44	3000	2400	223	68.69	42.27

Table 10. Liu's Low Efficiency Chiller (C)

Performance comparisons were made on the compressors, evaporators and condensers. The figures below show the relative performance of these three chillers. Figure 28 shows the relative performance of the three chiller compressors. All three compressors have similar performance at full load. In fact, the chiller B appears to be more efficient than chiller A full load. As load decreases, the chillers A and B continue to perform similarly. At 33% load the chiller A's compressor is somewhat more efficient than that of chiller B but by only a small amount. Chiller C's compressor performance drops off dramatically as load decreases. This performance trend may be attributed to increased design focus on achieving a high integrated part load value (IPLV), rather than full load performance. The IPLV places great importance on part load efficiency.



**Figure 28. Compressor Performance Comparison**

Figure 29 shows that the evaporator heat exchangers have a similar UAs at 33% load. As loads increase, the chillers B and C continue to have similar UA's. The chiller A's UA increases dramatically with load. At full load the current chiller's evaporator performs much better than both older chillers.

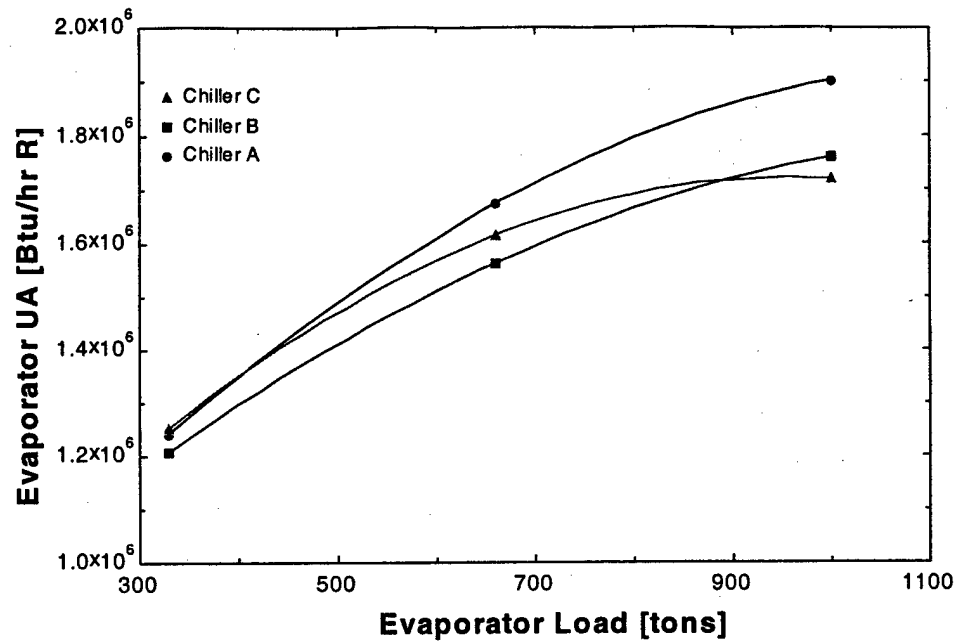


Figure 29. Evaporator Performance Comparison

Figure 30 shows that chiller A's condenser UA is much higher than the other two chillers at all loads depicted, while the chillers A and B have similar UA's.

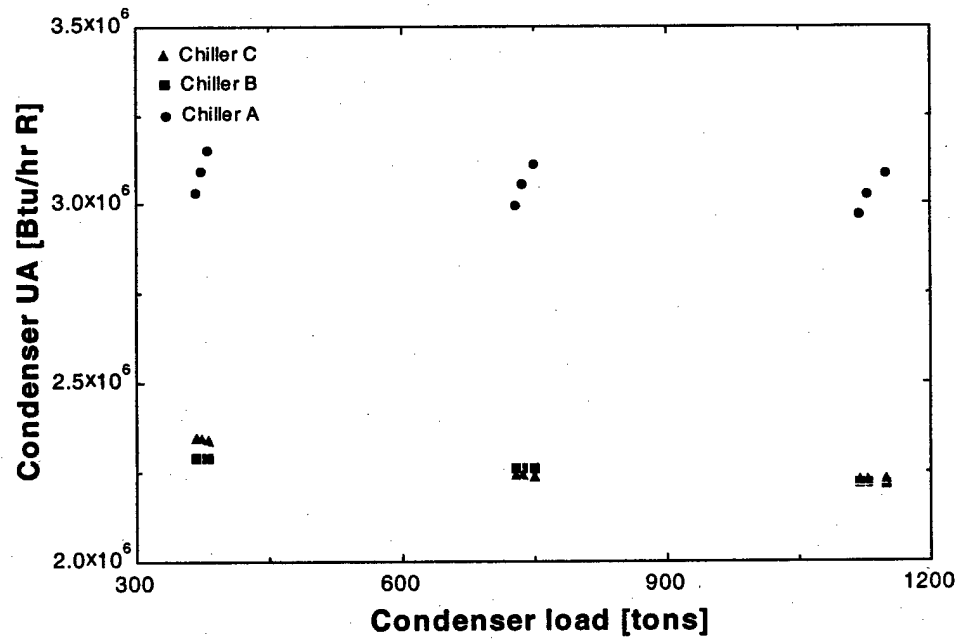


Figure 30. Condenser Performance Comparison

These figures indicate that chiller A's heat exchangers are significantly improved over the chillers used by Liu. The differences may include different tube surface treatments or larger heat exchangers. Both variations not only increase heat transfer but also could be expected to increase the chiller's first cost.

## 6. Performance Characteristics

The following discussion refers to the performance characteristics of chiller A. In order to appreciate chilled water system performance it is necessary to grasp how different conditions affect chiller operation. The figure below shows the effect that changing load has chiller efficiency.

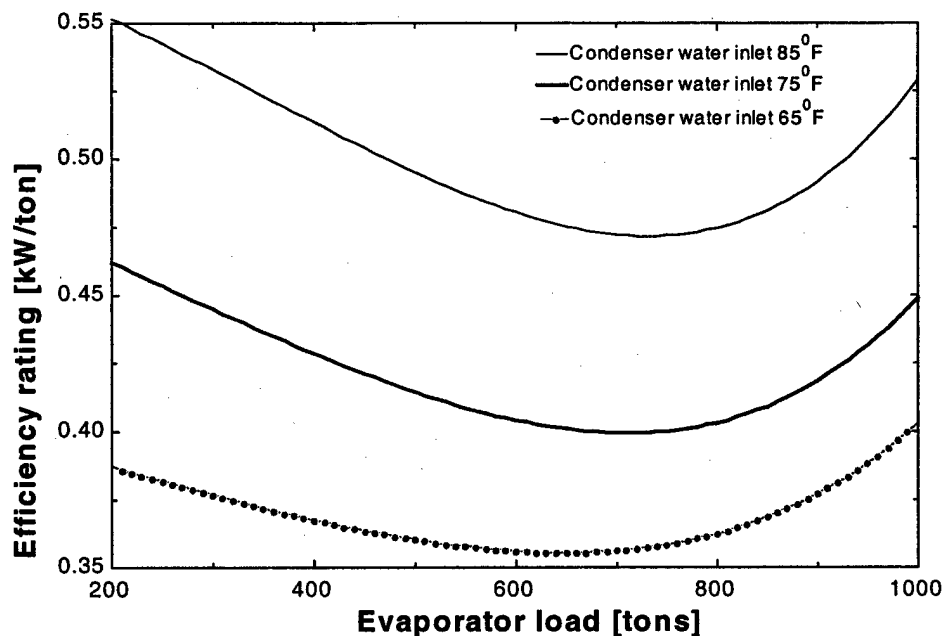
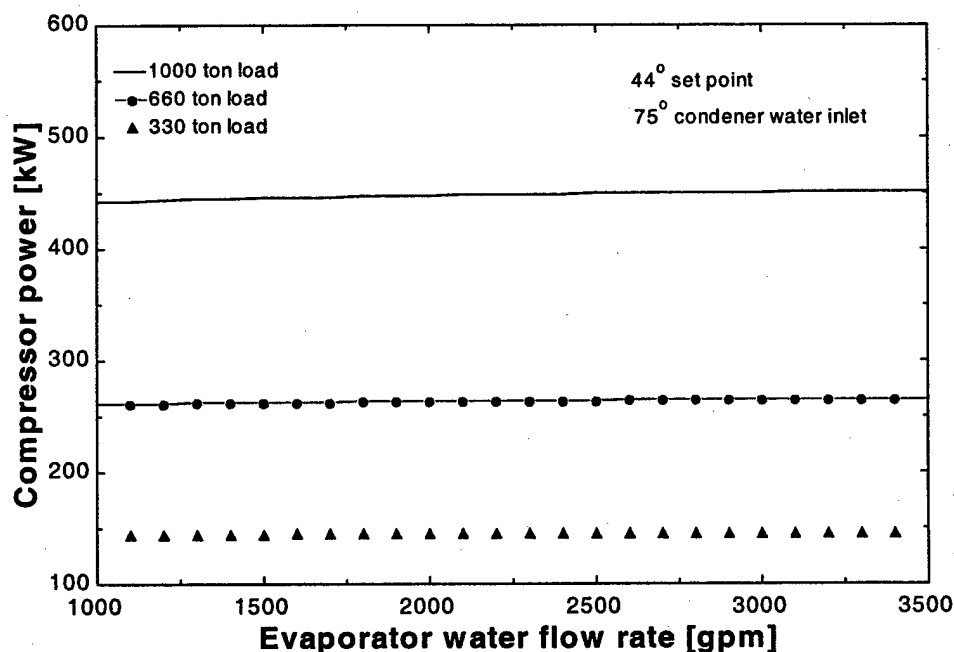


Figure 31. Chiller efficiency versus load

With high condenser water temperatures the chiller is most efficient at about 75% of maximum load. As the condensing water temperature is decreased the chiller becomes more efficient because compressor lift is reduced. Additionally, the chiller's best efficiency point shifts to lower loads as condenser temperature decreases. At a 65°F condenser inlet temperature the best efficiency is down to about 65%.

Increasing flow rate through the evaporator at fixed load has two different affects. First, the evaporator UA increases which tends to increase heat transfer rate. Meanwhile, at a fixed chilled water exit set point, the LMTD between the water and refrigerant is decreased. This tends to decrease the heat transfer rate. George Redden (1996) studied this phenomenon to determine variable flow effects on chiller performance. This was accomplished by modeling and bench testing a 225 ton capacity centrifugal chiller. In one case the evaporator flow rate was fixed while the load was varied. In another case the flow rate was varied proportional to the desired load reduction. Comparisons were made data at 71%, 45% and 25% load conditions. Similar chiller efficiencies were attained by either varying flow rate or inlet temperature. In fact the variable and constant flow results agreed to within 1% of one another. Redden's work concluded that varying evaporator water flow rate has little effect on chiller performance.



**Figure 32. Effect of variable flow on chiller performance**

Figure 32 shows that varying flow rate at a constant load has very little affect on this model's performance, as well. If the flow is kept within acceptable bounds, the chiller efficiency is a function only of load and lift. For this study's purpose maximum and minimum evaporator water velocities are taken to be three and 11 ft/sec respectively (Eppelheimer, 1996). These values agree with manufacturer's data. The

minimum flow rate is set to prevent laminar flow in the evaporator. Transition to laminar flow would significantly hinder water-side heat transfer coefficient. A velocity of three ft/sec corresponds to a Reynolds number of about 15,000, which is turbulent assuming the tube bundle is composed of rough pipes. The maximum flow limit is imposed to prevent tube bundle erosion. Operation with velocities in excess of 11 ft/sec also significantly increases evaporator head. The increased pressure drop can erode the tubes inner surfaces, shortening chiller life.

Another important characteristic of chiller performance is the effect that set point has on efficiency. If one increases the set point with a fixed load, the compressor lift is reduced. This, in turn, decreases the power requirement. Figure 33 how a chillers efficiency increases as the chiller set point is raised. This figure depicts a the chiller's efficiency rating in kW/ton while operating at 1000 tons.

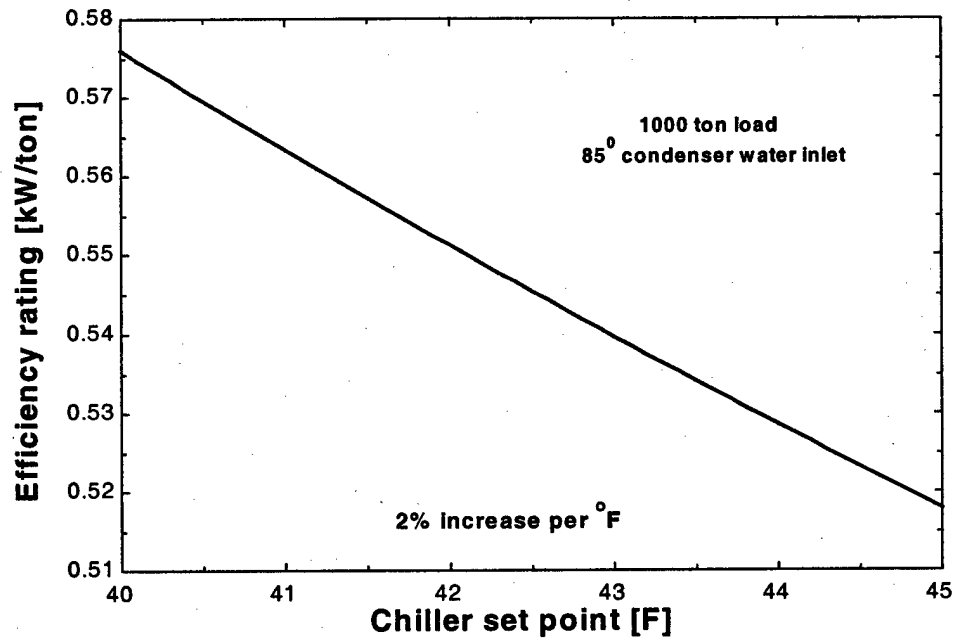


Figure 33. Efficiency versus set point

### **Pump Model**

Pumps for all models were selected using curves found in pump selection software (Goulds, 1995). An effort was made to ensure all pumps had similar best efficiency points (BEPs). For example, the best pump available for use as the secondary pump in a primary/secondary system, had a 83% BEP. As a result, a variable speed primary pump with a 83% BEP was selected for the single loop system even though more efficient options were available. Pumps were selected by first determining the flow rate and head required under the conditions of greatest annual system energy consumption. Pumps with an 83% BEP at this head and flow rate were chosen. Next, the maximum system flow rate and head were determined. All selected pumps were required to meet these maximum values. For example, the maximum flow required by the system may be 2800 gpm, however it operates most often at 2200 gpm. Thus, the selected pump would have a best efficiency point of 83% at 2200 gpm and may have an efficiency as low as 76% at maximum conditions.

#### **1. Constant Speed Pumping**

When constant speed pumps are used, the air handlers dictate system water flow rate. Pump head is a function of the flow rate, and the air handler's two-way valves modulate to accommodate the fluctuating head. Figure 34 shows how the system head is forced to increase as flow decreases.

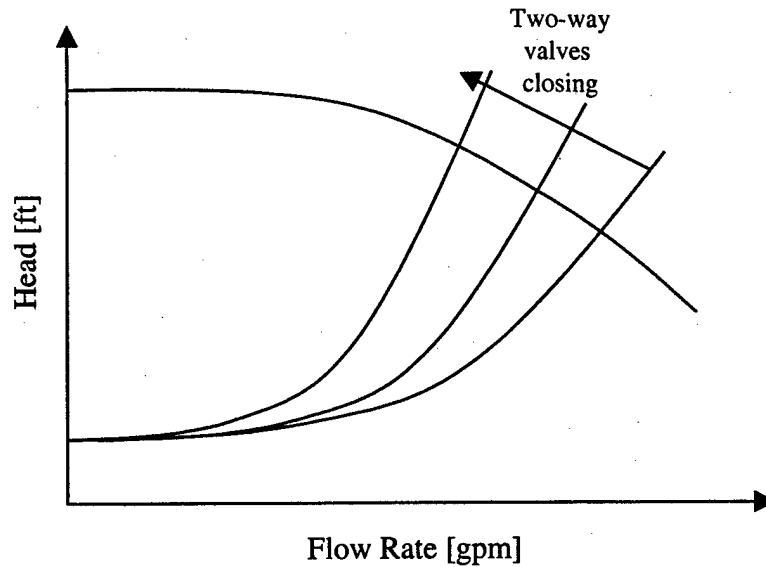


Figure 34. Centrifugal Pump and System Curves

Three separate pump equations are used to model constant speed pumps. These equations determine, pump head, efficiency and shaft power, all as a function of flow rate.

$$Head_{pump} = A_{head} + B_{head} \cdot GPM + C_{head} \cdot GPM^2 \quad \text{Equation 52}$$

$$\eta_{pump} = A_{\eta} + B_{\eta} \cdot GPM + C_{\eta} \cdot GPM^2 \quad \text{Equation 53}$$

$$W_{shaft} = A_{bhp} + B_{bhp} \cdot GPM \quad \text{Equation 54}$$

Here the constants in each equation are chosen to describe the particular pump. These values are given in the tables below.

	Head	eta	bhp
A	71.4	0.036	71600
B	0.0154	7.33E-04	16.9
C	-8.46E-06	-1.70E-07	N/A

Table 11. Single loop, constant speed, primary pump

	Head	eta	bhp
A	103	0.0859	94000
B	0.0105	5.97E-04	31.8
C	-6.31E-06	-1.20E-07	N/A

**Table 12. Primary-secondary system, constant speed, secondary pump**

Here the pump head and pump shaft power have units of feet and Btu/hr respectively. In order to find the total power required, the pump shaft power is divided by the constant motor efficiency, taken as 90%. This gives the relation for the total pumping power requirement.

$$\dot{W}_{pump} = \frac{\dot{W}_{shaft}}{\eta_{motor}} \quad \text{Equation 55}$$

Since the pressure at the pump exit is determined by equation 52 only one other quantity is needed to fix the pump exit state. The enthalpy is chosen and is determined by:

$$h_{w,out} = \frac{\dot{W}_{shaft}}{\dot{m}_w} + h_{w,in} \quad \text{Equation 56}$$

## 2. Variable Speed Pumping

When variable speed pumps are used, the air handler dictates flow rate. System head changes with flow rate. The pump speed is controlled by a pressure sensor in a remote air handler. The pump speed is adjusted to keep this differential pressure between the chilled water coil inlet and exit constant. Even though this distant chilled water coil's pressure drop is constant, the pump head varies. This is because there are other components that contribute to the total system head. These include piping, tube bends and evaporator head losses. As a result, the pump operates at the speed which allows it to maintain the flow rate and head determined by the system. Figure 35 describes a variable speed pump under normal operating conditions.

A pump is selected to operate most efficiently at some specific flow rate and head. These conditions are defined as the pump's best efficiency point. This point is labeled as 1 in the figure. If the air handler requires more flow the pump speed increases, pumping more water. The pump head increases and the pump operates at a new point, 1'. On the other hand, if the air handler requires less flow, the pump will slow, diminishing the pump head. In this case the new operating point is denoted by 1''.

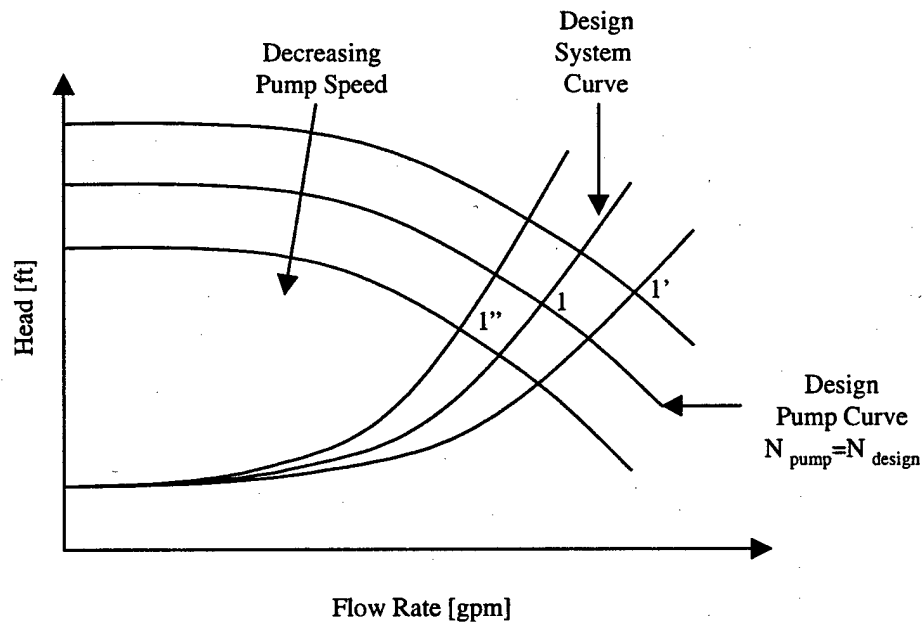


**Figure 35. Effects of Changing Speed on the Pump Curve**

In order to determine the pump operating characteristics two equations are needed. The first determines the head as a function of flow rate when the pump is operating at its design speed. This design speed is chosen for the condition that the pump will operate most frequently. This equation describes a curve called the design pump curve (DPC). The second equation describes pump efficiency as a function of flow rate when operating at design speed. This equation describes the curve called the design efficiency curve shown below.

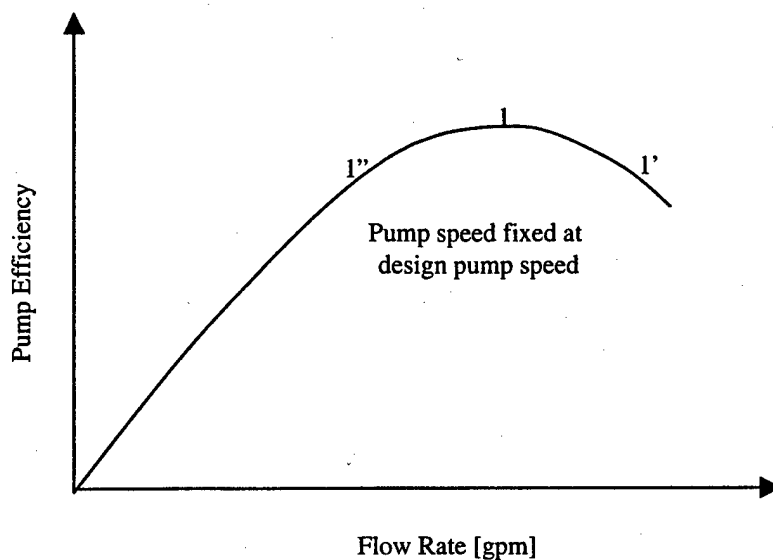


**Figure 36. Design efficiency curve**

However, the pump may not be operating at the design speed. Therefore it is first necessary to determine the actual speed of the pump. This is done by use of the affinity laws.

$$N_{actual} = \left( \frac{GPM_{actual}}{GPM_{DPC}} \right) N_{design} \quad \text{Equation 57}$$

In this equation, the term  $GPM_{DPC}$  and  $N_{design}$  are the flow rate and speed of the pump when operating on the design pump curve. The corresponding design pump curve head is also found using an affinity relation.

$$Head_{DPC} = \left( \frac{N_{design}}{N_{actual}} \right)^2 Head_{actual} \quad \text{Equation 58}$$

The design pump curve head and efficiency are known as a function of the design curve flow rate given by two equations.

$$\eta_{DPC} = A_{\eta} + B_{\eta} \cdot GPM_{DPC} + C_{\eta} \cdot GPM_{DPC}^2 \quad \text{Equation 59}$$

$$Head_{DPC} = A_{head} + B_{head} \cdot GPM_{DPC} + C_{head} \cdot GPM_{DPC}^2 \quad \text{Equation 60}$$

The constants in these equations are chosen to describe a particular pump. These values are displayed in the tables below.

	Head	eta
A	103	0.0859
B	0.0105	5.97E-04
C	-6.31E-06	-1.20E-07

**Table 13. Single loop, variable speed, primary pump**

	Head	eta
A	71.4	0.036
B	0.0154	7.33E-04
C	-8.46E-06	-1.70E-07

**Table 14. Primary-secondary system, variable speed, secondary pump**

The four preceding equations can be used to define the pump's operating conditions. However, actual pump efficiency decreases as pump speed is reduced. This reduction in efficiency is small when the pump is operating within 45% of its design speed. At slower speeds the efficiency starts to diminish more rapidly (Rishel, 1996). The actual efficiency is determined using a relation taking the form

$$\eta_{pump} = \eta_{DPC} \cdot f\left(\frac{N_{actual}}{N_{design}}\right) \quad \text{Equation 61}$$

where:

$$f\left(\frac{N_{actual}}{N_{design}}\right) = 0.815 + 0.403 \cdot \left(\frac{N_{actual}}{N_{design}}\right) - 0.218 \left(\frac{N_{actual}}{N_{design}}\right)^2 \quad \text{Equation 62}$$

The exit conditions are then determined by equation 60.

$$h_{w,out} = \left( \frac{h_{w,out,rev} - h_{w,in}}{\eta_{pump}} \right) + h_{w,in} \quad \text{Equation 63}$$

The total pumping power is calculated using:

$$\dot{W}_{pump} = \frac{\dot{m}_w (h_{w,out} - h_{w,in})}{\eta_{motor/vsd}} \quad \text{Equation 64}$$

where the term  $\eta_{motor/vsd}$  is assumed to be a function of speed. It is a combination of motor and variable speed drive efficiency. This hardware is selected to operate most efficiently at the BEP and will perform less efficiently at greater or lesser speeds. The expression for this combined efficiency is taken from Joyce (1990).

$$\eta_{motor/vsd} = 0.0498 + 1.85 \left( \frac{N_{actual}}{N_{design}} \right) - 1.03 \left( \frac{N_{actual}}{N_{design}} \right)^2 \quad \text{Equation 65}$$

The motor and variable speed drive efficiency is shown in Figure 37.

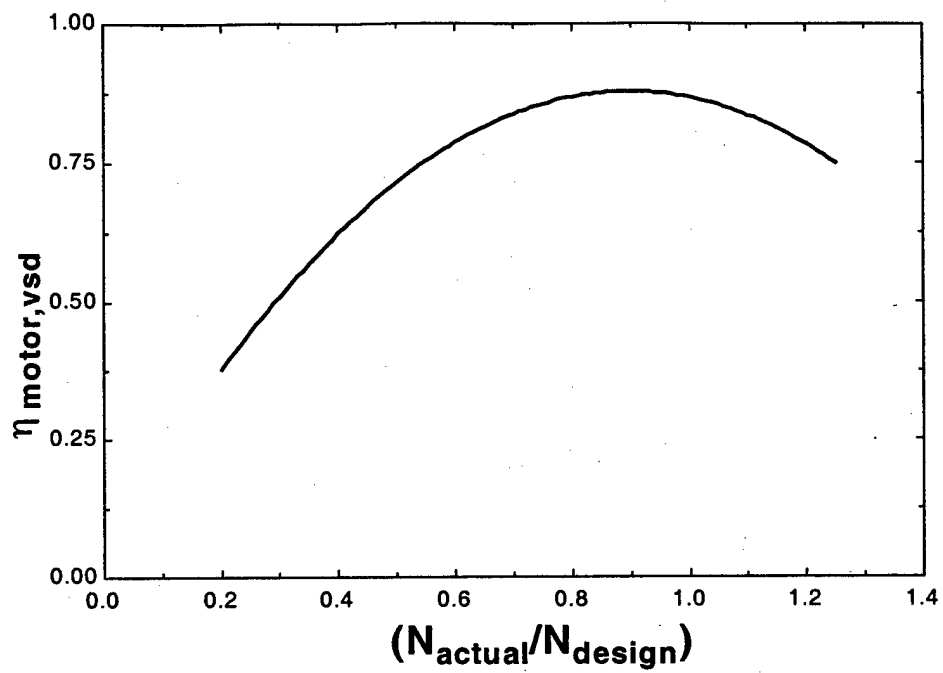


Figure 37. Motor and Variable Speed Drive Efficiency versus Pump Speed

### Cooling Tower Model

It was necessary to include a cooling tower as a component of the system, because cooling tower operation dictates condenser water inlet temperature, which affects compressor lift. As a result, the ambient weather conditions affect system performance through the cooling tower as well as air handlers.

The cooling tower used in this study was adapted from the model developed by Weber(1988). However, it includes the counterflow NTU-effectiveness model developed by Braun(1988) then used by Liu (1997) and Lilly(1998). The reader should consult these works for the complete development of the mass, energy and diffusion equations used to model the cooling tower.

The following assumptions were made in modeling the cooling tower:

- 1) Heat and mass transfer only in the direction normal to water and air flow.
- 2) Heat and mass transfer through the tower walls to the environment are negligible.
- 3) Constant air and water specific heats for a given operational situation.
- 4) Heat transfer from the tower fans to the air is negligible.
- 5) Uniform temperature throughout the water stream in any cross section normal to the flow.
- 6) Uniform tower cross sectional area.

Using steady state energy and mass balances on a differential control volume, Braun developed three differential equations. The first of these is derived from an energy balance on the water stream.

$$\dot{m}_{w,in} C_w \frac{dT_w}{dV} - \dot{m}_a (\omega_{a,out} - \omega_a) C_w \frac{dT_w}{dV} + \dot{m}_a C_w (T_w - T_{ref}) \frac{d\omega_a}{dV} = \dot{m}_a \frac{dh_a}{dV} \text{ Equation 66}$$

The next equation is taken from an energy balance on the air stream.

$$\frac{dh_a}{dV} - \frac{Le \cdot NTU}{V_T} \left[ (h_a - h_{s,w}) + (\omega_a - \omega_{s,w}) \left( \frac{1}{Le} - 1 \right) h_{ref,w} \right] \text{ Equation 67}$$

The third equation is derived from an overall mass balance,

$$\frac{dh_a}{dV} - \frac{Le \cdot NTU}{V_T} \left[ (h_a - h_{s,w}) + (\omega_a - \omega_{s,w}) \left( \frac{1}{Le} - 1 \right) h_{ref,w} \right] \quad \text{Equation 68}$$

where:

$$Le = \frac{h}{h_D C p_a} \quad \text{Equation 69}$$

$$NTU = \frac{h_D A_V V_T}{\dot{m}_a} \quad \text{Equation 70}$$

Given the inlet conditions equations 63, 64 and 65 can be solved for the water stream exit condition. This solution requires integration over the entire tower volume from inlet to exit. The process is simplified using Merkel's assumptions. Merkel neglects the effect the water loss due to evaporation on water flow rate and sets the Lewis number equal to unity. Equations 63 and 64 reduce to equation 68.

$$\frac{dT_w}{dV} = \frac{\dot{m}_a}{\dot{m}_w C_w} \left( \frac{dh_a}{dV} \right) \quad \text{Equation 71}$$

$$\frac{dh_a}{dV} = -\frac{NTU}{V_T} (h_a - h_{s,w}) \quad \text{Equation 72}$$

Braun then introduced a saturation specific heat,  $C_s$ . The saturation specific heat is the derivative of saturation air enthalpy with respect to the air temperature at the air/water interface. At this interface the temperature is assumed equal to the water temperature. So  $C_s$  is defined as,

$$C_s = \left[ \frac{dh_s}{dT} \right]_{T=T_w}$$

Equation 73

Equation 71 may then be expressed in terms of air enthalpies.

$$\frac{dh_{s,w}}{dV} = \frac{\dot{m}_a C_s}{\dot{m}_w C_w} \left( \frac{dh_a}{dV} \right)$$

Equation 74

The exit conditions can be analyzed using equations 69 and 71, assuming that the saturated air-water vapor enthalpy is a linear function of temperature. In other words the saturation specific heat,  $C_s$ , is assumed to be uniform throughout the tower.

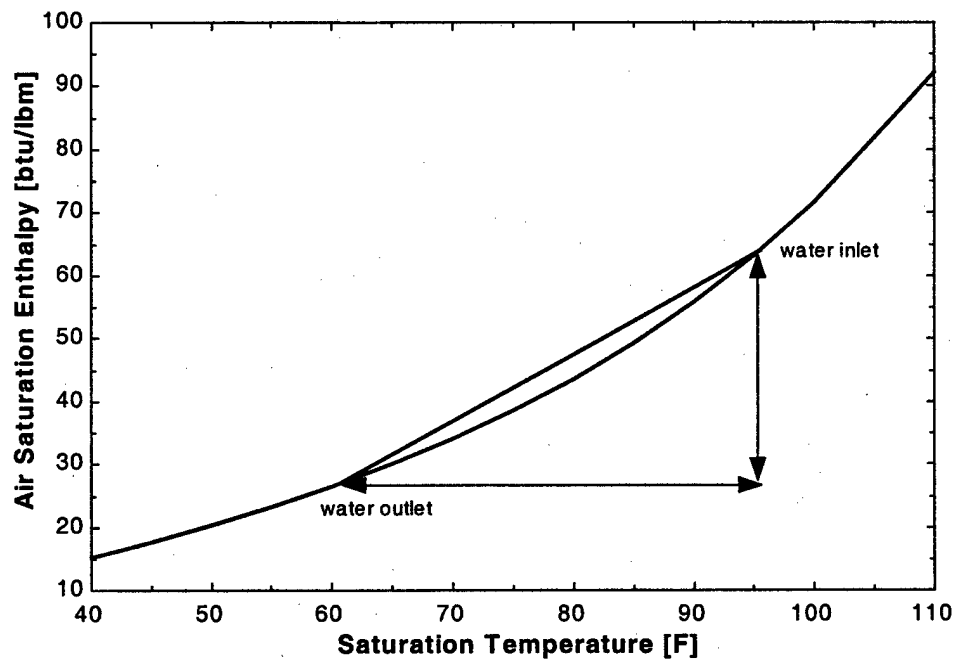


Figure 38. Defining a Linear Saturation Enthalpy

Figure 38 depicts how the saturation enthalpy varies with the saturation temperature. It is obvious that the saturation enthalpy does not vary linearly with temperature. Although, by choosing an appropriate average

slope between the inlet and outlet conditions, as seen in the figure, an effective relationship is found in terms of  $C_s$ .

$$C_s = \frac{h_{s,w,in} - h_{s,w,out}}{T_{w,in} - T_{w,out}} \quad \text{Equation 75}$$

The air-side effectiveness is defined as the ratio of the actual heat transfer to the maximum heat transfer possible if the exiting air stream were saturated at the incoming water temperature. The actual heat transfer in terms of the effectiveness is,

$$\dot{Q} = \varepsilon_a \dot{m}_a (h_{s,w,in} - h_{a,in}) \quad \text{Equation 76}$$

where the air-side effectiveness is found by using the common counter-flow heat exchanger relation.

$$\varepsilon_a = \frac{1 - \exp[-NTU(1 - C_r)]}{1 - C_r \exp[-NTU(1 - C_r)]} \quad \text{Equation 77}$$

Here  $C_r$  is the heat capacity ratio, given by equation 13.

$$C_r = \frac{\dot{m}_a C_s}{\dot{m}_{w,i} C_w} \quad \text{Equation 78}$$

The outlet water enthalpy is then be determined by performing an overall energy balance.

$$\dot{Q} = \dot{m}_w (h_{w,in} - h_{w,out}) \quad \text{Equation 79}$$

## 1. Cooling Tower NTU Calculation

The cooling tower NTU is given by the equation developed by Lowe and Christie (1960).

$$NTU = c \left[ \frac{m_w}{m_a} \right]^{1+n} \quad \text{Equation 80}$$

In this expression  $c$  and  $n$  constants, specific to a particular tower cooling box geometry. Manufacturers offer towers that have many different box sizes, each having its own cooling capacity. To calculate the coefficients and verify model accuracy, Liu (1997) correlated manufacturer's data for a number of box sizes. Manufacturer's data gives tower outlet water temperature for specified water and air flow rates. The reader should consult Liu's work for a complete development. The cooling tower box size used in this study is given below (Lilly, 1998):

Length	Width	Height
13' 11 1/8"	24' 1/2"	18' 7 5/8"

Table 15. Tower box geometry

## 2. Cooling Tower Fan Model

Many different fan motors are available for each box size. A manufacturer typically gives the fan shaft power for each air flow rate specified with a particular box size. Liu shows the relationship between fan horsepower and air flow rate. He also provides curve fits for each box size used in the tower model to translate the flow rate into fan power. The equation for fan horsepower is (Liu 1997):

$$hp = EXP \left( -A + \left( \frac{\ln(cfm) - 10.5}{2} \right) B \right) \quad \text{Equation 81}$$

where  $A$  and  $B$  are constants which correspond to a specific box size and  $cfm$  is the air flow rate in cubic feet per minute. In this study values for  $A$  and  $B$  were taken to be 2.31 and 6.38 respectively (Lilly, 1998).

In order to maintain a minimum condenser water inlet set point fans are assumed to be turned on and off as appropriate. A 70° F tower minimum set point was used in this study, which means that fans run continuously when the tower exit water temperature exceeds 70° F. When the water temperature is equal to

70° F, the fans are cycled on and off to maintain that temperature. The ratio of time that the fans are in use is called the fan duty. Additionally, it was assumed that heat transfer from the tower with fans off usage is 10% of the heat transfer attained with all fans on. The fan power was then found by multiplying the fan horsepower by the fan duty.

### Piping Model

The component models detailed above were combined to form system models. In order to combine models all pipe flow was considered at constant enthalpy. Pipe head was determined using the relation:

$$Head_{pipe} = \frac{\Delta P_{pipe}}{\rho_w g} + \Delta Z \quad \text{Equation 82}$$

where,

$$\Delta P_{pipe} = \frac{f_t L_t}{D_i} \left( \frac{1}{2} \rho_w V_w^2 \right) \quad \text{Equation 83}$$

the friction factor was found using the equation (White, 1986):

$$\frac{1}{f_t^{1/2}} = -1.8 \cdot \log \left[ \frac{6.9}{Re_{D_i}} + \left( \frac{\epsilon_t / D_i}{3.7} \right)^{1.11} \right] \quad \text{Equation 84}$$

Where  $Re_{D_i}$  is the Reynolds number based on the tube inner diameter,  $\epsilon_t$  is the tube roughness and  $D_i$  is the inner diameter. The roughness was assumed to be 0.00015 ft. A tube diameter was chosen such that the water velocity at design conditions approximately 10 ft/sec. As a result, all single chiller systems have pipes with 10" inner diameters while multiple chiller system piping has 13" inner diameters. This 10 ft/sec value is a common rule for office building design, where little growth is anticipated. Industrial applications normally use a lower value, typically as low as 7.5 ft/sec. This allows for growth without additional piping.

A 10 ft/sec water velocity will result in head losses close to 3 feet per 100 feet of pipe. The primary loop of each primary-secondary system has 500 equivalent pipe feet. This length accounts for the

elbows and fittings as well as the actual pipe. Thus, at design conditions, the primary loop head is approximately 35 feet. This accounts for 15 of pipe head and a 20 foot evaporator head. The secondary loop is 1500 equivalent feet. A differential pressure sensor across a distant air handler maintains a constant 20 foot head across its chilled water coil and two-way valve. As a result, the secondary loop head is 65 feet at design load. Finally, the single loop system is assumed to have 2000 equivalent feet of piping. Therefore, the chilled water loop head is 100 feet at design conditions. This value represents 20 feet from the evaporator, 20 feet from the air handler and the remaining 60 feet comes from pipe losses. All air handlers are assumed to be at the same elevation as the chiller. The condenser loop is assumed to be 500 feet long. The cooling tower is elevated 200 feet above the chiller. The cooling tower is assumed to be elevated because these towers are normally placed on roofs of large office buildings. These lengths were imposed to add realism to the system models. However, the actual lengths make little difference in the comparative results found in the study.

## CHAPTER III

### OPERATIONAL STRATEGIES

An effort has been made to ensure the system designs compared in this study use control strategies common throughout the HVAC industry. Additionally, similar strategies were employed in all designs which were compared with one another. The only difference between design pairs was bypass inclusion or omission. This was done in order to highlight only how the bypass loop affects system performance. The control strategies employed were not optimized because ideal operation will differ in each case. Instead each model was controlled consistent with current industry methods. In order to analyze system results, an understanding of the different methods is vital.

#### **Chilled Water Reset**

A common chilled water plant practice is to raise the centrifugal chiller's set point as the facility's cooling load drops. This is referred to as chilled water reset. It is believed to be an inexpensive energy savings method (Erth, 1987). By increasing the chilled water supply temperature the compressor lift is attenuated. Since compressor power is a function of load and lift, decreasing the lift while maintaining a constant cooling load reduces the power requirement. When the chiller set point is raised, the air handler's inlet water temperature is increased as well. This decreases the air handler's air to water LMTD. In order to maintain a similar heat transfer rate the coil's UA must increase. This may only be done by increasing the water and air velocities. This translates to an increased fan and pump power. Recent studies have shown the chiller to be the chilled water system's largest energy consumer. The chiller is responsible for approximately 62% of the energy, while fans and pumps account for only 38% (Eppelheimer, 1996).

Reset was employed in this study by increasing the chiller set point and as the outdoor temperature decreases in order to fix the system flow rate. This strategy is initiated only when the outdoor temperature falls below a prescribed level. Initially, air handlers control water flow rate by modulating two-way valves in order to maintain a 58°F cold deck temperature. Once the prescribed outdoor temperature is reached, the

system flow rate is fixed and chiller set point is raised to maintain the deck temperature. In reality this ideal control is not possible. Outdoor temperature affects various building zones differently. As a result, air handler cold deck temperatures fluctuate differently depending on location. In practice, the chiller set point is increased incrementally as outdoor temperature drops. For example, the set point may be raised one degree when the outdoor temperature reaches 55°F and then another degree at 50°F. Figure 39 shows this strategy as employed in this research. Here, Atlanta weather data was used where design conditions are 95°F dry bulb and 78°F wet bulb. The chiller set point was increased starting at an outdoor temperature of 74°F and water velocity in the evaporator was fixed at the minimum three ft/sec.

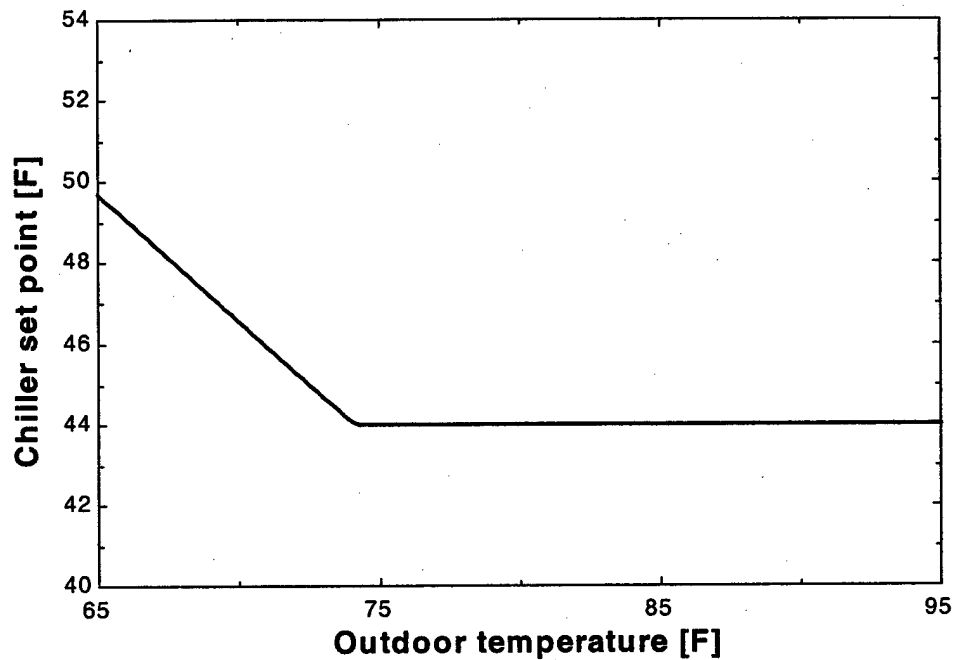


Figure 39. Chilled water reset

One can see the chilled water supply temperature is held at a constant 44°F until the outdoor temperature reaches 74°F. The chilled water set point then increases inversely with cooling load.

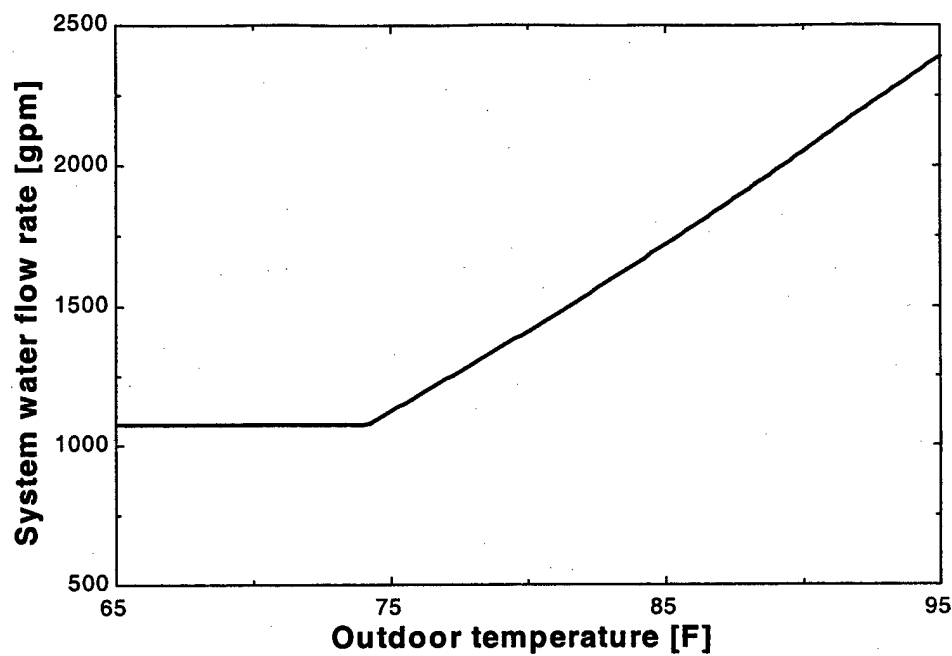


Figure 40. Flow rate variation with reset

Figure 40 represents the system flow rate response to this procedure. At large loads the system flow rate decreases with load. However, after reset is employed the system flow rate is fixed.

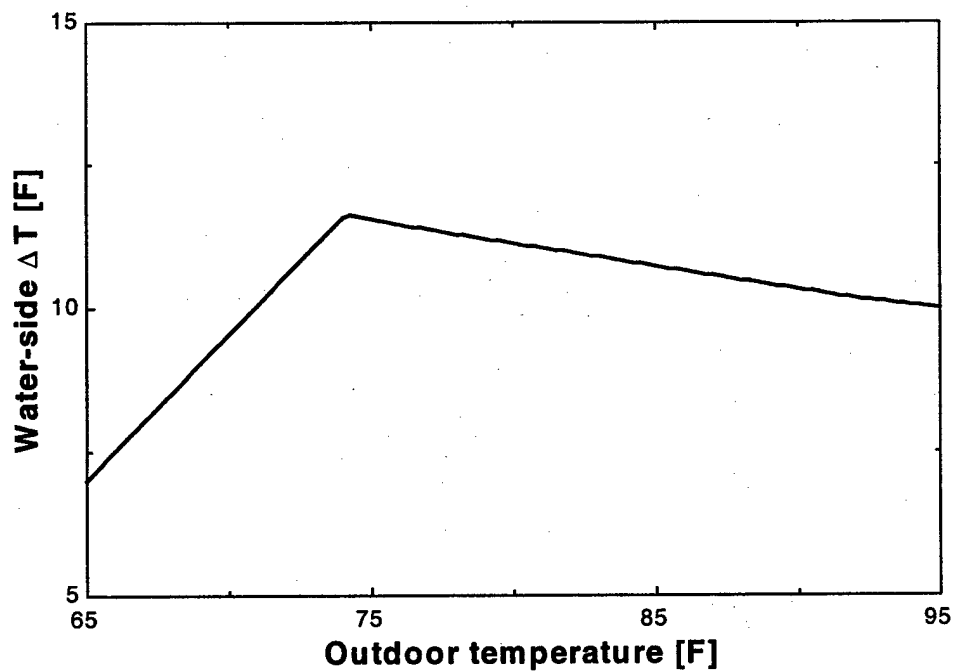


Figure 41. System  $\Delta T$  response to reset

Figure 41 depicts the manner in which chilled water  $\Delta T$  is affected by reset. At design load the temperature difference between the air handler water inlet and exit is  $10^{\circ}\text{F}$ . As the load is reduced the temperature difference increases. This trend continues until the reset condition is reached, at which point the water flow rate is fixed, but the cooling load requirement continues to decline with outdoor temperature. As a result temperature difference across the water-side of the air handler starts to decrease. The temperature difference after reset decreases because the amount of heat being carried away by this constant stream is reduced.

Chilled water reset was used in all systems analyzed in this study. The technique was not optimized because the results would only apply to a particular design and be of no great worth to the industry. Instead, reset was employed to ensure the evaporator water velocity in single loop systems stayed within manufacturer's limits. The same reset conditions were applied to all single loop/primary-secondary system design comparisons. In each case the application of reset improved annual system efficiency.

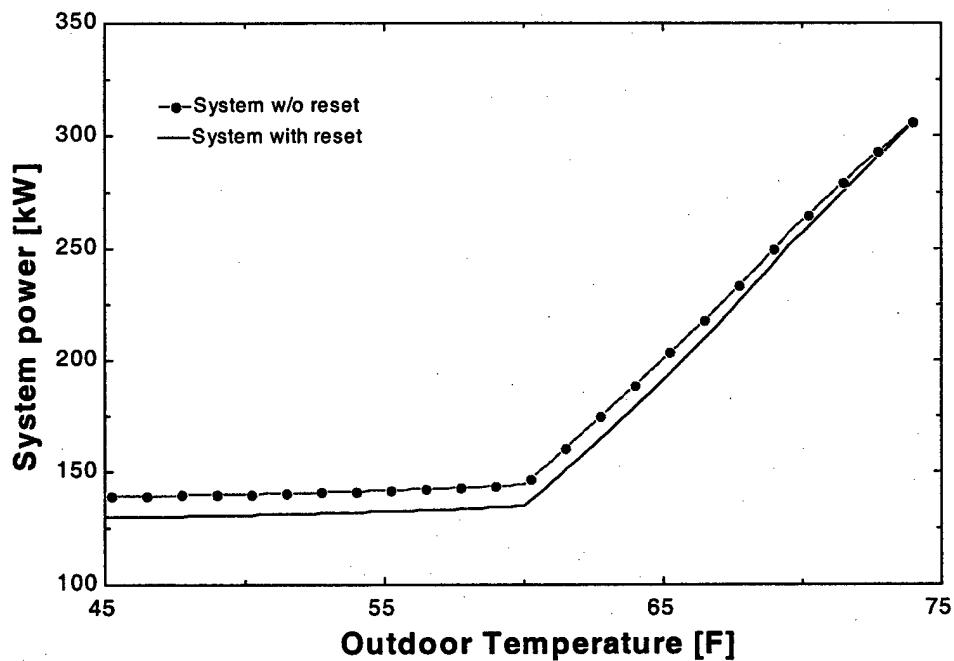


Figure 42. Energy savings resulting from reset

Figure 42 describes the total power requirement for a primary-secondary system. The lower curve is the power required for the system using reset while the upper curve is the power required by the system

without reset. At small loads chilled water reset can result in a 19% energy savings. Chilled water reset is required in some single loop systems to meet the minimum evaporator flow requirements, however this should not be viewed as a deficiency. Reset should be used in any chilled water system in the interest of efficiency. As a result, the use of this strategy is commonplace in industry today.

### **Tower minimum set point**

Most facilities attempt to save tower fan power by imposing a minimum tower set point. When the tower exit water exceeds this temperature, all tower fans run continuously. As the water drops to the set point, the tower fans are cycled to maintain the set point. For example, if a tower has five fans it will run only the fans required to maintain the set point. In order to extend the tower fans' lives, a lead/lag fan rotation is imposed. If water temperature continues to fall eventually all fans are turned off. Tower minimum set point has two advantages. The first is a trade off, as is the chilled water reset procedure. The tower set point dictates the condenser inlet temperature. Thus, when the tower set point is increased the compressor lift is raised as well. This reduces the chiller efficiency, but this is offset by diminished tower fan power requirements. Tower minimum set point also lengthens chiller life. When condenser inlet temperature is too low, the compressor lift becomes small. Compressors are not designed to operate with small lifts and this use may damage them. Liu (1997) found the optimum tower set point to be between 65°F and 68°F. Joyce (1990) recommends a set point of 80°F. The optimal set point is largely a function of the system design and component performance.

For the purposes of this study, 70°F was used as a set point. A fan duty is determined. Fan duty is the percentage of time the fans are operational. For example, if three of the five fans are running the fan duty is 0.6. The fan power requirement is then found by multiplying the fan duty by the power required when all fans are on. Additionally, it was assumed that the tower heat transfer rate without fans is 10% the rate with all fans running.

## Free Cooling

Many chiller plants shut down all chillers when the outdoor temperature falls below some designated level. At this point, the heat is transported to the outdoor air by a more direct path, free cooling. Free cooling is divided into two methods, air-side and water-side.

Air-side free cooling meets the required cooling load by circulating outside air directly into a building. When this method is used all chillers and pumps sit idle. The only power requirement is fan power needed to blow the air into ventilation ducts. This technique is applicable when temperatures fall below about 55°F. These factors make this a very efficient method. Nonetheless, its use is uncommon in large facilities. Normally, at low outdoor temperatures only internal zones require cooling. Circulating air to these areas requires a ventilation shaft. The shaft is usually placed vertically down the center of the building and takes outdoor air from the roof. Building owners seldom approve this method because it is more cost effective for a building owner to lease the space that would be occupied by the shaft. These profits, typically, more than offset the additional energy cost required by other designs.

Water-side free cooling is a method by which outdoor air cools system water without chiller use. It is normally used when ambient temperatures fall below about 45°F. This type of free cooling may be completed directly or indirectly. Direct, water-side, free cooling is accomplished by taking chilled water and passing it directly from air handler to tower. The problem with this technique is that it causes the chilled water loop to be open to the atmosphere. Since direct, water-side, free cooling vents the chilled water vapor directly to the atmosphere, oxygen is dissolved by the water. This oxygen then causes corrosion in chilled water system components. Additionally, the use of additives in this design is prohibited because they may be vented to the atmosphere. These stipulations make direct water-side free cooling an unattractive option.

Indirect, water-side, free cooling keeps the evaporator and condenser streams separate. It does so by using an additional flat plate heat exchanger, an economizer. Its use requires additional pumping power on both the condenser and evaporator sides. The additional power results from economizer pressure drop.

However, this option maintains a closed chilled water system which reduces corrosion and waterside fouling.

For this study, it was assumed the free cooling energy required for a primary-secondary and single loop system is identical. As a result, energy expenditures are not compared for ambient temperatures below 45°F.

### **Multiple Chiller Scheduling**

Optimum chiller loading in multiple chiller plants is a point of discussion throughout the HVAC field. Most multiple chiller plants operate based on the widely accepted rule that optimum chiller loading is between 60% and 80% of full load. As a result, a lead chiller is rarely allowed to exceed 80% capacity. Austin (1991) conducted a study that disputes this strategy. He found that optimal scheduling may involve operating the lead chiller at loads as large as 100%, depending on system design. Much of the confusion regarding scheduling results from Air-Conditioning & Refrigeration Institute (ARI) standards, which are applicable only to single chiller facilities. Chiller efficiency curves are normally rated at ARI conditions. These curves are not adequate tools by which to formulate a scheduling procedure. ARI standards dictate a 85°F condenser inlet temperature at 100% load. The condenser inlet temperature is then reduced to 75°F at 75% load and further to 65° at 50% and 25% load. Figure 43 shows is the efficiency curve for the chiller used in this study rated with ARI conditions.

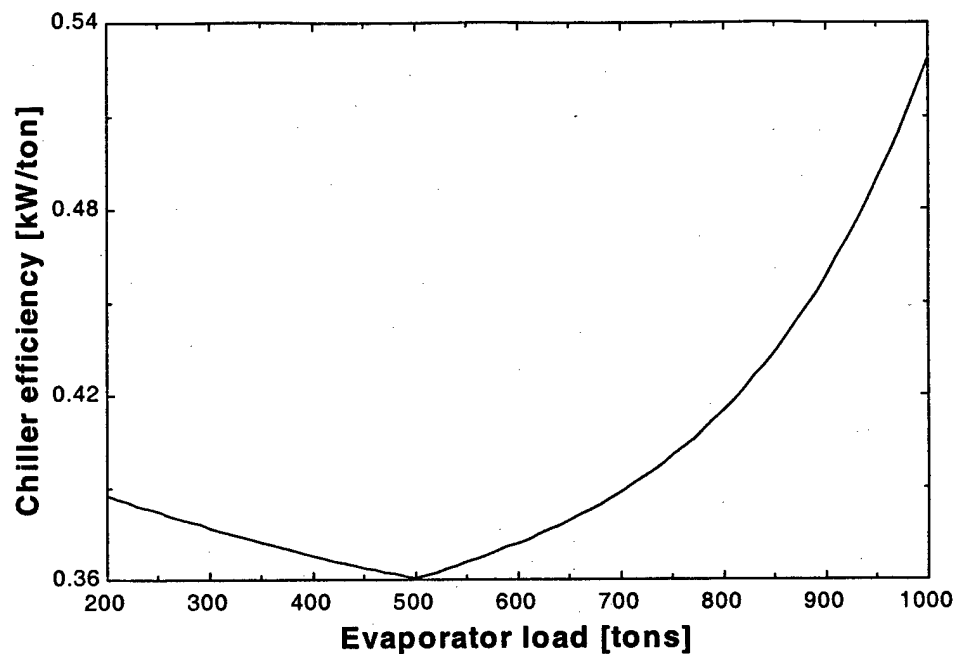


**Figure 43. ARI efficiency curve**

Inspection of this curve would lead one to believe that optimal scheduling would require energizing the lag chiller when the lead is only 65% loaded. Use of these standards is only applicable for single chiller system analysis. In multiple chiller plants condenser water inlet temperatures do not vary with load as they do in single chiller facilities. When focused on scheduling, it is more informative to know relative efficiencies at a constant condenser inlet temperature. Figure 44 is an efficiency curve for the same chiller at a constant 70°F condenser inlet temperature.

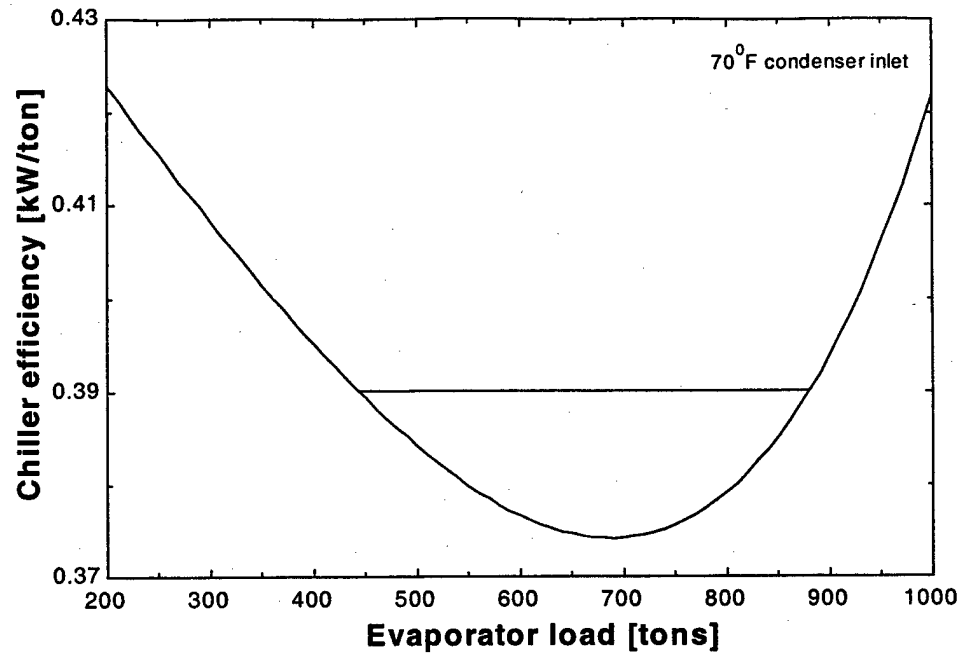


**Figure 44. Chiller efficiency curve with constant condenser inlet temperature**

This curve leads one to believe the optimal loading requires energizing a lag chiller when the load reaches 88% load. This conclusion is more reasonable but a more appropriate method still exists.

A lag chiller should be energized only when the total system energy requirement is decreased by doing so (Austin, 1991). In the case highlighted above, it is more efficient to operate two chillers at 45% load than one at 90%. However, one must consider the additional auxiliary power requirements associated with a lag chiller. Figure 45 shows a comparison of the total system power requirement for a system using one and two chillers. This figure shows that optimal chiller scheduling requires starting up the lag chiller when the outdoor temperature is about 73°F.

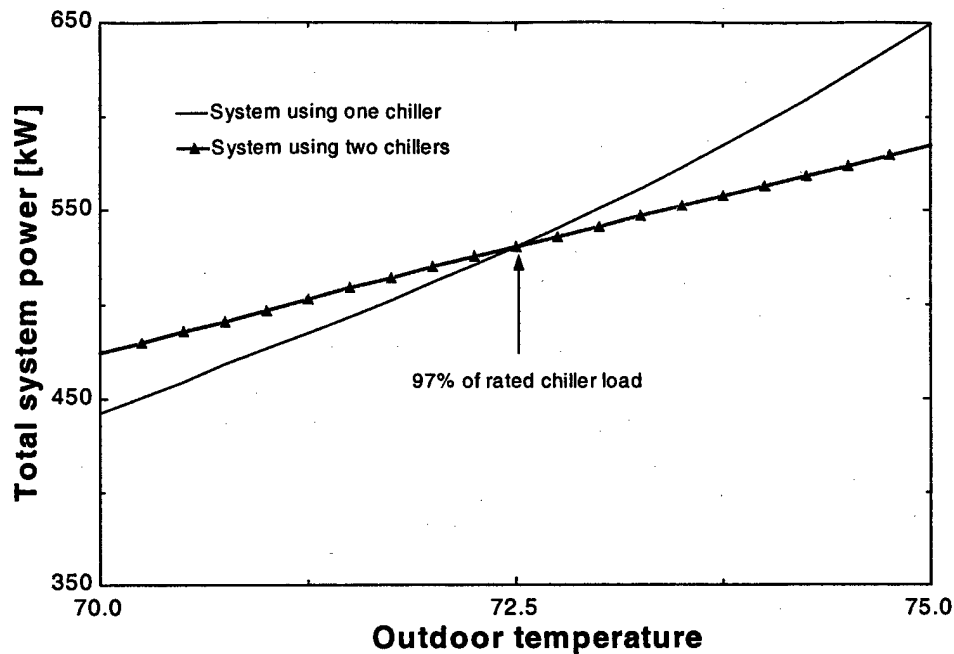
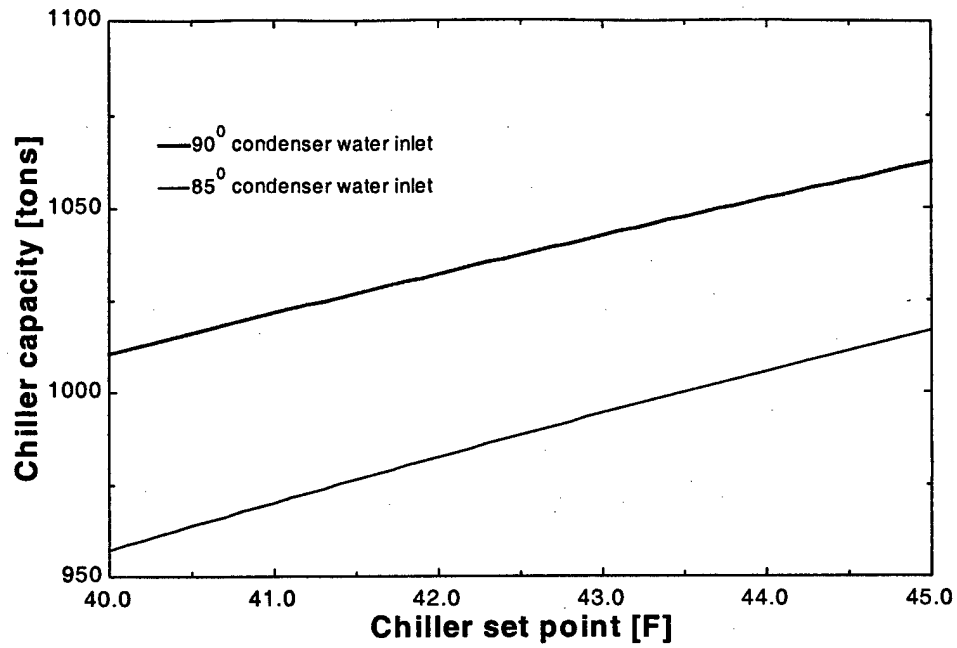


Figure 45. Chiller scheduling

This temperature corresponds to a load of 970 tons. Thus, in this situation optimal scheduling requires energizing the lag chiller when the lead is at about 97% of its rated load. Although this criteria differs depending on system design, and condenser water temperature.

### **Chilled Water Set Point Reduction**

Central plant operators often reduce chiller set point in an attempt to increase chilled water system capacity. This strategy not only fails to increase capacity, but also hurts efficiency. When the chiller set point is reduced the compressor lift is increased. This raises compressor power requirement. If a chiller is operating at maximum capacity lowering the set point decreases its capacity. Figure 46 represents the maximum capacity of the chiller as calculated by the system model using 588 kW as the maximum chiller motor power.



**Figure 46. Effect of reducing chiller set point**

Notice that this 1000 ton nominally rated chiller is able to deliver more than 1000 tons depending on the ambient conditions. This figure also verifies the trend that lowering the chiller set point reduces chiller capacity.

## CHAPTER IV

### DESIGN OPTIONS

Engineers have introduced some design changes to the typical primary-secondary system in an to minimize the problems associated with low chiller  $\Delta T$ . These changes are discussed below.

#### **Increasing Air Handler Capacity**

Typically, a facility is designed to deliver a 10°F chilled water temperature difference across the air handler at some specified design condition. In effect, the chilled water coil is sized to meet the design load while increasing the water temperature by 10°F. Increasing this temperature difference requires a larger chilled water coil. Engineers may design facilities to have excess capacity. This is done for a number of reasons. First, it is impossible to accurately calculate all the factors that contribute to the building load. Also, additional zones may be added to a particular air handler's load after construction is complete. Additionally, pumping power is reduced with the reduced flow rate. Over-sizing air handlers will compensate for some fouling, minimizing a possible low temperature differential problem. Finally, increasing the design  $\Delta T$  may raise a system's capacity. By decreasing secondary loop flow rate, bypass mixing in the chilled water supply is minimized. Furthermore, increasing chilled water coil size raises the UA.

Increasing design  $\Delta T$  has a down side as well. Doing so means purchasing and installing much larger air handlers. This raises the equipment's first cost as well as the space requirement.

#### **Check Valve**

Kirsner (1998) recommends another solution to prevent bypass mixing from chilled water return to supply. He proposes placing a check valve in the bypass preventing this flow. Including this valve allows primary loop flow to exceed secondary loop flow, but not the converse. The primary-secondary

system shown in Figure 47 operates normally when the secondary loop flow rate is less than or equal to the primary loop rate.

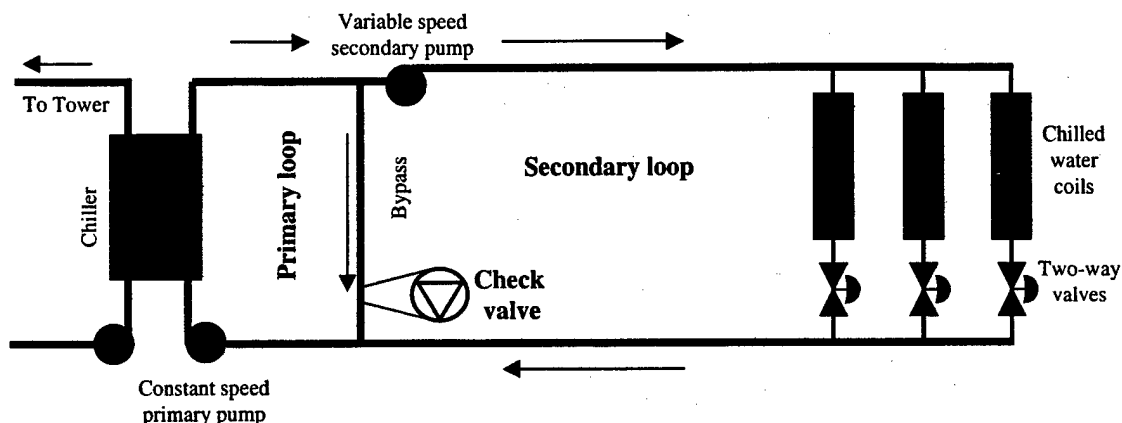


**Figure 47. Primary-secondary system with check valve**

As the load requirement increases from the design condition, the secondary flow rate increases. However, the check valve prevents secondary flow from exceeding primary flow. As a result, both primary and secondary flow rates increase together. The problem with this arrangement, in relation to a single loop design, is that it maintains a constant evaporator water pressure drop below design conditions. Additional savings are available by reducing the evaporator pressure drop with load.

### **Single Loop, Variable Flow Rate**

The primary (single loop) system referred to here should not be confused with the old, constant flow primary system with three-way valves in the chilled water coils. The single loop system has variable speed primary pumps and two-way valves in the chilled water coils. There are no secondary pumps and the bypass loop is omitted. Single loop systems have a number of advantages over the primary-secondary system. First there is no possibility of detrimental mixing from return to supply. Thus for overloaded situations, this design operates much like the primary-secondary arrangement with check valve. Additional advantages are realized in part load operation. Variable evaporator flow reduces water-side pressure drop at small cooling loads, decreasing pumping power requirements. This system eliminates the need for secondary pumps, diminishing system first cost. Finally, since single loop chiller scheduling is determined

by chiller load as opposed to flow, this design is able to adapt to low temperature differential without losing system capacity.

## CHAPTER V

### LOAD PROFILES AND WEATHER DATA

The analysis in this study has been divided into two categories. All systems compared are able to deliver the cooling load at design conditions. However, some designs deliver this cooling load more efficiently than others. Efficiency is critical during part load operation because a chilled water system operates at part load the vast majority of its life. System capacity is only a consideration when the required cooling load is greater than the design value. Some system designs have greater capacity than others. The performance categories compared in this study are:

- 1) System capacity is analyzed for all situations where the actual cooling load exceeds the system's design load.
- 2) System efficiency is studied for all loads equal to or less than the system design load.

Efficiency is quantified by annual energy requirements and an integrated energy rating (IER). In order to assign values to these quantities a load profile was developed. This profile expresses system load as a function of outdoor dry bulb temperature. Ambient conditions and number of annual hours spent at a specified load is defined by annual weather data.

The load profile used here is a modified version of that used by Weber (1988), Liu (1997) and Lilly (1998). Their profiles assumed 100% design load at 95°F. The load drops linearly with temperature to 20% at 60°F. The load requirement is then fixed at 20% for all temperatures below 60°F. Additionally, this profile stays a constant 100% at all temperatures above 95°F. This represents the maximum system capacity when operating above design conditions. The building load is assumed to continue its linear increase above 95°F.

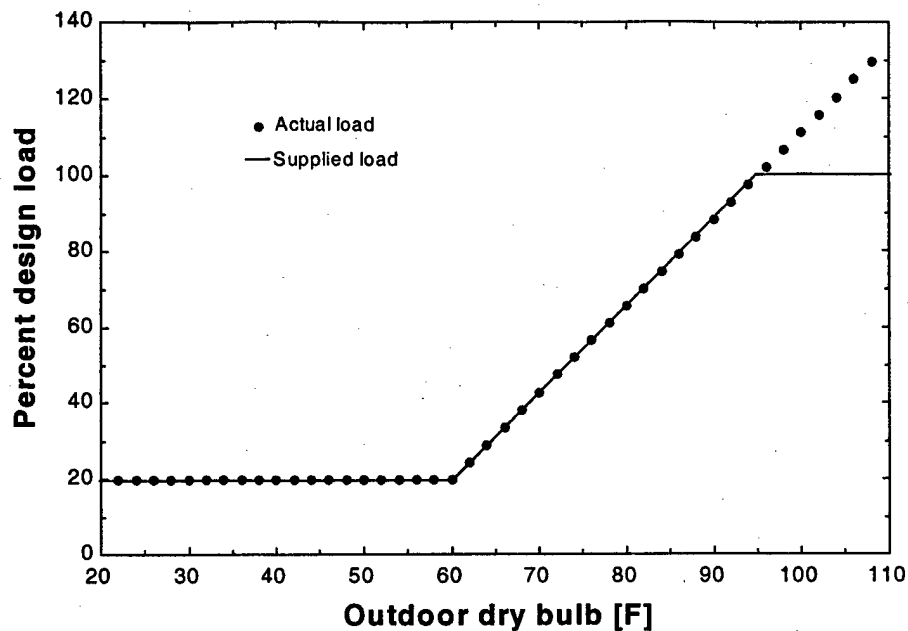


**Figure 48. Previous load profile**

A number of modifications have been made to this profile in the course of this research. First, the supplied load is not assumed to be equal to the design load when operating above design conditions. The supplied load, above design conditions, is set equal to the calculated system capacity. This capacity is a function of ambient conditions and system design. For example, a particular single loop system may be able to meet the actual load up to 100°F. While a similar primary-secondary system may only meet the load up to 95°F. Once a system is operating at full capacity its maximum load may increase or decrease with variations in ambient conditions. Another change made to the profile is the addition of free cooling at 45°F. As a result, it is assumed that there is no load below 45°F. In actuality there is some cooling load present, although the energy required by free cooling is not compared. Finally, the design dry bulb temperature is adjusted for different locations. For example, the design dry bulb in Atlanta is 95°F while in Phoenix it is 107°F. The load profiles and weather data are presented below. Only weather data at or below design conditions is represented. This is because annual efficiency comparisons only deal with temperature bins at or below design conditions.

**Atlanta**

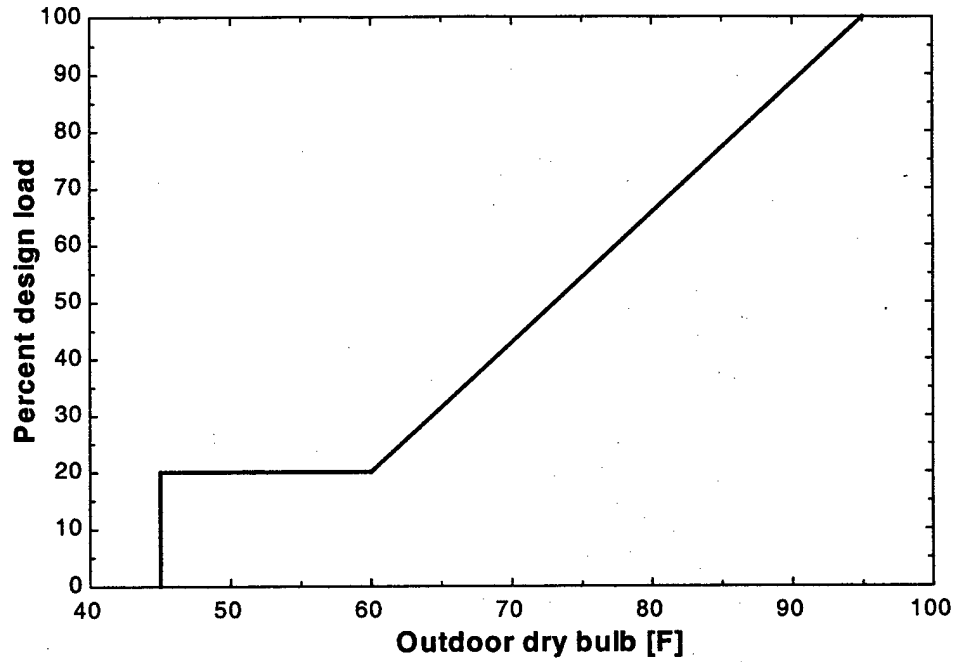
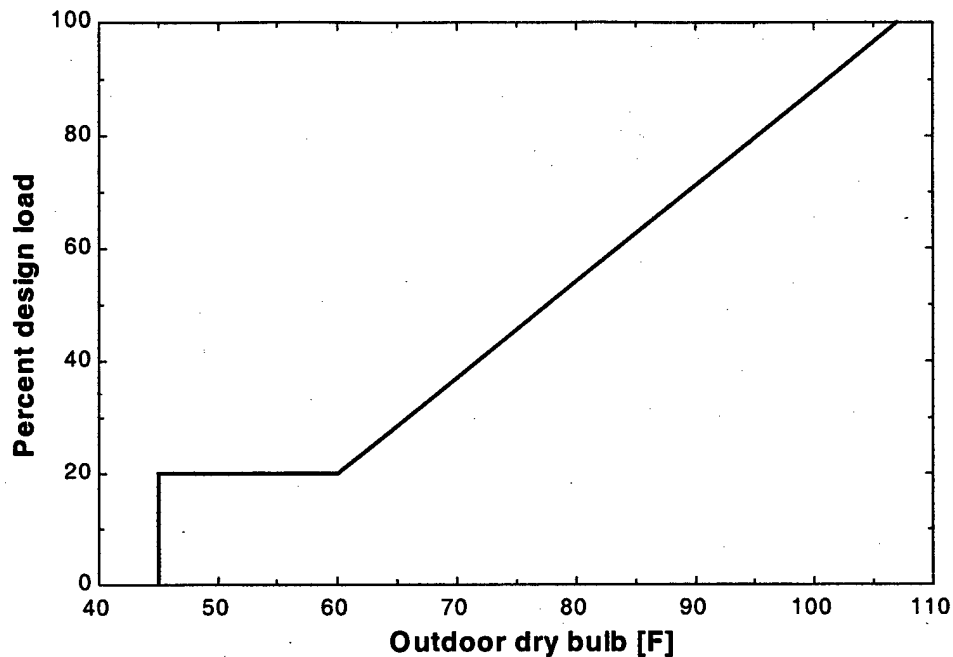


Figure 49. Atlanta Load Profile

Dry Bulb [F]	Wet Bulb [F]	Total Observations [hours]
95	74	N/A
92	74	135
87	72	367
82	70	612
77	69	839
72	67	1201
67	62	986
62	57	845
57	52	773
52	47	709
47	42	665
45	40	N/A
<b>Design Condition</b>	<b>95° [F] dry bulb</b>	<b>78° [F] wet bulb</b>

Table 16. Atlanta weather data

**Phoenix**



**Figure 50. Phoenix Load Profile**

Dry Bulb [F]	Wet Bulb [F]	Total Observations [hours]
107	71	154
102	70	329
97	68	463
92	67	592
87	65	709
82	62	753
77	59	730
72	55	710
67	52	759
62	49	801
57	47	801
52	44	725
47	41	573
45	39	N/A
<b>Design Condition</b>	<b>107<sup>o</sup> [F] dry bulb</b>	<b>75<sup>o</sup> [F] wet bulb</b>

**Table 17. Phoenix weather data**

**Chicago**

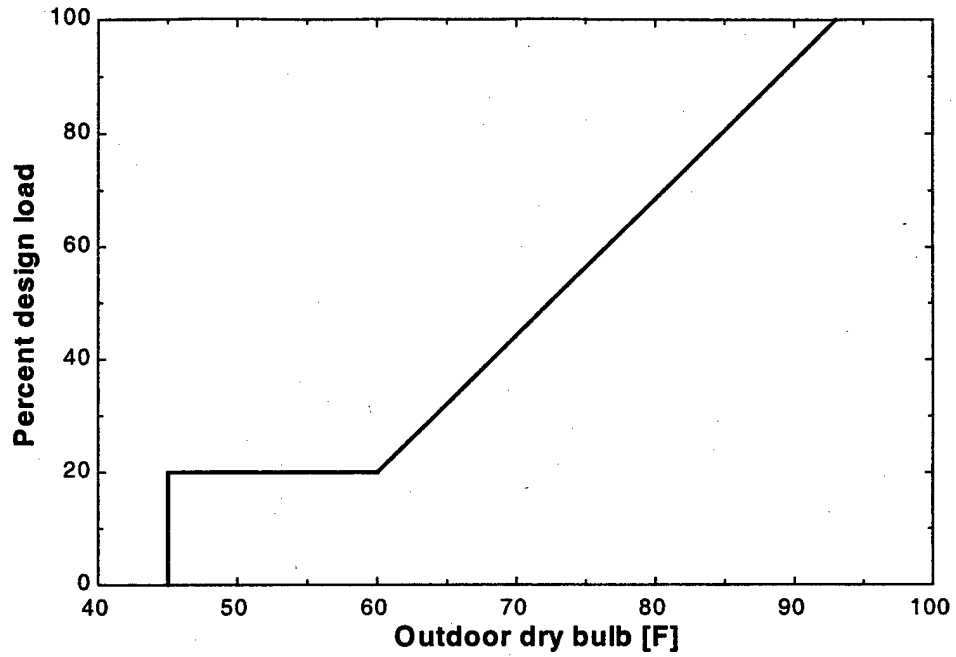


**Figure 51. Chicago Load Profile**

Dry Bulb [F]	Wet Bulb [F]	Total Observations [hours]
93	74	N/A
92	74	58
87	72	165
82	70	324
77	67	487
72	64	681
67	61	759
62	57	700
57	52	604
52	47	581
47	43	565
45	41	N/A
<b>Design Condition</b>	<b>93<sup>0</sup> [F] dry bulb</b>	<b>77<sup>0</sup> [F] wet bulb</b>

**Table 18. Chicago weather data**

**Air Conditioning & Refrigeration Institute**

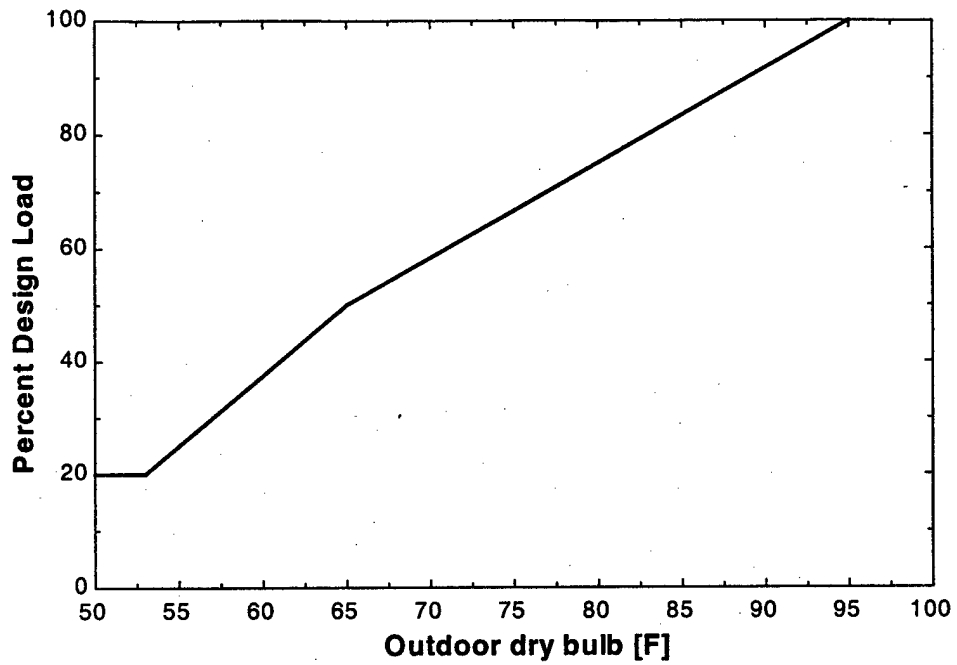


Figure 52. ARI Load Profile

Percent load	Dry Bulb [F]	Wet Bulb [F]	Condenser water inlet [F]	Percent cooling hours
100%	95	75	85	1%
75%	80	68.75	75	42%
50%	65	62.5	65	45%
25%	55	56.25	65	12%

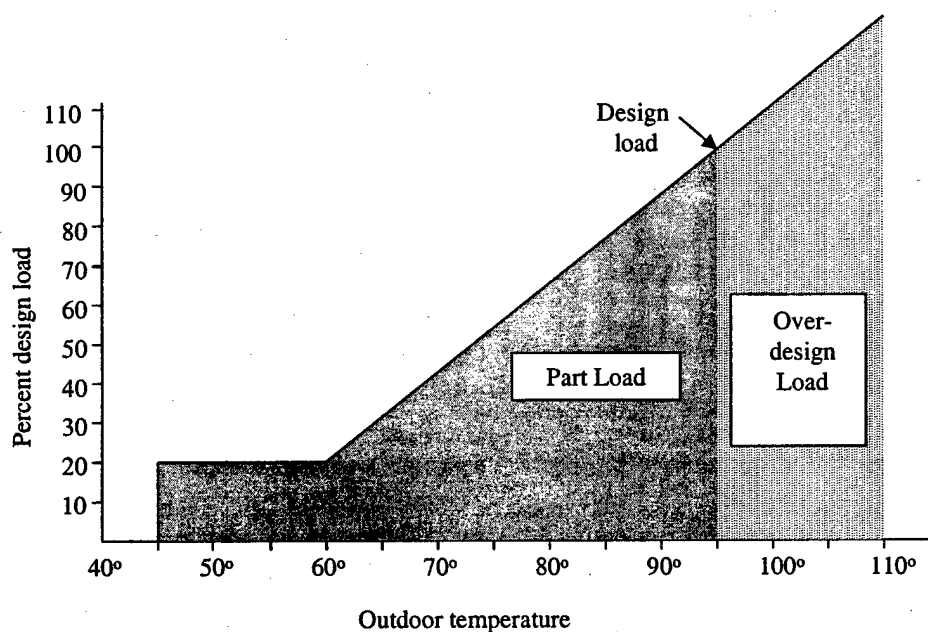
Design Condition	95° [F] dry bulb	75° [F] wet bulb	85° [F] condenser inlet
------------------	------------------	------------------	-------------------------

Table 19. ARI conditions

## CHAPTER VI

### PERFORMANCE STUDIES

Chilled water system analysis has been divided into two areas. These areas are operation below and above design load. They are shown in Figure 53. The analysis was separated into two regions because some designs are able to match load requirements at high temperatures while others cannot. All systems are able to meet the requirement below the design temperature.



**Figure 53. Load profile**

This is because a system is designed to have the necessary capacity to meet the design load. As a result, each design is able to meet the required load when conditions are equal to or below design conditions. However, some designs perform more efficiently than others under these conditions. Two parameters are calculated to compare system efficiency. One parameter calculated is each design's annual energy requirement. These values are compared to determine the energy saved or lost as a result of omitting the bypass loop. Integrated energy ratings (IER) are also compared. These values include the

system, chiller and evaporator auxiliary IERs. The system IER is the annual kW/ton rating which compares the system power required to handle the building cooling load. Chiller IER is a similar rating which compares compressor power to evaporator load. Evaporator auxiliary IER rates the efficiency of all air handler fans and evaporator side pumps. IER values are determined using the formula,

$$IER = \frac{1}{\sum_{i=1}^n \frac{hr_i / hr_{tot}}{kw_i / ton_i}} \quad \text{Equation 85}$$

where,  $hr_i$ ,  $kw_i$  and  $ton_i$  are the number of hours, kilowatts and tons in the  $i^{\text{th}}$  temperature bin respectively. The variable  $n$  is the total number of temperature bins considered.

System capacity is used to compare each design's ability to meet load requirements above design weather conditions. This over-design analysis is done by comparing a primary-secondary system's capacity to that of a similar single loop design.

### **Annual efficiency**

#### **1. Base Case**

This case compares the efficiency of a single loop with a primary-secondary system. Atlanta weather data and load profile are used. Design conditions are at 95°F dry bulb and 78°F wet bulb. All handlers are sized for a 100 ton load and a 10°F water-side temperature differential at design conditions. Each model has ten air handlers, giving the system a 1000 ton capacity at design conditions. The two systems are depicted in Figure 54.

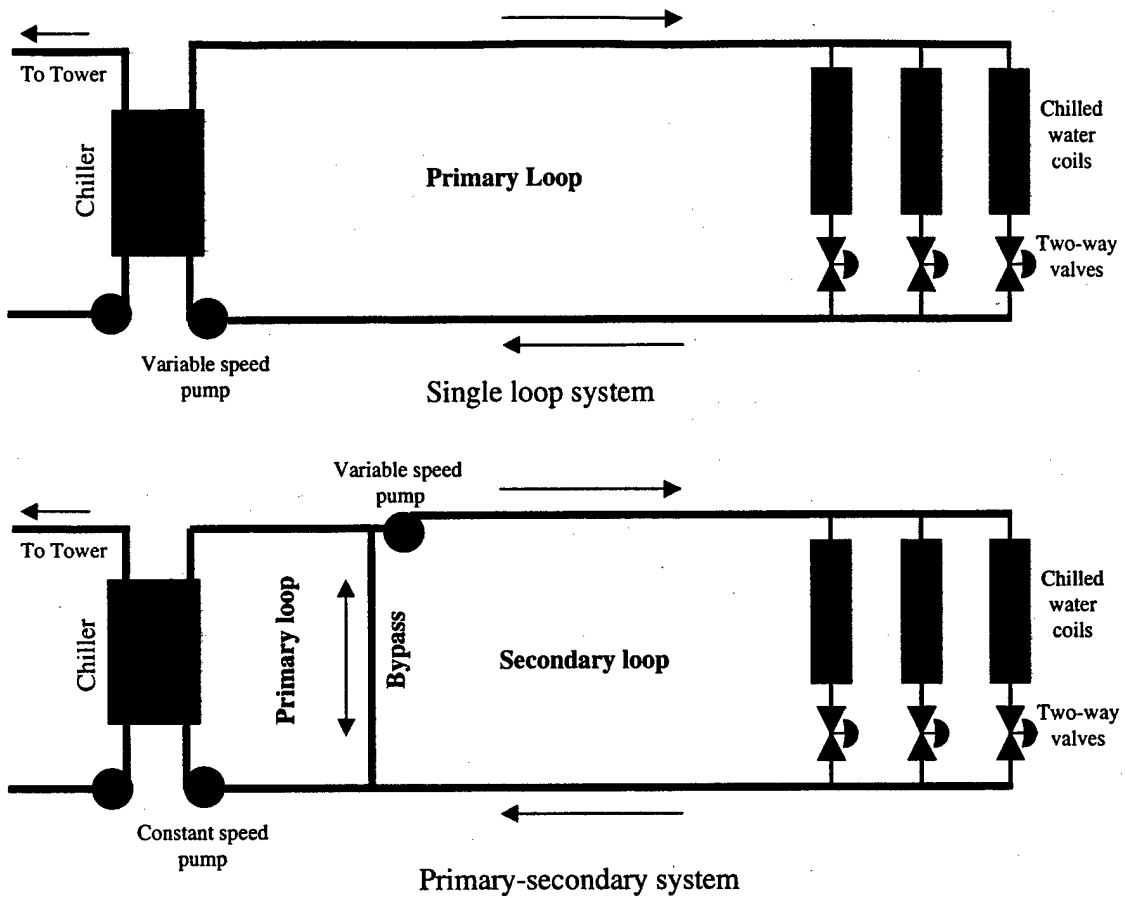


**Figure 54. Base case designs**

The single loop system gives a 7.8% annual energy savings over the primary-secondary system under these conditions. The vast majority of this savings is derived from the reduced pump head at part load. The decreased head is a result of lower part load evaporator flow rates. Figure 55 shows the single loop pump power reduction.

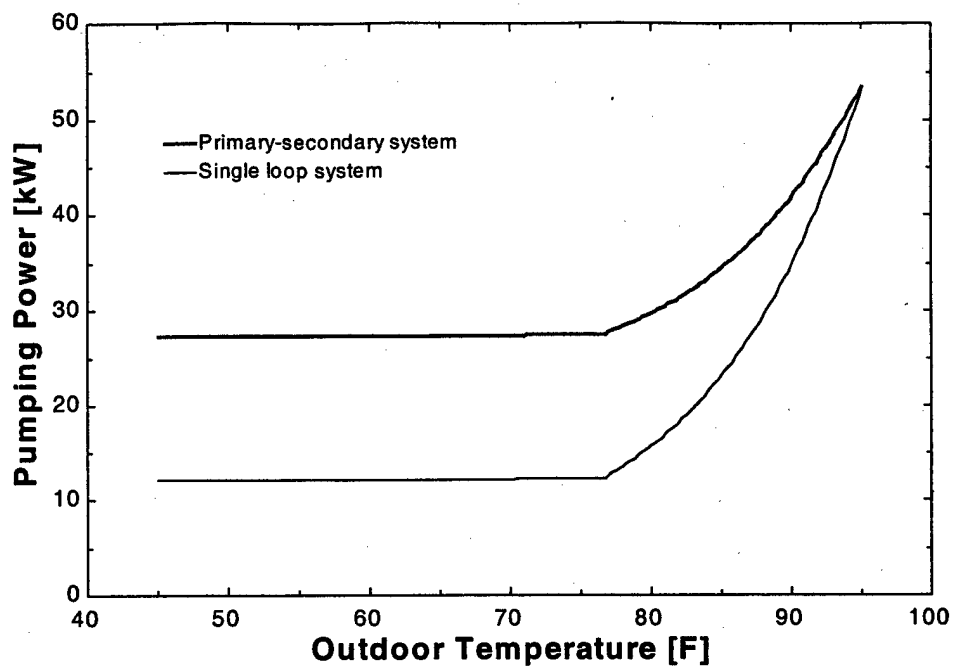


Figure 55. Base case pump power

The compressor power required by the primary-secondary system is slightly larger as well. More pump power means that more shaft work is added to the water stream. This energy has to leave through the evaporator as heat. In fact, the primary-secondary compressor power is larger but by a very small amount. The energy added by pumps as shaft work is much smaller than that added by air handlers as heat. The relative compressor power comparison is seen in Figure 56.

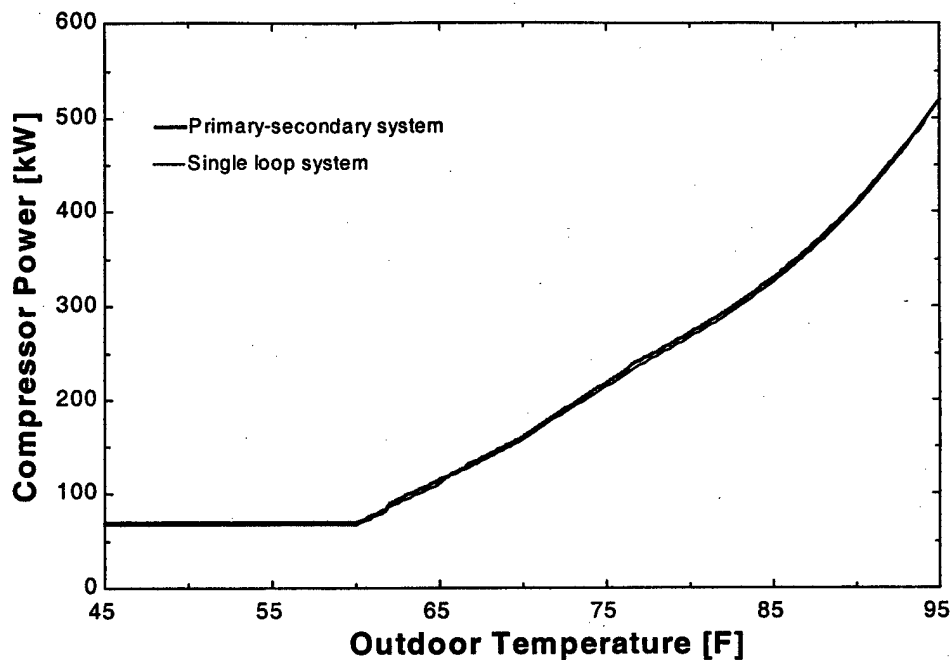


Figure 56. Base case compressor power

The IER analysis is seen in Table 20. This table shows that the savings is primarily a result of reduced evaporator side pump power. The single loop chiller IER is somewhat larger than that of the primary-secondary system, however the difference is less than one percent. The values here are only carried to two significant digits because the model is not meant to predict absolute values within one percent accurately. It should be viewed as a comparative tool designed to point out trends.

System type	Single loop	Primary-secondary
Evaporator Auxiliary IER	0.042 [kW/ton]	0.085 [kW/ton]
Chiller IER	0.37 [kW/ton]	0.37 [kW/ton]
System IER	0.55 [kW/ton]	0.61 [kW/ton]

Table 20. Base case IER analysis

The chiller IER value may seem smaller than expected. This indicates very high chiller efficiency. The chiller efficiency, here, is increased because chiller reset was used.

## 2. Constant Speed Pumping Design

The design and conditions for this comparison are almost the same as the base case. The only change is the replacement of all variable with constant speed pumps. This situation was included because of the higher cost of variable speed drives. Certainly when attempting to capitalize on savings available by varying evaporator flow rate, energy costs will be less for a variable speed pumping scheme. However, constant pumps require less shaft power when flow rate is reduced. One would then expect the single loop system to also offer a small savings over the primary-secondary system.

The single loop system discussed here reduces the annual energy use by 3.2%. This is a much smaller savings than was available with variable speed pumping. Table 21 shows that the single loop efficiency increase is again derived from a reduced pump power. It is also interesting to note both auxiliary efficiency ratings are much worse than their variable speed counterparts.

<b>System type</b>	<b>Single loop</b>	<b>Primary-secondary</b>
<b>Evaporator Auxiliary IER</b>	<b>0.11 [kW/ton]</b>	<b>0.13 [kW/ton]</b>
<b>Chiller IER</b>	<b>0.37 [kW/ton]</b>	<b>0.37 [kW/ton]</b>
<b>System IER</b>	<b>0.65 [kW/ton]</b>	<b>0.67 [kW/ton]</b>

**Table 21. Constant speed pumping IER analysis**

## 3. Other Load Profiles

Weather data and load profiles were selected from different cities within the United States. This was done to verify the savings available in different HVAC markets. The tables below show the comparison of single loop to primary-secondary loop performance using these different profiles. All single loop systems are more efficient than their primary-secondary loop counterpart. Bypass loop omission results in 5.2%, 7.8% and 8.8% annual energy savings in Phoenix, Atlanta and Chicago respectively. The

single loop system saves much more energy in Chicago and Atlanta than it does in Phoenix. This is because the single loop saves energy from the smaller evaporator pressure drop at diminished loads. When the average load is lower the system saves more energy. The average load in Phoenix is 45% of design, while the average in Atlanta and Chicago is 40.8% and 38% respectively.

System type	Single loop	Primary-secondary
Evaporator Auxiliary IER	0.048 [kW/ton]	0.084 [kW/ton]
Chiller IER	0.38 [kW/ton]	0.38 [kW/ton]
System IER	0.54 [kW/ton]	0.59 [kW/ton]

Table 22. Phoenix IER analysis

System type	Single loop	Primary-secondary
Evaporator Auxiliary IER	0.045 [kW/ton]	0.092 [kW/ton]
Chiller IER	0.37 [kW/ton]	0.37 [kW/ton]
System IER	0.55 [kW/ton]	0.62 [kW/ton]

Table 23. Chicago IER analysis

a) ARI

Comparisons using the ARI load profile were included because it is an industry standard for rating chillers. As such, these values may easily be compared to real world systems with comparable components. The chiller IER here is somewhat lower than the actual chiller rating. This is because chiller reset was initiated at approximately 75°F.

System type	Single loop	Primary-secondary
Evaporator Auxiliary IER	0.038 [kW/ton]	0.067 [kW/ton]
Chiller IER	0.37 [kW/ton]	0.37 [kW/ton]
System IER	0.64 [kW/ton]	0.68 [kW/ton]

Table 24. ARI Load analysis

System IPLV is much higher in this comparison than for other cooling load profiles. This is because the average system load using this data is 58% of design. Since this system weights the higher loads more heavily, one would expect a smaller savings. The single loop system saves 5.5% compared to the primary-secondary system when using this profile.

#### 4. Effects of Air Handler Degradation

This case, again, compares the annual performance of single loop and primary-secondary systems. All air handlers are fouled to the point that there is a 7°F design temperature differential between the chilled water supply and return. Atlanta weather data and load profile are used. Since there is a 7°F ΔT at design conditions, the system requires a much higher flow rate. At full load this flow is greater than the constant 2400 gpm primary loop flow in the primary-system. As a result, the secondary flow rate exceeds primary loop flow rate. The return water is mixed with the chilled water supply, increasing the supply temperature. This situation will be explained further in the over-design load analysis. In this case, the secondary flow rate exceeds the primary flow when the building load reached 85% of its design value. The system is still able to meet the load requirement but does so much less efficiently it requires because more fan and pump power. The single loop design is able to increase water flow rate to air handlers without mixing.

System type	Single loop	Primary-secondary
Evaporator Auxiliary IER	0.045 [kW/ton]	0.089 [kW/ton]
Chiller IER	0.38 [kW/ton]	0.38 [kW/ton]
System IER	0.56 [kW/ton]	0.61 [kW/ton]

Table 25. Fouled system IER analysis

In this case the single loop system requires 9.4% less energy annually than the primary-secondary system. In this situation a fouled air handler was chosen for simplicity. The low temperature differential caused here by fouling may result from a number of other factors. This analysis shows that the single loop system is more capable of adapting to load problems that lead to low temperature differential.

## 5. Increased Air Handler Capacity

This case determines the effect that increasing air handler size has on system efficiency. This situation is the same as the base case except it employs larger air handlers. This system is designed to produce a 12<sup>0</sup>F  $\Delta T$  at design conditions. As a result, the air handlers are much larger. The system's 10 air handlers are capable of transferring 145 tons each with a 10<sup>0</sup>F water-side temperature change.

System type	Single loop	Primary-secondary
Evaporator Auxiliary IER	0.037 [kW/ton]	0.050 [kW/ton]
Chiller IER	0.37 [kW/ton]	0.37 [kW/ton]
System IER	0.54 [kW/ton]	0.60 [kW/ton]

Table 26. Increased air handler capacity IER analysis

In this case use of the single loop system results in an annual 8.2% energy reduction. This is somewhat larger than the 7.8% seen in the base case. Most of the extra savings is a result of reduced pumping power requirement. It is interesting to note that increasing air handler size raised the single loop and primary-secondary system efficiencies by 1.2% and 1.0% respectively.

## 6. Low Efficiency Chiller Analysis

The chiller used in the analysis to this point has been a modern, high efficiency chiller. Its IPLV rating is 0.38. Few existing chilled water plants have high efficiency chillers. Most plants operate with equipment that was purchased 10 to 12 years ago. These chillers operate inefficiently by today's standards. Since the single loop system derives its savings from a decreased pump power at low loads, similar savings should be available with lower efficiency chillers. Table 27 shows the relative performance of the two systems with an older chiller.

System type	Single loop	Primary-secondary
Evaporator Auxiliary IER	0.042 [kW/ton]	0.085 [kW/ton]
Chiller IER	0.71 [kW/ton]	0.71 [kW/ton]
System IER	0.89 [kW/ton]	0.95 [kW/ton]

Table 27. Low efficiency chiller analysis

This system was modeled using chiller C from the preceding chiller comparison study. It has a 0.59 IPLV rating. Curiously, the chiller IER is much lower than the IPLV rating indicates. This is because this chiller performs very poorly at small loads, as was seen in the chiller comparison study. When using Atlanta weather data and load profile the average load and the average condenser water inlet temperature are approximately 400 tons and 75°F respectively. Under these conditions the chiller efficiency rating is 0.72 kW/ton, much worse than the IPLV value. The single loop system uses 5.9% less energy annually than the

primary-secondary system in this case. Although this is somewhat less than the 7.8% savings seen in the base case, the absolute savings is larger.

## 7. Multiple Chiller Plant Analysis

Most large central plants have more than one chiller, so multiple chiller plant analysis is critical. This case compares the two plant designs, each with two chillers. Atlanta weather data and load profile are used. As discussed earlier, chillers are scheduled to minimize total system electrical energy requirements. Optimal scheduling for the single loop system is almost identical to that of the primary-secondary system. In this case proper scheduling requires starting up the lag chiller when the lead chiller is delivering 97% of its rated load.

<b>System type</b>	<b>Single loop</b>	<b>Primary-secondary</b>
<b>Evaporator Auxiliary IER</b>	<b>0.025 [kW/ton]</b>	<b>0.044 [kW/ton]</b>
<b>Chiller IER</b>	<b>0.38 [kW/ton]</b>	<b>0.38 [kW/ton]</b>
<b>System IER</b>	<b>0.51 [kW/ton]</b>	<b>0.53 [kW/ton]</b>

**Table 28. Multiple chiller plant IER analysis**

It can be seen that the chiller IER values for the two chiller system are larger than those of single chiller systems. This is because chiller scheduling was based on overall system power rather than just compressor power analysis. Auxiliary and total system IER values are lower here than in single chiller results. This is because the chillers in these multiple chiller systems are operated at a higher average load than the single chiller systems. In this example, the average load is 1382 tons when the temperature is greater than 73°F. Two chillers are operated when above 73°F, so the average load is 69%. When the temperature falls below 73°F, the average load is 603 tons, but only one chiller is used. Thus, this one chiller operates at about 60%. As a result, the average annual chiller load in this multiple chiller system is

63%. Since the average load is higher the energy savings available by use of the single loop system is somewhat smaller. The savings here is 3.9%.

### **Over-design Load Operation**

A chilled water system's capacity is determined by a number of factors. These include chiller size, maximum compressor motor power, maximum water flow rate and maximum air flow rate. In both the single loop and primary-secondary systems the maximum compressor power is taken to be 588kW. This value was acquired from the chiller's manufacturer. The maximum system water flow rate is taken as 2800 gpm. This flow rate was chosen to be about 15% greater than the design value. Finally, the maximum air flow rate into an air handler is 400 cfm per design ton. For example, an air handler with a 100 ton capacity will have fans capable of a 40,000 cfm air flow rate. This is the standard industry accepted value for air flow rates.

The assumed control strategy is important when analyzing its capacity. The system constantly adjusts to changes attempting to meet the building load. When a room starts to heat up the air handler fans increase speed to deliver more cool air. As the air flow rate increases, the cold deck temperature starts to rise. This triggers the two-way valves to open, calling for more chilled water. As two-way valves open the chilled water coil head drops, sending a signal for the pumps to increase speed. As the system flow rate increases the chiller water exit temperature increases momentarily. This increase signals the compressor to increase capacity, cooling the water to the chiller set point again. This sequence works well as long as the system is not above design load.

#### **1. Base Case**

As the actual load moves above the design value, the single loop and primary-secondary systems operate much differently. The primary loop of a primary-secondary system is constrained by a constant 2400 gpm flow rate. When secondary flow rate exceeds 2400 gpm the return water is mixed with the supply through the bypass.

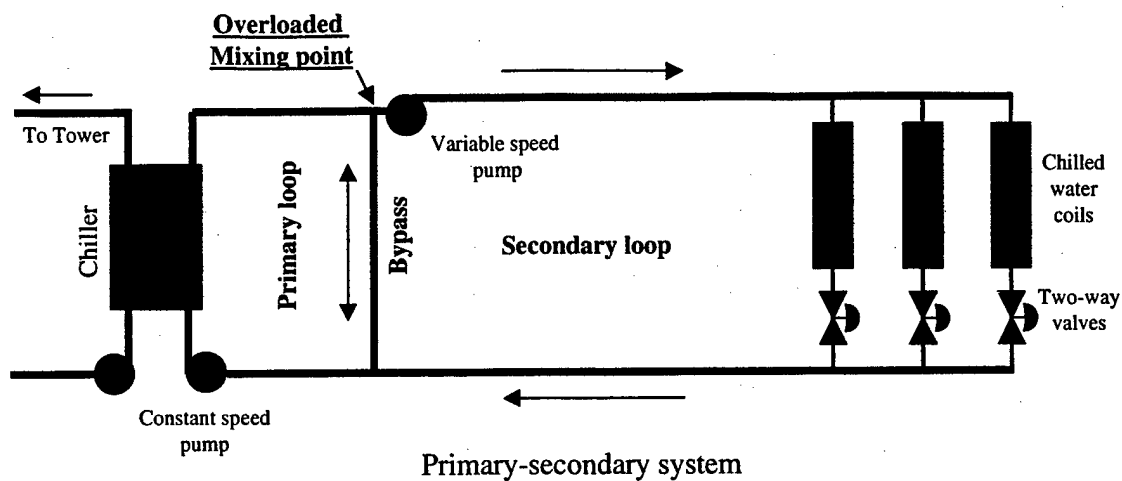


**Figure 57. Mixing on over-design primary-secondary system**

This mixing increases the air handler's water inlet temperature, which reduces the air to water-side LMTD and with it the heat transfer. The air flow rate increases to compensate, but this lifts the cold deck temperature. The air handler calls for more water, attempting to drop the cold deck, further increasing the inlet temperature. This sequence progresses until the secondary loop reaches its maximum flow rate.

Figure 58 shows how the air handler water inlet temperature increases with the secondary loop flow rate.

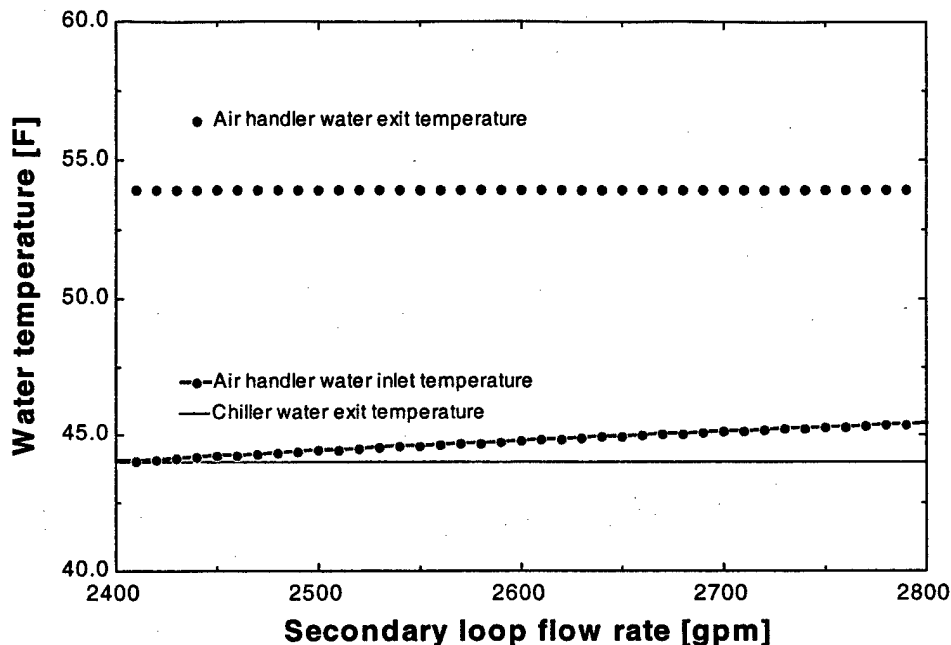


Figure 58. Over-loaded primary-secondary system

In this figure the chiller is able to hold the 44°F set point because the compressor is operating below 588kW. The building load is met because the air handler fans are running below maximum levels. However, the air handler cold deck temperature is no longer maintained at the constant 58°F. Figure 59 shows how the primary-secondary mixing adversely affects system load. The negative slope on the primary-secondary system capacity curve relates the fact that this is an unstable situation. As soon as the secondary flow exceeds primary loop flow rate the system will proceed to a “wide open” position. The time that it takes this process to proceed depends on chilled water system length, water velocity and air handler/pump control scheme. Typically these controls are adjusted to be slow enough that they do not hunt for an adequate operating point but fast enough to adjust to changing demand.

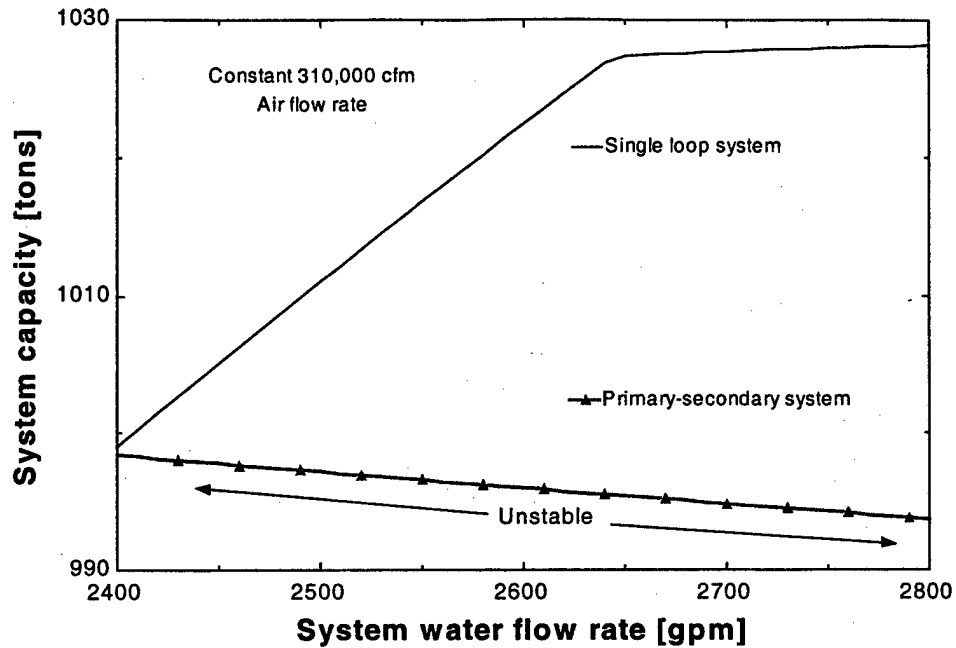


Figure 59. System capacity versus water flow rate

The single loop system, having no mixing, maintains a positive slope throughout the flow rate variation. The initial steep slope represents the area where the chiller maintains the 44°F set point. At approximately 2650 gpm the compressor reaches the maximum power level. The set point then rises while the compressor continually operates at maximum power. Notice the single loop system curve maintains a positive slope after the chiller reaches full capacity. Since the chiller is delivering a warmer supply temperature, the chilled water return stream is warmer as well. This decreases the compressor lift, which raises chiller capacity. Chiller capacity is increased in the primary-secondary system as well, but it is primary loop flow rate not chiller capacity that constrains that design. The single loop design capacity is constrained by chiller capacity. Thus, increased chiller capacity directly increases system capacity.

Throughout this process the system is attempting to meet the building load. Even though the chilled water has reached its maximum flow rate the system may still be able to meet the load. The air handler fans increase the air velocity across the chilled water coil. This increases the airside heat transfer coefficient, resulting in a larger UA and LMTD. The affect of air speed on system capacity is seen in Figure 60. This graph assumes that the water flow rate is fixed at the maximum value of 2800 gpm. Also the ambient temperatures are set at design weather conditions. The primary-secondary system capacity

increases steeply until the air flow equals 33,000 cubic feet per minute. That is the point that the primary-secondary system's compressor reaches maximum load. Prior to that point the chiller maintains its set point. Since the water flow rate is fixed at 2800 gpm the air handler inlet temperature is fixed.

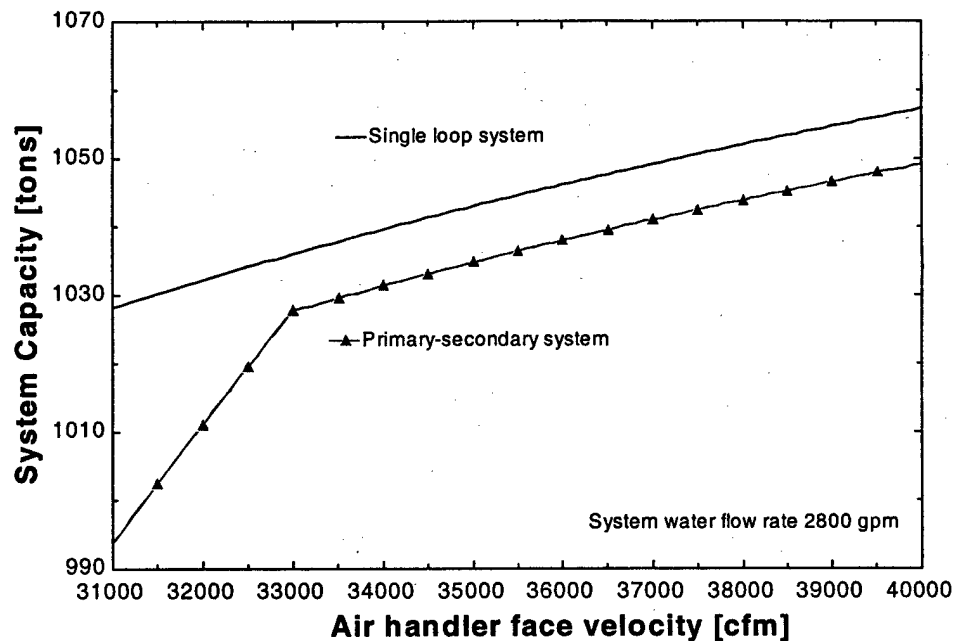


Figure 60. System capacity versus air flow rate

The single loop system's chiller is already at full power, thus the set point is increasing. Once the compressor is operating at maximum power in each the curves become parallel. The primary-secondary system continues to exhibit lesser capacity because its air handler inlet water temperature is increased by mixing. Eventually, both systems reach their maximum capacity. This is the point where the chiller, pumps and fans are all running at maximum power.

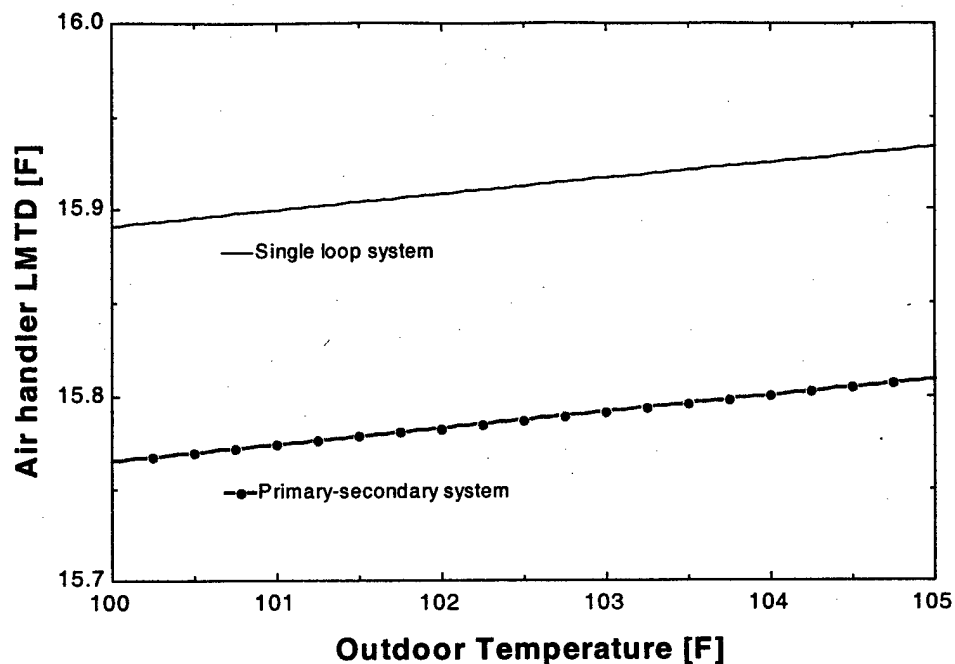


Figure 61. Air handler LMTD

At maximum capacity, the primary-secondary system's air handler water inlet temperature is greater than the corresponding temperature in a single loop design. As a result, the primary-secondary air to water LMTD is smaller. The chilled water coil UAs are identical because the designs have equal air and water velocities. Figure 61 represents each system operating "wide open". The smaller air handler LMTD limits the primary-secondary system capacity. Both systems exhibit increasing temperature differences. This shows that the air inlet temperature is raising with outdoor conditions faster than the water inlet temperature. Figure 62 shows how the system capacities compare.

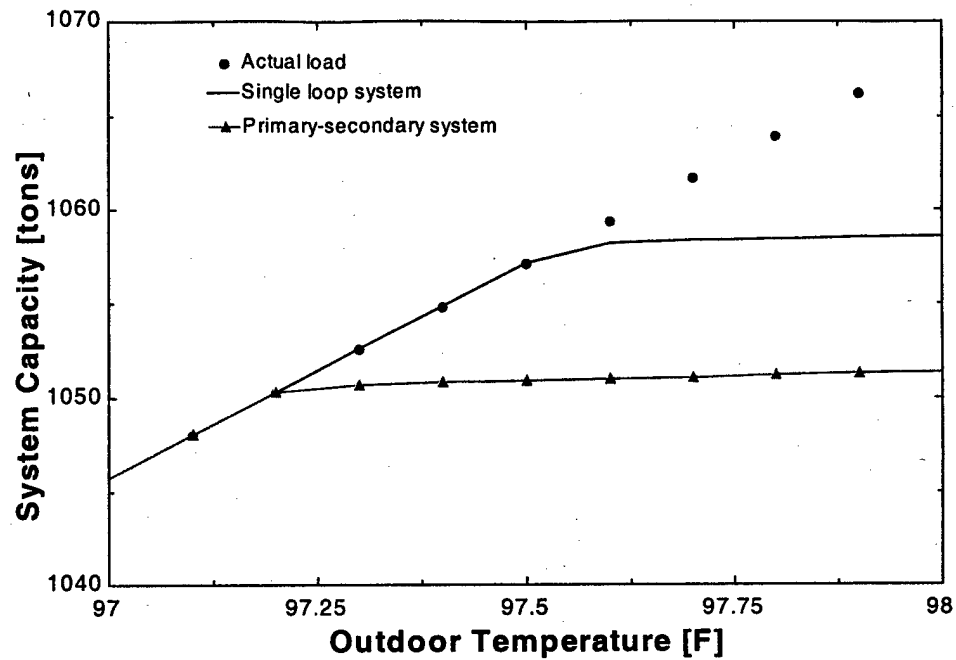


Figure 62. System capacity

The single loop system is able to meet the building load requirement to higher outdoor temperatures. Additionally, this system has more capacity when it is no longer able to meet the actual load.

## 2. Reducing Chilled Water Set Point

One might reason that reducing the chiller set point has the potential to increase primary-secondary design's capacity. Initially, the system is constrained by primary flow rate and not chiller capacity. When the set point is reduced the chiller becomes more fully loaded. Also, the air handler water inlet temperature is lowered. This increases the LMTD and thus the heat transfer.

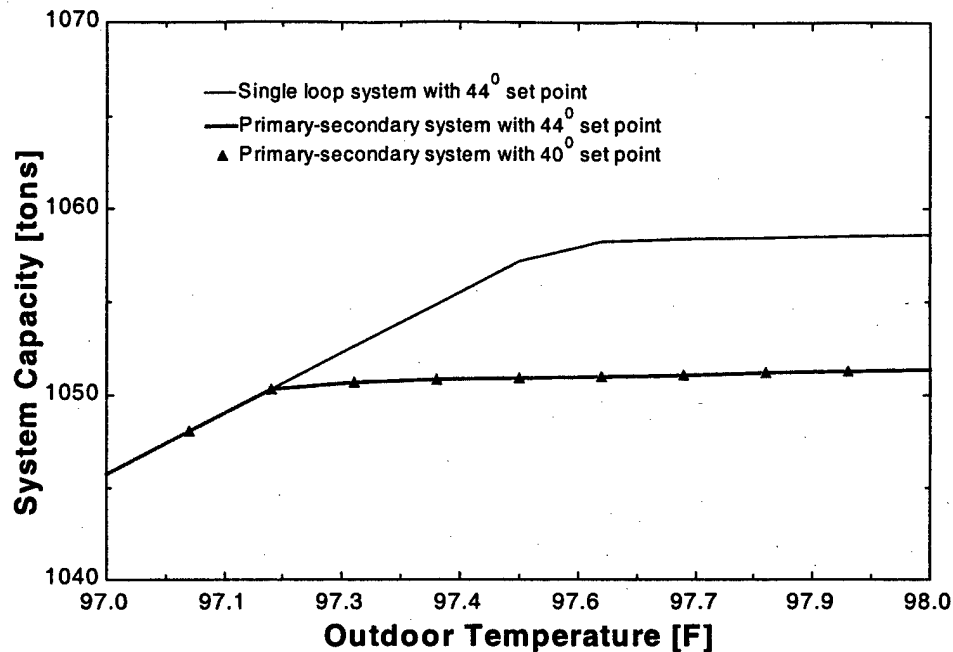


Figure 63. Adjusting the chiller set point

The problem with this reasoning is the fact that the set point is no longer maintained once the compressor reaches maximum power. Figure 63 shows the effect that set point reduction has on system capacity. Each system is able to meet the load requirement until long after the compressor is at full power. As a result, the system capacity remains unchanged from the original performance with a 44°F set point.

While this strategy fails to increase system capacity, it hurts system efficiency. Figure 64 shows how chiller efficiency is affected by reducing the evaporator outlet temperature. Initially, all three systems are meeting the load. However, the system with the 40° set point is the most inefficient. Both primary-secondary systems have equal efficiency once the compressors reach maximum power. The systems are essentially identical thereafter because the set point is no longer maintained. When all three systems move to maximum capacity the single loop chiller operates most efficiently. This is because it has a higher cooling capacity using the same power.

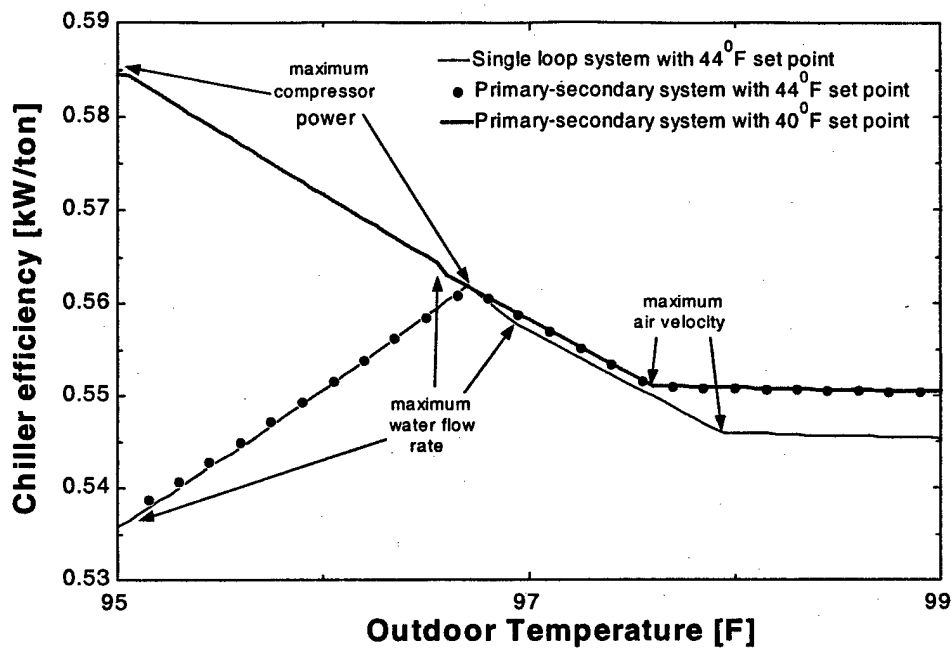


Figure 64. Chiller efficiency with reduced set point

It is able to do so because there is no mixing. Consequently, the evaporator outlet temperature can be higher than the primary-secondary system's temperature. This reduces the compressor lift, increasing the chiller capacity.

### 3. Effects of Air Handler Degradation on System Capacity

This case compares the capacity of a single loop and primary-secondary system with fouled air handlers. The air handlers are fouled to the point that the chilled water system  $\Delta T$  is reduced to  $7^{\circ}\text{F}$ . As a result, system pumps are operating at maximum flow rate with loads considerably smaller than the design value. However, both systems are still able to meet the design load requirement by increasing the air handler face velocity. Air handler fouling does not only affect system efficiency, it hurts system capacity as well. The air handler UA is reduced due to fouling, thus at maximum air and water flow rates the air handler is not able to deliver the same cooling load. In this case air handler fouling results in a 2% capacity decrease when compared with similar unfouled designs. Figure 65 shows that the single loop system is still

able to deliver a larger cooling load than the primary-secondary system. In fact, the single loop outperforms the primary-secondary design by the same percentage as it did in the unfouled analysis.

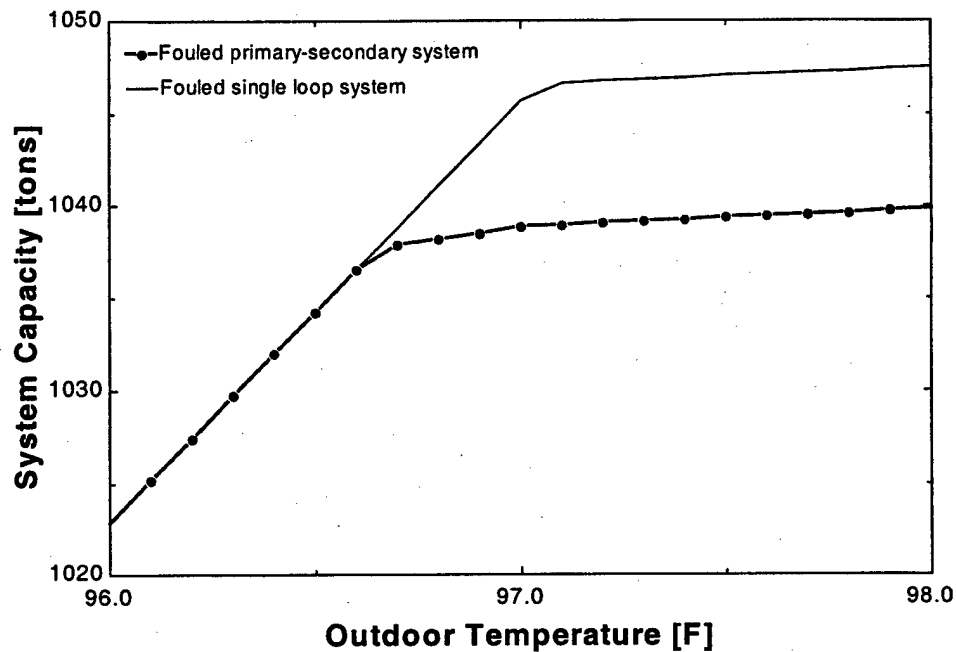
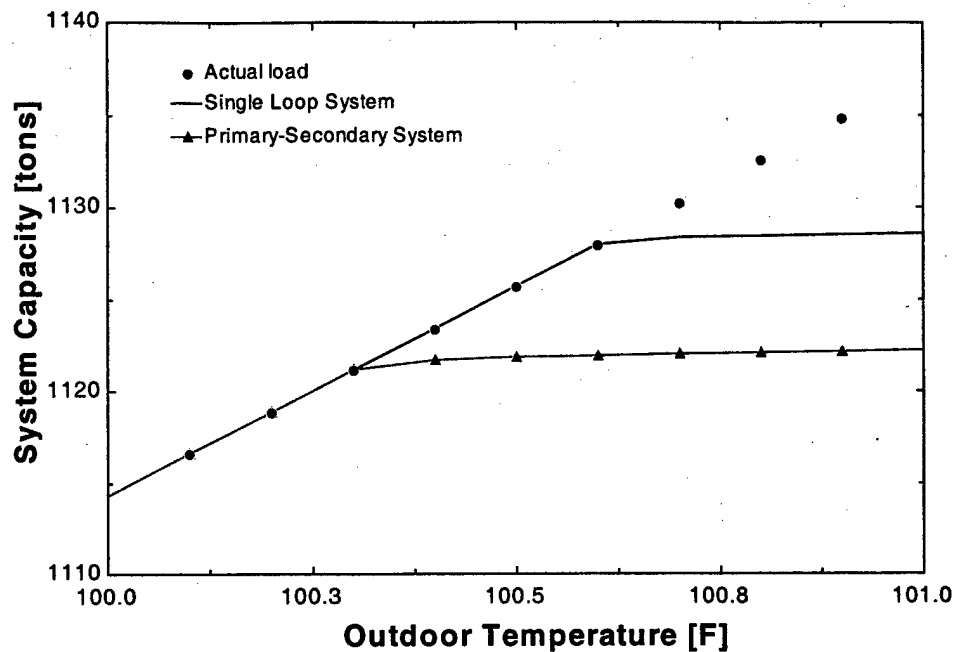


Figure 65. Effect of fouling on system capacity

#### 4. Increasing Air Handler Capacity

The final area analyzed is the affect that increasing the air handler sizes. In this case it was assumed that the air handlers were the only components altered. Therefore, the maximum compressor power and water flow rate remain 588kW and 2800 gpm respectively. One would expect bigger fans to accompany the larger chilled water coil. Due to the larger air handlers the design system  $\Delta T$  is increased to 12°F. By doing so a 145 ton air handler is needed. Using the 400 cfm per design ton value, the maximum air flow rate is 58,000 cfm. This air handler was given greater capacity by simply increasing the face area. Thus the larger air flow rate converts to a similar face velocity.



**Figure 66. Increased design  $\Delta T$  system capacity**

Both system capacities are larger here than in previous examples. This is because the air handler UA is substantially increased. The Reynolds number and heat transfer coefficients are similar to their previous values because the maximum water and air velocities remain unchanged. The UA is raised because the air and water-side heat transfer area is greater. With a larger UA the air to water LMTD may reduce. As a result, the evaporator exit temperature may increase, reducing the compressor lift. The reduced compressor lift gives the chiller more capacity. Figure 66 shows that the single loop system still outperforms the primary-secondary system by the same percentage it did previously.

## CHAPTER VII

### CONCLUSIONS

This study has analyzed chilled water system performance from two perspectives. Using a variety of load profiles and system designs annual efficiency was compared. A number control strategies were then compared to determine a system's ability to meet load demands when they exceed the design load. Air handler fouling was introduced to determine each design's ability to adapt to low chilled water temperature differential, a common chilled water system ailment. In each case analyzed the single loop system outperforms the corresponding primary-secondary design.

#### **Part Load efficiency**

Single loop, variable flow, chilled water system efficiency exceeds primary-secondary loop efficiency under a variety of conditions. These situations include:

1. Single and multiple chiller systems
2. Diverse load profiles
3. Constant and variable speed pumping schemes
4. Different design temperature differentials

#### **Greater Capacity**

Single loop systems are capable of meeting larger load demands at over design conditions, because there is no mixing from the return to the supply chilled water across the bypass leg. Various design and control strategies were studied to determine their ability to increase primary-secondary loop capacity to that of the single loop design. These include:

1. Reducing the chiller set point
2. Increasing air handler capacity
3. Inserting a check valve in the chiller bypass

The first two strategies fail to close the performance gap between single loop and primary-secondary system capacity. Including a check valve allows the primary-secondary loop to have equal capacity but fails to increase annual system efficiency.

### **Adapts to Load Problems**

Single loop systems are more efficient and have greater capacity when the chilled water  $\Delta T$  is low. Low chilled water  $\Delta T$  is a common problem among chilled water systems caused by air handler problems. These deficiencies include fouling, uncalibrated sensors and poor air handler control. The single loop system is able to adapt to these conditions by increasing chilled water flow rate through evaporators with little adverse performance affects.

### **Minimum Evaporator Water Flow Rate**

Evaporator water flow rate must be high enough for the flow to remain turbulent. This is often thought to be a shortcoming of the single loop, variable flow rate design. Evaporator flow rate is not an issue because the problem is resolved when chilled water reset is employed. Reset not only ensures turbulent flow in the evaporator, but saves energy as well. Consequently, reset is a common practice used with primary-secondary systems today. Multiple chiller use also resolves this issue.

### **Control Strategy**

The single loop, variable flow system is much simpler to operate than the primary-secondary design. The single loop system eliminates the possibility of detrimental mixing. Pumps are controlled to maintain a constant pressure drop across a distant chilled water coil, while the chillers are scheduled as a function of cooling load.

### **Summary**

The single loop design with variable speed pumps is advantageous to the popular primary-secondary system. This proposed design change does not suggest that it is better to change to an older primary system with constant speed pumps and three-way valves. Rather, this change is the next logical step in chilled water system design advancement. Primary-secondary systems were designed in order to take advantage of the reduced pressure drop resulting from variable water flow rates in the air handlers. The single loop design extends this reasoning to varying water flow rate in the evaporator, further reducing system pressure drop.

## CHAPTER VIII

### RECOMMENDATIONS

This study's results should be verified by analyzing a sufficiently instrumented facility. This instrumentation must be able to measure small building load variations. Additionally, water flow rate and temperature readings are required throughout the system. This exceptional instrumentation is necessary to ensure a similar load and proper control strategy in each case. The system's performance should be measured with the bypass loop open and closed under similar conditions. These conditions should include operation above and below design levels.

Additionally, this model should be revised as more efficient chilled water system components are developed. The results shown in this study only reflect system performance with components available today. As component performance changes the system performance will be affected. This may affect the comparative analysis presented here, but not the advantages of the single loop design over the primary-secondary system.

Multiple chiller analysis should be extended to include three and four chiller systems. Low system  $\Delta T$  complicates primary-secondary chiller scheduling to a greater degree when more chillers are involved. Single loop chiller scheduling is a function of load, while primary-secondary scheduling is tied to system flow rate. These effect of these different strategies would be pronounced by adding chillers to the systems.

## APPENDIX A

### BASE CASE, SINGLE LOOP MODEL

"Base Case, Single Loop, Chilled Water System"

{Section I. Procedures}

{A. Air Handler Procedures}

{This PROCEDURE determines the load based on out door dry bulb temperature}

Procedure loadprofile(T\_amb:Q\_ton\_ah)

IF (T\_amb<=60) Then

Q\_ton\_ah=20

Endif

IF (T\_amb>60) AND (T\_amb<=105) Then

Q\_ton\_ah=16/7\*T\_amb-117.143

Endif

IF (T\_amb>105) Then

Q\_ton\_ah=100

Endif

END

{This procedure determines the flow regime and assigns a Nusselt number and friction factor}

Procedure regime(Re\_D\_i\_ah,Pr\_w\_ah,D\_i\_ah,epsilon\_pipe\_ah:Nus\_ah,f\_i\_ah)

IF (Re\_D\_i\_ah<=2000) Then

Nus\_ah=4.36

{eqn 3.65 ref[1]}

f\_i\_ah=64/Re\_D\_i\_ah

{eqn 3.29 ref[1]}

Endif

IF (Re\_D\_i\_ah>2000) Then

Nus\_ah=0.023\*Re\_D\_i\_ah<sup>0.8</sup>\*Pr\_w\_ah<sup>0.4</sup>

{eqn 11.16 ref[2]}

f\_i\_ah=1/(-1.8\*log10(6.9/Re\_D\_i\_ah+(epsilon\_pipe\_ah/(D\_i\_ah\*3.7))<sup>1.11</sup>))<sup>2</sup>

{eqn 6.64a ref[5]}

Endif

END

{This PROCEDURE determines the relative heat capacities}

Procedure heat(C\_a\_ah,C\_w\_ah:C\_min\_ah,C\_max\_ah)

IF (C\_a\_ah/C\_w\_ah<=1) THEN

C\_min\_ah=C\_a\_ah

C\_max\_ah=C\_w\_ah

Endif

IF (C\_a\_ah/C\_w\_ah>1) THEN

C\_min\_ah=C\_w\_ah

C\_max\_ah=C\_a\_ah

ENDIF

End

```

{This procedure determines the heat exchanger efficiency given that the air flow is
unmixed and the water is mixed}
Procedure transfer(C_a_ah,C_w_ah,NTU_ah,C_r_ah:epsilon_ah)
IF (C_a_ah/C_w_ah>1) THEN
    epsilon_ah=1-exp((-1/C_r_ah)*(1-exp(-C_r_ah*NTU_ah)))    {eqn 11.35a ref[3]}
Endif
IF (C_a_ah/C_w_ah<=1) THEN
    epsilon_ah=(1/C_r_ah)*(1-exp(-C_r_ah*(1-exp(-NTU_ah))))    {eqn 11.34a ref[3]}
Endif
END

{This procedure determines the f for air flow over bare tubes.}
Procedure baretube(Re_D_o_ah:f_tube_ah)
IF (Re_D_o_ah<1000) THEN
    f_tube_ah=3.680886*Re_D_o_ah^(-0.3090731)                {Figure 7.13 ref[1]}
Endif
IF (Re_D_o_ah>=1000) THEN
    f_tube_ah=0.42275-5.53e-6*Re_D_o_ah-3.598e-10*Re_D_o_ah^2{Figure 7.13 ref[1]}
Endif
END

{This procedure determines the effective specific heat for air of the air handler}
Procedure latentheat(T_a_ah_in,T_a_ah_out,T_a_ah_ave,D_a_ah_in,HMRT_a_ah_in,P_atm,
P_a_ah_in,h_a_ah_in:HMRT_a_ah_out,h_a_ah_out,h_a_ah_out_eff,Cp_eff)
IF (T_a_ah_out>D_a_ah_in) Then
    HMRT_a_ah_out=HMRT_a_ah_in
    h_a_ah_out=enthalpy(AIRH2O,T=T_a_ah_out,P=P_atm,W=HMRT_a_ah_out)
    h_a_ah_out_eff=h_a_ah_out
    Cp_eff=specheat(AIRH2O,T=T_a_ah_ave,P=(P_a_ah_in+P_atm)/2,D=D_a_ah_in)
Endif
IF (T_a_ah_out<=D_a_ah_in) Then
    HMRT_a_ah_out=humrat(AIRH2O,T=T_a_ah_out,P=P_atm,R=1)
    h_a_ah_out=enthalpy(AIRH2O,T=T_a_ah_out,P=P_atm,R=1)
    h_a_ah_out_eff=h_a_ah_out+(HMRT_a_ah_in-
HMRT_a_ah_out)*enthalpy(WATER,P=P_atm,T=T_a_ah_out)
    Cp_eff=(h_a_ah_in-h_a_ah_out_eff)/(T_a_ah_in-T_a_ah_out)
Endif
END

```

{B. Chilled water reset procedure}

{This procedure first sets mass flow rate as a function of temperature, then at a specified outdoor dry bulb, it switches to make the evaporator exit temperature a function of flow rate.}

Procedure

reset(T\_amb,Q\_dot\_evap,h\_w\_evap\_in,h\_w\_evap\_out,P\_w\_evap\_out:m\_dot\_w\_evap,T\_w\_evap\_out)

IF (T\_amb=>77) Then

    T\_w\_evap\_out=44

    m\_dot\_w\_evap=Q\_dot\_evap/(h\_w\_evap\_in-h\_w\_evap\_out)

Endif

IF (T\_amb<77) Then

    m\_dot\_w\_evap=538300

    T\_w\_evap\_out=temperature(WATER,h=(h\_w\_evap\_in-Q\_dot\_evap/m\_dot\_w\_evap)

,P=P\_w\_evap\_out)

Endif

END

{C. Tower procedures.}

{This procedure determines the tower fan duty}

Procedure

towerfan(Q\_dot\_tow,epsilon\_tow,m\_dot\_a\_tow,h\_s\_w\_tow\_in,h\_a\_tow\_in,T\_w\_tow\_out1:

fanduty,T\_w\_tow\_out)

IF (T\_w\_tow\_out1>70) Then

    fanduty=1

    T\_w\_tow\_out=T\_w\_tow\_out1

Endif

IF (T\_w\_tow\_out1<70) AND ((Q\_dot\_tow-0.1\*epsilon\_tow\*m\_dot\_a\_tow\*(h\_s\_w\_tow\_in-h\_a\_tow\_in))/(0.9\*epsilon\_tow\*m\_dot\_a\_tow\*(h\_s\_w\_tow\_in-h\_a\_tow\_in))>0) Then

    fanduty=(Q\_dot\_tow-0.1\*epsilon\_tow\*m\_dot\_a\_tow\*(h\_s\_w\_tow\_in-h\_a\_tow\_in))/(0.9\*epsilon\_tow\*m\_dot\_a\_tow\*(h\_s\_w\_tow\_in-h\_a\_tow\_in))

    T\_w\_tow\_out=70

Endif

IF (T\_w\_tow\_out1<70) AND ((Q\_dot\_tow-0.1\*epsilon\_tow\*m\_dot\_a\_tow\*(h\_s\_w\_tow\_in-h\_a\_tow\_in))/(0.9\*epsilon\_tow\*m\_dot\_a\_tow\*(h\_s\_w\_tow\_in-h\_a\_tow\_in))<=0) Then

    fanduty=0

    T\_w\_tow\_out=T\_w\_tow\_out1

Endif

END

{Section II. Inputs}

Hours=1 {hrs}

T\_amb=95 {F}

ODWB=78 {F}

{Section III. Overall Calculations}

{A. Energy analysis}

W\_dot\_total=W\_dot\_comp+W\_dot\_pump+W\_dot\_pump\_cond+10\*W\_dot\_fan+W\_dot\_fan\_tow {btu/hr}

KW\_total=W\_dot\_total\*convert(btu/hr,kW) {kW}

KWh\_total=KW\_total\*Hours {kWh}

{These calculations sum to the inverse of the IER }

$$\text{IER\_chiller} = (\text{Hours}/\text{Hours\_total}) / (\text{KW\_comp}/\text{Q\_ton\_evap})$$

$$\text{IER\_system} = (\text{Hours}/\text{Hours\_total}) / (\text{kW\_total}/(10 * \text{Q\_ton\_ah}))$$

$$\text{IER\_aux\_evap} = (\text{Hours}/\text{Hours\_total}) / ((\text{W\_dot\_pump} + 10 * \text{W\_dot\_fan}) * \text{convert}(\text{btu}/\text{hr}, \text{kW}) / (10 * \text{Q\_ton\_ah}))$$

$$\text{Hours\_total} = 7132$$

{B. Entropy Analysis}

$$\text{S\_dot\_gen\_fan\_ah} = 10 * \text{m\_dot\_a\_ah} * (\text{s\_a\_fan\_out} - \text{s\_a\_fan\_in}) \quad \{\text{btu}/\text{hr R}\}$$

$$\text{S\_dot\_gen\_ah} = 10 * (\text{m\_dot\_w\_ah} * (\text{s\_w\_ah\_out} - \text{s\_w\_ah\_in}) - \text{Q\_load\_ah} / (\text{T\_amb} + 459.67)) \quad \{\text{btu}/\text{hr R}\}$$

$$\text{S\_dot\_gen\_pump} = \text{m\_dot\_w\_pump} * (\text{s\_pump\_out} - \text{s\_pump\_in}) \quad \{\text{btu}/\text{hr R}\}$$

$$\text{S\_dot\_gen\_evap} = \text{m\_dot\_w\_evap} * (\text{s\_w\_evap\_out} - \text{s\_w\_evap\_in}) - (\text{Q\_dot\_evap} / (\text{T\_evap} + 459.67))$$

$$\text{S\_dot\_gen\_cond} = \text{m\_dot\_w\_cond} * (\text{s\_w\_cond\_out} - \text{s\_w\_cond\_in}) - (\text{Q\_dot\_cond} / (\text{T\_cond} + 459.67))$$

$$\text{S\_dot\_gen\_comp} = (\text{W\_dot\_comp} - \text{W\_dot\_carnot}) / \text{T\_amb} \quad \{\text{btu}/\text{hr R}\}$$

$$\text{S\_dot\_gen\_tower} = \text{m\_dot\_w\_tow} * (\text{s\_w\_tow\_out} - \text{s\_w\_tow\_in}) - (\text{Q\_dot\_tow} / (\text{T\_w\_tow\_ave} + 459.67))$$

$$\text{S\_dot\_gen\_pump\_cond} = \text{m\_dot\_w\_cond} * (\text{s\_pump\_cond\_out} - \text{s\_pump\_cond\_in}) \quad \{\text{btu}/\text{hr R}\}$$

$$\text{S\_dot\_gen\_loop\_pri} = \text{m\_dot\_w\_pump} * (\text{s\_pump\_in} - \text{s\_w\_ah\_out} + \text{s\_w\_ah\_in} - \text{s\_w\_evap\_out})$$

$$\text{S\_dot\_gen\_loop\_cond} = \text{m\_dot\_w\_cond} * (\text{s\_pump\_cond\_in} - \text{s\_w\_tow\_out} + \text{s\_w\_tow\_in} - \text{s\_w\_cond\_out})$$

$$\text{S\_dot\_gen\_tot} = \text{S\_dot\_gen\_fan\_ah} + \text{S\_dot\_gen\_ah} + \text{S\_dot\_gen\_pump} + \text{S\_dot\_gen\_evap} + \text{S\_dot\_gen\_cond} +$$

$$\text{S\_dot\_gen\_comp} + \text{S\_dot\_gen\_tower} + \text{S\_dot\_gen\_pump\_cond} + \text{S\_dot\_gen\_loop\_pri} + \text{S\_dot\_gen\_loop\_cond}$$

$$\text{W\_dot\_lost} = \text{S\_dot\_gen\_tot} * \text{T\_amb} \quad \{\text{btu}/\text{hr}\}$$

{Section IV. Air handler model}

{A. Air handler fan}

{1. Fluid properties}

$$\text{T\_room} = 75 \quad \{\text{F}\}$$

$$\text{T\_a\_fan\_in} = \text{temperature}(\text{AIRH2O}, \text{h} = \text{h\_a\_fan\_in}, \text{P} = \text{P\_atm}, \text{W} = \text{HMRT\_fan\_in}) \quad \{\text{F}\}$$

$$\text{T\_a\_fan\_out} = \text{temperature}(\text{AIRH2O}, \text{h} = \text{h\_a\_fan\_out}, \text{P} = \text{P\_atm} + \text{DELTA P\_a\_ah}, \text{W} = \text{HMRT\_fan\_in})$$

$$\text{HMRT\_amb} = \text{humrat}(\text{AIRH2O}, \text{T} = \text{T\_amb}, \text{P} = \text{P\_atm}, \text{B} = \text{ODWB})$$

$$\text{HMRT\_room} = \text{humrat}(\text{AIRH2O}, \text{T} = \text{T\_room}, \text{P} = \text{P\_atm}, \text{R} = \text{R\_room})$$

$$\text{HMRT\_fan\_in} = 0.85 * \text{HMRT\_room} + 0.15 * \text{HMRT\_amb}$$

$$\text{R\_room} = .5549$$

$$\text{h\_amb} = \text{enthalpy}(\text{AIRH2O}, \text{T} = \text{T\_amb}, \text{P} = \text{P\_atm}, \text{B} = \text{ODWB}) \quad \{\text{btu}/\text{lbm}\}$$

$$\text{h\_room} = \text{enthalpy}(\text{AIRH2O}, \text{T} = \text{T\_room} + 5, \text{P} = \text{P\_atm}, \text{R} = \text{R\_room}) \quad \{\text{btu}/\text{lbm}\}$$

$$\text{h\_a\_fan\_in} = 0.85 * \text{h\_room} + 0.15 * \text{h\_amb} \quad \{\text{btu}/\text{lbm}\}$$

$$\text{h\_a\_fan\_out\_rev} = \text{enthalpy}(\text{AIRH2O}, \text{P} = \text{P\_atm} + \text{DELTA P\_a\_ah}, \text{T} = \text{T\_a\_fan\_out\_rev}, \text{W} = \text{HMRT\_fan\_in})$$

$$\text{s\_a\_fan\_in} = \text{entropy}(\text{AIRH2O}, \text{T} = \text{T\_a\_fan\_in}, \text{P} = \text{P\_atm}, \text{W} = \text{HMRT\_fan\_in}) \quad \{\text{btu}/\text{lbm R}\}$$

$$\text{s\_a\_fan\_in} = \text{entropy}(\text{AIRH2O}, \text{T} = \text{T\_a\_fan\_out\_rev}, \text{P} = \text{P\_atm} + \text{DELTA P\_a\_ah}, \text{W} = \text{HMRT\_fan\_in})$$

$$\text{s\_a\_fan\_out} = \text{entropy}(\text{AIRH2O}, \text{T} = \text{T\_a\_fan\_out}, \text{P} = \text{P\_atm} + \text{DELTA P\_a\_ah}, \text{W} = \text{HMRT\_fan\_in})$$

{2. Fan Calculations}

$$\text{eta\_fan} = .65$$

$$\text{eta\_fan} = (\text{h\_a\_fan\_in} - \text{h\_a\_fan\_out\_rev}) / (\text{h\_a\_fan\_in} - \text{h\_a\_fan\_out})$$

$$\text{W\_dot\_fan} = -\text{m\_dot\_a\_ah} * (\text{h\_a\_fan\_in} - \text{h\_a\_fan\_out}) \quad \{\text{btu}/\text{hr}\}$$

$$\text{KW\_fan} = \text{W\_dot\_fan} * \text{convert}(\text{btu}/\text{hr}, \text{kW}) \quad \{\text{kW}\}$$

{B. Inputs for Air Handler}

$h_{w\_ah\_in} = h_{w\_evap\_out}$  {btu/lbm}  
 $h_{a\_fan\_out} = h_{a\_ah\_in}$  {btu/lbm}  
 $P_{a\_ah\_in} = P_{atm} + \Delta P_{a\_ah}$  {psia}  
 $P_{w\_ah\_in} = P_{w\_evap\_out} - (\text{Head}_{pipe}/2 + \text{Elev}_{load} + \text{Head}_{valve}) * \rho_{w\_ah} * g * \text{convert}(\text{lbm}/\text{ft}^3 * \text{s}^2, \text{psia})$   
 $\text{Head}_{valve} = 20 - \text{Head}_{coil}$  {ft}  
 $\text{HMRT}_{a\_ah\_in} = \text{HMRT}_{fan\_in}$

{C. Air Handler overall heat transfer coefficient calculation}

$1/UA_{tot\_ah} = 1/(h_{i\_ah} * A_{i\_ah}) + \ln(D_{o\_ah}/D_{i\_ah}) / (2 * \pi * k_{pipe} * \text{Length}_{ah} * n_{row} * n_{column})$   
 $+ 1/(h_{o\_ah} * A_{o\_ah} * \eta_{o\_ah})$  {eqn 11.5 ref[3]}

{D. Geometry}

$\text{Length}_{ah} = 7.555$  {ft}  
 $\text{Height}_{ah} = 5$  {ft}  
 $\text{Depth}_{ah} = 8.5 * \text{convert}(\text{in}, \text{ft})$  {ft}  
 $\text{fin}_{pitch} = 12 / \text{convert}(\text{in}, \text{ft})$  {1/ft}  
 $D_{o\_ah} = .75 * \text{convert}(\text{in}, \text{ft})$  {ft}  
 $D_{i\_ah} = .666 * \text{convert}(\text{in}, \text{ft})$  {ft}  
 $t_{fin} = .006 * \text{convert}(\text{in}, \text{ft})$  {ft}  
 $n_{row} = 4$   
 $n_{column} = 40$   
 $\text{Elev}_{load} = 0$  {ft}

{E. Airside calculations}

{1. Air properties}

Call latentheat( $T_{a\_ah\_in}, T_{a\_ah\_out}, T_{a\_ah\_ave}, D_{a\_ah\_in}, \text{HMRT}_{a\_ah\_in}, P_{atm}, P_{a\_ah\_in}, h_{a\_ah\_in}, \text{HMRT}_{a\_ah\_out}, h_{a\_ah\_out}, h_{a\_ah\_out\_eff}, C_{p\_eff}$ )  
 $\text{HMRT}_{a\_ah\_ave} = (\text{HMRT}_{a\_ah\_in} + \text{HMRT}_{a\_ah\_out}) / 2$   
 $k_{a\_ah} = \text{conductivity}(\text{AIRH2O}, T = T_{a\_ah\_ave}, P = P_{a\_ah\_ave}, W = \text{HMRT}_{a\_ah\_ave})$  {Btu/hr-ft-R}  
 $\mu_{a\_ah} = \text{viscosity}(\text{AIRH2O}, T = T_{a\_ah\_ave}, P = P_{a\_ah\_ave}, W = \text{HMRT}_{a\_ah\_ave})$  {lbm/ft-hr}  
 $\rho_{a\_ah} = \text{density}(\text{AIRH2O}, T = T_{a\_ah\_ave}, P = P_{a\_ah\_ave}, W = \text{HMRT}_{a\_ah\_ave})$  {lbm/ft^3}  
 $v_{m\_ah} = 1 / \rho_{a\_ah}$  {ft^3/lbm}  
 $Pr_{a\_ah} = C_{p\_eff} * \mu_{a\_ah} / k_{a\_ah}$

{2. Air flow properties}

$G_{a\_ah} = \dot{m}_{a\_ah} / (\sigma_{ah} * A_{fr\_ah})$  {lbm/ft^2-hr} {eqn 11.37 ref[3]}  
 $Re_{D_{o\_ah}} = G_{a\_ah} * D_{o\_ah} / \mu_{a\_ah}$  {eqn 14.37 ref[4]}  
 $Re_{L_{ah}} = G_{a\_ah} * b_{ah} / \mu_{a\_ah}$  {eqn ref[4]}

{3. Airside geometry calculations}

$a_{ah} = \text{Height}_{ah} / n_{column}$  {ft}  
 $b_{ah} = \text{Depth}_{ah} / n_{row}$  {ft}  
 $A_{fr\_ah} = \text{Height}_{ah} * \text{Length}_{ah}$  {ft^2}  
 $\sigma_{ah} = (a_{ah} - D_{o\_ah}) / a_{ah}$   
 $A_{f\_ah} = (2 * a_{ah} * b_{ah} * \pi * D_{o\_ah}^2 / 2) * \text{fin}_{pitch} * \text{Length}_{ah} * n_{row} * n_{column}$  {ft^2}  
 $A_{t\_ah} = \pi * D_{o\_ah} * \text{Length}_{ah} * n_{row} * n_{column}$  {ft^2}  
 $A_{o\_ah} = A_{f\_ah} + A_{t\_ah}$  {ft^2}

{4. Airside Heat Transfer Calculations}

$h_{o\_ah} = (Cp\_eff * G_{a\_ah} * j_n / Pr_{a\_ah}^{(2/3)})$  {Btu/ft<sup>2</sup>-hr-R} {eqn14.36 ref[4]}

$j_4 = 0.2618 * JP + 0.0014$  {eqn ref[4]}

$JP = Re_{D_{o\_ah}}^{-0.4} * (A_{o\_ah} / A_{t\_ah})^{-0.15}$  {eqn14.46 ref[4]}

$j_n / j_4 = (1 - 1280 * n_{row} * Re_{L\_ah}^{-1.2}) / (1 - 1280 * 4 * Re_{L\_ah}^{-1.2})$  {eqn14.50 ref[4]}

{5. Fin Calculations}

$eta_{o\_ah} = 1 - (A_{f\_ah} / A_{o\_ah}) * (1 - eta_{fin})$  {eqn 11.3 ref[3]}

$eta_{fin} = .95$

{F. Waterside calculations}

{1. Water properties}

$Cp_{w\_ah} = specheat(WATER, T = T_{w\_ah\_ave}, P = P_{atm})$  {Btu/lbm-R}

$k_{w\_ah} = conductivity(WATER, T = T_{w\_ah\_ave}, P = P_{atm})$  {Btu/hr-ft-R}

$mu_{w\_ah} = viscosity(WATER, T = T_{w\_ah\_ave}, P = P_{atm})$  {lbm/ft-hr}

$rho_{w\_ah} = density(WATER, T = T_{w\_ah\_ave}, P = P_{atm})$  {lbm/ft<sup>3</sup>}

$Pr_{w\_ah} = Cp_{w\_ah} * mu_{w\_ah} / k_{w\_ah}$

{2. Flow properties}

$G_{w\_ah} = m_{dot\_w\_ah} / ((n_{column} - 1) * pi * D_{i\_ah}^2 / 4)$  {lbm/ft<sup>2</sup>-hr}

$Re_{D_{i\_ah}} = G_{w\_ah} * D_{i\_ah} / mu_{w\_ah}$  {eqn 11.10 ref[2]}

{3. Waterside geometry calculations}

$A_{i\_ah} = pi * D_{i\_ah} * Length_{ah} * n_{row} * n_{column}$  {ft<sup>2</sup>}

{4. Waterside heat transfer calculations}

Call Regime( $Re_{D_{i\_ah}}, Pr_{w\_ah}, D_{i\_ah}, epsilon_{pipe\_ah}, Nus_{ah}, f_{i\_ah}$ )

$h_{i\_ah} = Nus_{ah} * k_{w\_ah} / D_{i\_ah}$  {Btu/ft<sup>2</sup>-hr-R} {eqn 3.66 ref[1]}

{G. Pipe and fin properties}

$k_{pipe} = 401 * convert(W/m*K, Btu/hr*ft*R)$  {Btu/hr-ft-R}

$k_{fin} = 237 * convert(W/m*K, Btu/hr*ft*R)$  {Btu/hr-ft-R}

$epsilon_{pipe\_ah} = .00015$  {ft}

{H. Load conditions.}

CALL loadprofile( $T_{amb}, Q_{ton\_ah}$ )

CALL Transfer( $C_{a\_ah}, C_{w\_ah}, NTU_{ah}, C_{r\_ah}, epsilon_{ah}$ )

Call heat( $C_{a\_ah}, C_{w\_ah}, C_{min\_ah}, C_{max\_ah}$ )

$Q_{load\_ah} = Q_{ton\_ah} * convert(ton, Btu/hr)$  {Btu/hr}

$Q_{load\_ah} = m_{dot\_w\_ah} * (h_{w\_ah\_out} - h_{w\_ah\_in})$  {Btu/hr}

$Q_{load\_ah} = m_{dot\_a\_ah} * Cp\_eff * DELTAT_{a\_ah}$  {Btu/hr}

$Q_{load\_ah} = epsilon_{ah} * C_{min\_ah} * (T_{a\_ah\_in} - T_{w\_ah\_in})$  {Btu/hr}

$Q_{max\_ah} = C_{min\_ah} * (T_{a\_ah\_in} - T_{w\_ah\_in})$  {Btu/hr}

$C_{w\_ah} = m_{dot\_w\_ah} * cp_{w\_ah}$  {Btu/hr R}

$C_{a\_ah} = m_{dot\_a\_ah} * Cp\_eff$  {Btu/hr R}

$C_{r\_ah} = C_{min\_ah} / C_{max\_ah}$

$NTU_{ah} = UA_{tot\_ah} / C_{min\_ah}$  {eqn 11.25 ref[3]}

## {I. Temperature}

$T_{w\_ah\_in}$ =temperature(WATER,H=h\_w\_ah\_in,P=P\_w\_ah\_in) {F}  
 $T_{w\_ah\_out}$ =temperature(WATER,h=h\_w\_ah\_out,P=P\_w\_ah\_out) {F}  
 $DELTA T_{w\_ah}$ = $T_{w\_ah\_out}$ - $T_{w\_ah\_in}$  {F}  
 $DELTA T_{a\_ah}$ = $T_{a\_ah\_in}$ - $T_{a\_ah\_out}$  {F}  
 $T_{w\_ah\_ave}$ =( $T_{w\_ah\_in}$ - $T_{w\_ah\_out}$ )/ln( $T_{w\_ah\_in}$ / $T_{w\_ah\_out}$ ) {F}  
 $T_{a\_ah\_ave}$ =( $T_{a\_ah\_in}$ - $T_{a\_ah\_out}$ )/ln( $T_{a\_ah\_in}$ / $T_{a\_ah\_out}$ ) {F}  
 $T_{a\_ah\_in}$ =temperature(AIRH2O,h=h\_a\_ah\_in,P=P\_a\_ah\_in,W=HMRT\_a\_ah\_in) {F}  
 $T_{a\_ah\_out}$ =58 {F}  
 $D_{a\_ah\_in}$ =dewpoint(AIRH2O,T= $T_{a\_ah\_in}$ ,P=P\_a\_ah\_in,W=HMRT\_a\_ah\_in) {F}

## {J. Entropy}

$s_{w\_ah\_in}$ =entropy(WATER,P=P\_w\_ah\_in,T= $T_{w\_ah\_in}$ ) {btu/lbm R}  
 $s_{w\_ah\_out}$ =entropy(WATER,P=P\_w\_ah\_out,T= $T_{w\_ah\_out}$ ) {btu/lbm R}

## {K. Flow rates}

## {1. Water flow}

$V_{w\_ah}$ =FPS\_w\_ah\*(n\_column-1)\*pi\*D\_i\_ah^2/4\*convert(1/s,1/min) {cfm}  
 $GPM_{w\_ah}$ = $V_{w\_ah}$ \*convert(ft^3,gal) {gpm}  
 $m_{dot\_w\_ah}$ = $V_{w\_ah}$ \*rho\_w\_ah\*60 {lbm/hr}

## {2. Air flow}

$V_{a\_ah}$ =FPM\_a\_ah\*Length\_ah\*Height\_ah {cfm}  
 $m_{dot\_a\_ah}$ = $V_{a\_ah}$ \*rho\_a\_ah\*60 {lbm/hr}  
 $FPH_{a\_ah}$ =FPM\_a\_ah\*convert(1/min,1/hr) {ft/hr}  
 $FPS_{a\_ah}$ =FPM\_a\_ah\*convert(1/min,1/s) {ft/s}

## {L. Pressure drop calculations}

## {1. Waterside pressure drop}

$DELTA P_{i\_ah}$ =rho\_w\_ah\*g\*Head\_coil\*convert(lbm/ft\*s^2,psia) {psia}  
 $DELTA P_{tube\_ah}$ =f\_i\_ah\*Length\_ah\*n\_row/D\_i\_ah\*(rho\_w\_ah\*FPS\_w\_ah^2/2)  
\*convert(lbm/s^2\*ft,psia) {psia} {eqn 3.27 ref[1]}  
 $Head_{tube\_ah}$ = $DELTA P_{tube\_ah}$ /(rho\_w\_ah\*g)\*convert(psia\*ft^2\*s^2/lbm,ft) {eqn 6.25 ref[6]}  
 $Head_{bend}$ =5\*K\*FPS\_w\_ah^2/(2\*g) {ft}  
 $Head_{coil}$ = $Head_{tube\_ah}$ + $Head_{bend}$  {ft}  
 $P_{w\_ah\_out}$ = $P_{w\_ah\_in}$ - $DELTA P_{i\_ah}$  {psia}  
 $P_{w\_ah\_ave}$ =( $P_{w\_ah\_in}$ + $P_{w\_ah\_out}$ )/2 {psia}  
 $K=4$

## {2. Airside pressure drop}

CALL Baretube(Re\_D\_o\_ah:f\_tube\_ah)  
 $DELTA P_{a\_ah}$ =deltaP\_o\_ah\*convert(lbm/hr^2\*ft,psia) {psia}  
 $P_{a\_ah\_ave}$ =( $P_{a\_ah\_in}$ + $P_{atm}$ )/2 {psia}  
 $f_{f\_ah}$ =(deltaP\_o\_ah-deltaP\_t\_ah)/(v\_m\_ah\*G\_a\_ah^2/(2\*sigma\_ah)) {eqn 7 ref[6]}  
 $f_{f\_ah}$ =1.7\*Re\_L\_ah^(-0.5) {eqn 9 ref[6]}  
 $a_{ah\_star}$ =a\_ah/D\_o\_ah {eqn 7.114 ref[1]}  
 $b_{ah\_star}$ =b\_ah/D\_o\_ah {eqn 7.114 ref[1]}  
 $Chi_{ah}$ =1 {Fig 7.13 ref[1]}  
 $delta P_{t\_ah}$ =n\_row\*f\_tube\_ah\*Chi\_ah\*(rho\_a\_ah\*(FPH\_a\_ah/sigma\_ah)^2/2) {lbm/hr^2 ft}  
{eqn 7.113 ref[1]}

{Section V. Primary pump model}

{A. Inputs for primary pump}

h\_pump\_in=h\_w\_ah\_out {btu/lbm}  
m\_dot\_w\_pump=10\*m\_dot\_w\_ah {lbm/hr}

{B. Pressure calculations}

DELTA\_P\_pump=rho\_w\_pump\*g\*Head\_loop\*convert(lbm/ft\*S^2,psia){psia}  
P\_pump\_out=P\_min+DELTA\_P\_pump {psia}  
P\_pump\_ave=P\_min+DELTA\_P\_pump/2 {psia}  
P\_min=125 {psia}

{C. Affinity calculations}

N\_pump\_act=N\_pump\_design\*(GPM\_pump/GPM\_design) {rpm} {eqn 6.1 ref[7]}  
N\_pump\_act=N\_pump\_design\*(Head\_loop/Head\_design)^(0.5) {rpm} {eqn 6.2 ref[7]}  
N\_pump\_design=1180 {rpm} {ref[8]}

{D. Pump curves}

Head\_design=103.3620 + 0.01053070\*GPM\_design - 0.00000631\*GPM\_design^2  
eta\_pump=(0.08592879 + 0.00059656\*GPM\_design - 0.00000012\*GPM\_design^2)\*  
(0.8158200 + 0.4025401\*N\_pump\_act/N\_pump\_design - 0.2183601\*(N\_pump\_act/N\_pump\_design)^2)  
eta\_motor=0.0498386+1.846339\*(N\_pump\_act/N\_pump\_design)-  
1.029\*(N\_pump\_act/N\_pump\_design)^2  
eta\_pump=(h\_pump\_out\_rev-h\_pump\_in)/(h\_pump\_out-h\_pump\_in)  
W\_dot\_pump=m\_dot\_w\_pump\*(h\_pump\_out-h\_pump\_in)/eta\_motor {Btu/hr}  
KW\_pump=W\_dot\_pump\*convert(Btu/hr,kW) {kW}

{E. Head calculation}

Head\_pipe=f\_loop\*Length\_loop/D\_i\_pipe\*(FPS\_pump^2/2)/g {ft} {eqn 6.30 ref[5]}  
Head\_loop=Head\_pipe+Head\_coil+Head\_evap+Head\_valve {ft}  
f\_loop=1/(-1.8\*log10(6.9/Re\_D\_i\_pump+(epsilon\_pipe/(D\_i\_pipe\*3.7))^1.11))^2 {eqn 6.64a ref[5]}

{F. Pipe geometry}

D\_i\_pipe=10\*convert(in,ft) {ft}  
Length\_loop=2000 {ft}  
epsilon\_pipe=.00015 {ft}

{G. Flow properties}

GPM\_pump=m\_dot\_w\_pump/rho\_w\_pump\*convert(ft^3/hr,gpm) {gpm}  
CFM\_pump=GPM\_pump\*convert(gpm,cfm) {ft^3/min}  
FPM\_pump=CFM\_pump/(pi\*D\_i\_pipe^2/4) {ft/min}  
FPS\_pump=FPM\_pump\*convert(1/min,1/s) {ft/s}  
FPH\_pump=FPM\_pump\*convert(1/min,1/hr) {ft/hr}  
Re\_D\_i\_pump=rho\_w\_pump\*FPH\_pump\*D\_i\_pipe/mu\_w\_pump

{H. Fluid properties}

rho\_w\_pump=density(WATER,T=T\_pump\_ave,P=P\_pump\_ave) {lbm/ft^3}  
mu\_w\_pump=viscosity(WATER,T=T\_pump\_ave,P=P\_pump\_ave) {lbm/ft hr}

## {I. Temperatures}

T\_pump\_in=temperature(WATER,P=P\_min,h=h\_pump\_in) {F}  
 T\_pump\_ave=(T\_pump\_out-T\_pump\_in)/ln((T\_pump\_out)/(T\_pump\_in)) {F}  
 T\_pump\_out\_rev=temperature(WATER,P=P\_pump\_out,s=s\_pump\_in) {F}  
 T\_pump\_out=temperature(WATER,P=P\_pump\_out,H=h\_pump\_out) {F}

## {J. Enthalpy and entropy}

h\_pump\_out\_rev=enthalpy(WATER,P=P\_pump\_out,T=T\_pump\_out\_rev) {Btu/lbm}  
 s\_pump\_in=entropy(WATER,P=P\_min,T=T\_pump\_in) {Btu/lb R}  
 s\_pump\_out=entropy(WATER,P=P\_pump\_out,T=T\_pump\_out) {Btu/lb R}

## {Section VI. Centrifugal chiller model}

## {A. Chiller inputs}

## {1. Evaporator Side}

P\_w\_evap\_in=P\_pump\_out {psia}  
 h\_w\_evap\_in=h\_pump\_out {btu/lbm}  
 m\_dot\_w\_evap=m\_dot\_w\_pump {lbm/lbm}

## {2. Condenser Side}

P\_w\_cond\_in=P\_pump\_cond\_out {psia}  
 h\_w\_cond\_in=h\_pump\_cond\_out {btu/lbm}

## {B. Compressor}

W\_dot\_carnot=Q\_dot\_evap\*((T\_cond+459.67)/(T\_evap+459.67)-1) {btu/hr}  
 KW\_comp=W\_dot\_comp\*convert(Btu/hr,kW) {kW}  
 W\_dot\_comp=a+b\*W\_dot\_carnot+c\*W\_dot\_carnot^2  
 a=3042.991 + 705.2175\*Q\_ton\_evap + 0.9521675\*Q\_ton\_evap^2  
 b=1.228996 - 0.00438602\*Q\_ton\_evap + 0.00000203\*Q\_ton\_evap^2  
 c=0.00000279 - 3.146E-09\*Q\_ton\_evap + 1.310E-12\*Q\_ton\_evap^2

## {C. Evaporator}

## {1. Evaporator heat transfer calculations}

Call

Reset(T\_amb,Q\_dot\_evap,h\_w\_evap\_in,h\_w\_evap\_out,P\_w\_evap\_out:m\_dot\_w\_evap,T\_w\_evap\_out)  
 Q\_dot\_evap=Q\_ton\_evap\*convert(ton,Btu/hr) {Btu/hr}  
 "Q\_dot\_evap=m\_dot\_w\_evap\*(h\_w\_evap\_in-h\_w\_evap\_out) {Btu/hr} {Blocked out for reset}"  
 Q\_dot\_evap=epsilon\_evap\*m\_dot\_w\_evap\*C\_w\_evap\*(T\_w\_evap\_in-T\_w\_evap) {Btu/hr}

epsilon\_evap=1-exp(-NTU\_evap) {eqn 11.19 ref[3]}  
 NTU\_evap=UA\_evap/(m\_dot\_w\_evap\*C\_w\_evap) {eqn 11.30a ref[3]}

1/UA\_evap=1/(hA\_i\_evap)+1/(hA\_o\_evap) {eqn 11.25 ref[3]}

hA\_i\_evap=6213\*(Re\_D\_i\_evap^0.5334881)\*Pr\_w\_evap^0.3  
 hA\_o\_evap=180935.0 + 6243.157\*Q\_ton\_evap - 1.474305\*Q\_ton\_evap^2

## {2. Evaporator pressure drop calculations}

f\_i\_evap=1/(-1.8\*log10(6.9/Re\_D\_i\_evap+(epsilon\_pipe\_evap/(D\_i\_evap\*3.7))^1.11))^2  
 {eqn 6.64a ref[5]}

DELTA\_P\_evap=Head\_evap\*rho\_w\_evap\*g\*convert(lbm/ft\*s^2,psia) {psia}  
 Head\_evap=f\_i\_evap\*Length\_evap\*n\_pass\_evap/D\_i\_evap\*(FPS\_evap^2/2)/g {ft}

{eqn 6.30 ref[5]}

P\_evap\_ave=P\_min+DELTA\_P\_evap/2 {psia}

P\_w\_evap\_out=P\_w\_evap\_in-DELTA\_P\_evap {psia}

## {3. Evaporator geometry}

$D_i_{evap}=0.824*\text{convert}(\text{in},\text{ft})$  {ft}  
 Length<sub>evap</sub>=14.2 {ft}  
 n<sub>tubes<sub>evap</sub></sub>=215  
 n<sub>pass<sub>evap</sub></sub>=4  
 epsilon<sub>pipe<sub>evap</sub></sub>=.00038731 {ft}

## {4. Evaporator fluid properties}

$C_{w_{evap}}=\text{specheat}(\text{WATER},T=T_{w_{evap\_ave}},P=P_{evap\_ave})$  {Btu/lbm R}  
 $\rho_{w_{evap}}=\text{density}(\text{WATER},T=T_{w_{evap\_ave}},P=P_{evap\_ave})$  {lbm/ft<sup>3</sup>}  
 $\mu_{w_{evap}}=\text{viscosity}(\text{WATER},T=T_{w_{evap\_ave}},P=P_{evap\_ave})$  {lbm/ft hr}  
 $k_{w_{evap}}=\text{conductivity}(\text{WATER},T=T_{w_{evap\_ave}},P=P_{evap\_ave})$  {Btu/ft hr R}  
 $Pr_{w_{evap}}=C_{w_{evap}}*\mu_{w_{evap}}/k_{w_{evap}}$   
 $Re_{D_i_{evap}}=\rho_{w_{evap}}*FPH_{evap}*D_i_{evap}/\mu_{w_{evap}}$

## {5. Evaporator flow rate}

$GPM_{w_{evap}}=m_{dot_{w_{evap}}}/\rho_{w_{evap}}*\text{convert}(\text{ft}^3/\text{hr},\text{gpm})$  {gal/min}  
 $CFM_{w_{evap}}=GPM_{w_{evap}}*\text{convert}(\text{gpm},\text{cfm})$  {ft<sup>3</sup>/min}  
 $FPM_{evap}=CFM_{w_{evap}}/((\pi*D_i_{evap}^2/4)*n_{tubes_{evap}})$  {ft/min}  
 $FPS_{evap}=FPM_{evap}*\text{convert}(1/\text{min},1/\text{s})$  {ft/s}  
 $FPH_{evap}=FPM_{evap}*\text{convert}(1/\text{min},1/\text{hr})$  {ft/hr}

## {6. Evaporator Temperatures}

$T_{w_{evap\_out}}=44$  {F} {Blocked out for reset}  
 $T_{w_{evap\_in}}=\text{temperature}(\text{WATER},h=h_{w_{evap\_in}},P=P_{w_{evap\_in}})$  {F}  
 $T_{w_{evap\_ave}}=(T_{w_{evap\_in}}-T_{w_{evap\_out}})/\ln(T_{w_{evap\_in}}/T_{w_{evap\_out}})$  {F}

## {7. Enthalpy and entropy}

$h_{w_{evap\_out}}=\text{enthalpy}(\text{WATER},T=T_{w_{evap\_out}},P=P_{w_{evap\_out}})$  {btu/lbm}  
 $s_{w_{evap\_in}}=\text{entropy}(\text{WATER},h=h_{w_{evap\_in}},P=P_{w_{evap\_in}})$  {btu/lbm R}  
 $s_{w_{evap\_out}}=\text{entropy}(\text{WATER},h=h_{w_{evap\_out}},P=P_{w_{evap\_out}})$  {btu/lbm R}

## {D. Condenser}

## {1. Condenser UA calculation}

$Q_{dot_{cond}}=\epsilon_{cond}*m_{dot_{w_{cond}}}*C_{w_{cond}}*(T_{cond}-T_{w_{cond\_in}})$  {Btu/hr}  
 {eqn 11.23 ref[3]}  
 $Q_{dot_{cond}}=m_{dot_{w_{cond}}}*C_{w_{cond}}*(T_{w_{cond\_out}}-T_{w_{cond\_in}})$  {Btu/hr}  
 $Q_{dot_{cond}}=Q_{dot_{evap}}+W_{dot_{comp}}$  {Btu/hr}  
 $Q_{ton_{cond}}=Q_{dot_{cond}}*\text{convert}(\text{btu/hr},\text{ton})$  {tons}  
 $\epsilon_{cond}=1-\exp(-NTU_{cond})$  {eqn 11.30 ref[3]}  
 $NTU_{cond}=UA_{cond}/(m_{dot_{w_{cond}}}*C_{w_{cond}})$   
 $UA_{cond\_1}=1845702 + 22792.36*T_{cond} - 96.24830*T_{cond}^2$   
 $UA_{cond\_2}=1.059937 - 0.00009226*Q_{ton_{cond}} + 0.00000001*Q_{ton_{cond}}^2$   
 $UA_{cond}=UA_{cond\_1}*UA_{cond\_2}$

## {2. Condenser fluid properties}

$\rho_{w_{cond}}=\text{density}(\text{WATER},T=T_{w_{cond\_ave}},P=P_{w_{cond\_ave}})$  {lbm/ft<sup>3</sup>}  
 $C_{w_{cond}}=\text{specheat}(\text{WATER},T=T_{w_{cond\_ave}},P=P_{w_{cond\_ave}})$  {Btu/lbm R}  
 $\mu_{w_{cond}}=\text{viscosity}(\text{WATER},T=T_{w_{cond\_ave}},P=P_{w_{cond\_ave}})$  {lbm/ft hr}  
 $k_{w_{cond}}=\text{conductivity}(\text{WATER},T=T_{w_{cond\_ave}},P=P_{w_{cond\_ave}})$  {Btu/hr ft R}



## {E. Flow rates}

$GPM\_pump\_cond = m\_dot\_w\_pump\_cond / rho\_w\_pump\_cond * convert(ft^3/hr, gpm)$  {gpm}  
 $CFM\_pump\_cond = GPM\_pump\_cond * convert(gpm, cfm)$  {ft<sup>3</sup>/min}  
 $FPM\_pump\_cond = CFM\_pump\_cond / (pi * D\_i\_pipe\_cond^2 / 4)$  {ft/min}  
 $FPS\_pump\_cond = FPM\_pump\_cond * convert(1/min, 1/s)$  {ft/s}  
 $FPH\_pump\_cond = FPM\_pump\_cond * convert(1/min, 1/hr)$  {ft/hr}  
 $Re\_D\_i\_pump\_cond = rho\_w\_pump\_cond * FPH\_pump\_cond * D\_i\_pipe\_cond / mu\_w\_pump\_cond$

## {F. Fluid Properties}

$rho\_W\_pump\_cond = density(WATER, T=T\_pump\_cond\_ave, P=P\_pump\_cond\_ave)$  {lbm/ft<sup>3</sup>}  
 $mu\_W\_pump\_cond = viscosity(WATER, T=T\_pump\_cond\_ave, P=P\_pump\_cond\_ave)$  {lbm/ft hr}

## {G. Temperatures}

$T\_pump\_cond\_in = temperature(WATER, h=h\_pump\_cond\_in, P=P\_pump\_cond\_ave)$  {F}  
 $T\_pump\_cond\_ave = (T\_pump\_cond\_out - T\_pump\_cond\_in) / ln((T\_pump\_cond\_out) / (T\_pump\_cond\_in))$   
 $T\_pump\_cond\_out\_rev = temperature(WATER, P=P\_pump\_cond\_out, s=s\_pump\_cond\_in)$  {F}  
 $T\_pump\_cond\_out = temperature(WATER, P=P\_pump\_cond\_out, H=h\_pump\_cond\_out)$  {F}

## {H. Enthalpy and entropy}

$h\_pump\_cond\_out\_rev = enthalpy(WATER, P=P\_pump\_cond\_out, T=T\_pump\_cond\_out\_rev)$  {btu/lbm}  
 $s\_pump\_cond\_in = entropy(WATER, P=P\_pump\_cond\_in, T=T\_pump\_cond\_in)$  {btu/lb R}  
 $s\_pump\_cond\_out = entropy(WATER, P=P\_pump\_cond\_out, T=T\_pump\_cond\_out)$  {btu/lb R}

## {Section VIII. Cooling tower model}

## {A. Inputs for cooling tower}

$h\_w\_tow\_in = h\_w\_cond\_out$  {btu/lbm}  
 $m\_dot\_w\_tow = m\_dot\_w\_cond$  {lbm/hr}

## {B. Cooling tower calculations}

Call towerfan(Q\_dot\_tow, epsilon\_tow, m\_dot\_a\_tow, h\_s\_w\_tow\_in, h\_a\_tow\_in, T\_w\_tow\_out, fanduty, T\_w\_tow\_out)  
 $Q\_dot\_tow = 0.9 * fanduty * epsilon\_tow * m\_dot\_a\_tow * (h\_s\_w\_tow\_in - h\_a\_tow\_in) + 0.1 * epsilon\_tow * m\_dot\_a\_tow * (h\_s\_w\_tow\_in - h\_a\_tow\_in)$  {Btu/hr}  
 $Q\_dot\_tow = m\_dot\_w\_tow * (h\_w\_tow\_in - h\_w\_tow\_out)$  {btu/hr}  
 $epsilon\_tow = (1 - exp(-NTU\_tow * (1 - Cr\_tow))) / (1 - Cr\_tow * exp(-NTU\_tow * (1 - Cr\_tow)))$  {eqn 11.30a ref[3]}  
 $NTU\_tow = 1.3936 * (m\_dot\_w\_tow / m\_dot\_a\_tow)^{1.7044}$  {eqn II.17 ref[9]}  
 $Cr\_tow = (m\_dot\_a\_tow * Cs) / (m\_dot\_w\_tow * Cp\_w\_tow)$  {eqn II.12 ref[9]}  
 $Cs = (h\_s\_w\_tow\_in - h\_s\_w\_tow\_out) / (T\_w\_tow\_in - T\_w\_tow\_out)$  {btu/lbm R} {eqn II.13 ref[9]}

## {C. Water properties}

$rho\_w\_tow = density(WATER, T=T\_w\_tow\_ave, P=P\_atm)$  {lbm/ft<sup>3</sup>}  
 $Cp\_w\_tow = specheat(WATER, T=T\_w\_tow\_ave, P=P\_atm)$  {Btu/lbm R}  
 $h\_s\_w\_tow\_in = enthalpy(AIRH2O, R=1, T=T\_w\_tow\_in, P=P\_atm)$  {Btu/lbm}  
 $h\_s\_w\_tow\_out = enthalpy(AIRH2O, R=1, T=T\_w\_tow\_out, P=P\_atm)$  {Btu/lbm}

## {D. Air Properties}

$rho\_a\_tow = density(AIRH2O, B=ODWB, T=T\_a\_tow\_in, P=P\_atm)$  {lbm/ft<sup>3</sup>}  
 $Cp\_a\_tow = specheat(AIRH2O, B=ODWB, T=T\_a\_tow\_in, P=P\_atm)$  {Btu/lbm R}  
 $h\_a\_tow\_in = enthalpy(AIRH2O, B=ODWB, T=T\_a\_tow\_in, P=P\_atm)$  {Btu/lbm}

## {E. Temperatures}

$T_{a\_tow\_in} = T_{amb}$  {F}  
 $T_{w\_tow\_in} = \text{temperature}(\text{WATER}, h=h_{w\_tow\_in}, P=P_{atm})$  {F}  
 $T_{w\_tow\_out1} = \text{temperature}(\text{WATER}, h=h_{w\_tow\_out}, P=P_{atm})$  {F}  
 $T_{w\_tow\_ave} = (T_{w\_tow\_in} - T_{w\_tow\_out}) / \ln((T_{w\_tow\_in}) / (T_{w\_tow\_out}))$  {F}

## {F. Entropy}

$s_{w\_tow\_in} = \text{entropy}(\text{WATER}, h=h_{w\_tow\_in}, P=P_{atm})$  {btu/lbm R}  
 $s_{w\_tow\_out} = \text{entropy}(\text{WATER}, h=h_{w\_tow\_out}, P=P_{atm})$  {btu/lbm R}

## {G. Flow rates}

$m_{dot\_a\_tow} = \rho_{a\_tow} * cfm_{tow} * \text{convert}(1/\text{min}, 1/\text{hr})$  {lbm/hr}  
 $cfm_{tow} = 250 * 1000$

## {H. Cooling tower fan model}

$FHPCA = -2.3084$  {Appendix A ref[10]}  
 $FHPCB = 6.3769$  {Appendix A ref[10]}  
 $W_{dot\_fan\_tow} = (\exp(FHPCA + ((\ln(cfm_{tow}) - 10.5)/2) * FHPCB) / .9) * f_{anduty} * \text{convert}(\text{hp}, \text{btu/hr})$  {btu/hr} {Appendix A ref[10]}  
 $KW_{fan\_tow} = W_{dot\_fan\_tow} * \text{convert}(\text{btu/hr}, \text{kW})$  {kW}

## {Section IX. Constants}

$P_{atm} = 14.7$  {psia}  
 $g = 32.2$  {ft/s<sup>2</sup>}

## {References:

- [1] Bejan, Convection Heat Transfer, 2ed.
- [2] Bejan, Advanced Engineering Thermodynamics, 2ed.
- [3] Incropera and DeWitt, Introduction to Heat Transfer, 1ed.
- [4] McQuiston, Faye and Parker, Jerald., Heating, Ventalating and Air Conditioning; Analysis and Design
- [5] White, Fluid Mechanics, 2ed.
- [6] Rich, Donald G., The effect of fin spacing on the heat transfer and friction performance of multirow smooth plate fin and tube heat exchangers, 1973.
- [7] Rishel, James B., HVAC Pump Handbook, 1996.
- [8] Goulds Pump Selection Software, 1995.
- [9] Liu, Hubert H., Analysis and Performance Optimization of Commercial Chiller/Cooling Tower System.

## APPENDIX B

### BASE CASE, PRIMARY-SECONDARY SYSTEM

"Base Case, Primary-Secondary, Chilled Water System"

{Section I. Procedures}

{A. Air handler procedures}

{This PROCEDURE determines the load based on out door dry bulb temperature}

Procedure loadprofile(T\_amb:Q\_ton\_ah)

IF (T\_amb<=60) Then

    Q\_ton\_ah=20

Endif

IF (T\_amb>60) AND (T\_amb<=105) Then

    Q\_ton\_ah=16/7\*T\_amb-117.143

Endif

IF (T\_amb>105) Then

    Q\_ton\_ah=100

Endif

END

{This procedure determines the flow regime and assigns a Nusselt number and friction factor}

Procedure regime(Re\_D\_i\_ah,Pr\_w\_ah,D\_i\_ah,epsilon\_pipe\_ah:Nus\_ah,f\_i\_ah)

IF (Re\_D\_i\_ah<=2000) Then

    Nus\_ah=4.36

{eqn 3.65 ref[1]}

    f\_i\_ah=64/Re\_D\_i\_ah

{eqn 3.29 ref[1]}

Endif

IF (Re\_D\_i\_ah>2000) Then

    Nus\_ah=0.023\*Re\_D\_i\_ah<sup>0.8</sup>\*Pr\_w\_ah<sup>0.4</sup>

{eqn 11.16 ref[2]}

    f\_i\_ah=1/(-1.8\*log10(6.9/Re\_D\_i\_ah+(epsilon\_pipe\_ah/(D\_i\_ah\*3.7))<sup>1.11</sup>))<sup>2</sup>{eqn 6.64a ref[5]}

Endif

END

{This PROCEDURE determines the relative heat capacities}

Procedure heat(C\_a\_ah,C\_w\_ah:C\_min\_ah,C\_max\_ah)

IF (C\_a\_ah/C\_w\_ah<=1) THEN

    C\_min\_ah=C\_a\_ah

    C\_max\_ah=C\_w\_ah

Endif

IF (C\_a\_ah/C\_w\_ah>1) THEN

    C\_min\_ah=C\_w\_ah

    C\_max\_ah=C\_a\_ah

ENDIF

End

{This procedure determines the heat exchanger efficiency given that the air flow is unmixed and the water is mixed}

```

Procedure transfer(C_a_ah,C_w_ah,NTU_ah,C_r_ah:epsilon_ah)
IF (C_a_ah/C_w_ah>1) THEN
  epsilon_ah=1-exp((-1/C_r_ah)*(1-exp(-C_r_ah*NTU_ah))) {eqn 11.35a ref[3]}
Endif
IF (C_a_ah/C_w_ah<=1) THEN
  epsilon_ah=(1/C_r_ah)*(1-exp(-C_r_ah*(1-exp(-NTU_ah)))) {eqn 11.34a ref[3]}
Endif
END

```

{This procedure determines the f for air flow over bare tubes.}

```

Procedure baretube(Re_D_o_ah:f_tube_ah)
IF (Re_D_o_ah<1000) THEN
  f_tube_ah=3.680886*Re_D_o_ah^(-0.3090731) {Figure 7.13 ref[1]}
Endif
IF (Re_D_o_ah>=1000) THEN
  f_tube_ah=0.42275-5.53e-6*Re_D_o_ah-3.598e-10*Re_D_o_ah^2{Figure 7.13 ref[1]}
Endif
END

```

{This procedure determines the effective specific heat for air of the air handler}

```

Procedure latentheat(T_a_ah_in,T_a_ah_out,T_a_ah_ave,D_a_ah_in,HMRT_a_ah_in,P_atm,
P_a_ah_in,h_a_ah_in:HMRT_a_ah_out,h_a_ah_out,h_a_ah_out_eff,Cp_eff)
IF (T_a_ah_out>D_a_ah_in) Then
  HMRT_a_ah_out=HMRT_a_ah_in
  h_a_ah_out=enthalpy(AIRH2O,T=T_a_ah_out,P=P_atm,W=HMRT_a_ah_out)
  h_a_ah_out_eff=h_a_ah_out
  Cp_eff=specheat(AIRH2O,T=T_a_ah_ave,P=(P_a_ah_in+P_atm)/2,D=D_a_ah_in)
Endif
IF (T_a_ah_out<=D_a_ah_in) Then
  HMRT_a_ah_out=humrat(AIRH2O,T=T_a_ah_out,P=P_atm,R=1)
  h_a_ah_out=enthalpy(AIRH2O,T=T_a_ah_out,P=P_atm,R=1)
  h_a_ah_out_eff=h_a_ah_out+(HMRT_a_ah_in-
HMRT_a_ah_out)*enthalpy(WATER,P=P_atm,T=T_a_ah_out)
  Cp_eff=(h_a_ah_in-h_a_ah_out_eff)/(T_a_ah_in-T_a_ah_out)
Endif
END

```

{B. Chilled water reset procedure}

{This procedure first sets mass flow rate as a function of temperature, then at a specified outdoor dry bulb, it switches to make the evaporator exit temperature a function of flow rate.}

Procedure

reset(T\_amb,Q\_load\_ah,h\_w\_ah\_in,h\_w\_ah\_out,h\_pump\_sec\_out,h\_pump\_sec\_in,m\_dot\_w\_ah,P\_w\_eva  
p\_out:m\_dot\_w\_pump\_sec,T\_w\_evap\_out)

IF (T\_amb=>77) Then

    T\_w\_evap\_out=44

    m\_dot\_w\_pump\_sec=10\*Q\_load\_ah/(h\_w\_ah\_out-h\_w\_ah\_in)

Endif

IF (T\_amb<77) Then

    m\_dot\_w\_pump\_sec=538300

    T\_w\_evap\_out=temperature(WATER,h=(h\_w\_ah\_out-h\_pump\_sec\_out+  
h\_pump\_sec\_in-Q\_load\_ah/m\_dot\_w\_ah),P=P\_w\_evap\_out)

Endif

END

{C. Tower procedures.}

{This procedure determines the tower fan duty}

Procedure

towerfan(Q\_dot\_tow,epsilon\_tow,m\_dot\_a\_tow,h\_s\_w\_tow\_in,h\_a\_tow\_in,T\_w\_tow\_out1:  
fanduty,T\_w\_tow\_out)

IF (T\_w\_tow\_out1>70) Then

    fanduty=1

    T\_w\_tow\_out=T\_w\_tow\_out1

Endif

IF (T\_w\_tow\_out1<70) AND ((Q\_dot\_tow-0.1\*epsilon\_tow\*m\_dot\_a\_tow\*(h\_s\_w\_tow\_in-  
h\_a\_tow\_in))/(0.9\*epsilon\_tow\*m\_dot\_a\_tow\*(h\_s\_w\_tow\_in-h\_a\_tow\_in))>0) Then

    fanduty=(Q\_dot\_tow-0.1\*epsilon\_tow\*m\_dot\_a\_tow\*(h\_s\_w\_tow\_in-h\_a\_tow\_in))/  
(0.9\*epsilon\_tow\*m\_dot\_a\_tow\*(h\_s\_w\_tow\_in-h\_a\_tow\_in))

    T\_w\_tow\_out=70

Endif

IF (T\_w\_tow\_out1<70) AND ((Q\_dot\_tow-0.1\*epsilon\_tow\*m\_dot\_a\_tow\*(h\_s\_w\_tow\_in-  
h\_a\_tow\_in))/(0.9\*epsilon\_tow\*m\_dot\_a\_tow\*(h\_s\_w\_tow\_in-h\_a\_tow\_in))<=0) Then

    fanduty=0

    T\_w\_tow\_out=T\_w\_tow\_out1

Endif

END

{D. Mixing procedures.}

Procedure mixing

(m\_dot\_w\_bypass,m\_dot\_w\_pump\_pri,m\_dot\_w\_pump\_sec,h\_w\_ah\_out,h\_w\_evap\_out:

h\_w\_bypass,h\_pump\_pri\_in,h\_pump\_sec\_in)

IF (m\_dot\_w\_bypass>=0) Then

h\_w\_bypass=h\_w\_evap\_out

h\_pump\_pri\_in=(m\_dot\_w\_bypass\*h\_w\_evap\_out+m\_dot\_w\_pump\_sec\*h\_w\_ah\_out)/

m\_dot\_w\_pump\_pri

h\_pump\_sec\_in=h\_w\_evap\_out

Endif

IF (m\_dot\_w\_bypass<0) Then

h\_w\_bypass=h\_w\_ah\_out

h\_pump\_pri\_in=h\_w\_ah\_out

h\_pump\_sec\_in=(m\_dot\_w\_pump\_pri\*h\_w\_evap\_out-m\_dot\_w\_bypass\*h\_w\_ah\_out)/

m\_dot\_w\_pump\_sec

Endif

END

{Section II. Inputs}

Hours=1

T\_amb=95 {F}

ODWB= 78 {F}

{Section III. Overall Calculations}

{A. Energy analysis}

W\_dot\_total=W\_dot\_comp+W\_dot\_pump\_tot+W\_dot\_pump\_cond+10\*W\_dot\_fan+W\_dot\_fan\_tow

KW\_total=W\_dot\_total\*convert(btu/hr,kW) {kW}

KWh\_total=KW\_total\*hours {kWh}

{These equations sum to the inverse of the IER value}

IER\_chiller=(Hours/Hours\_total)/(KW\_comp/Q\_ton\_evap))

IER\_system=(Hours/Hours\_total)/(kW\_total/(10\*Q\_ton\_ah))

IER\_aux\_evap=(Hours/Hours\_total)/((W\_dot\_pump\_tot+10\*W\_dot\_fan)\*convert(btu/hr,kW)/

(10\*Q\_ton\_ah))

Hours\_total=7132

## {B. Entropy Analysis}

$S_{\dot{gen\_fan\_ah}} = 10 * m_{\dot{a\_ah}} * (s_{a\_fan\_out} - s_{a\_fan\_in})$  {btu/hr R}  
 $S_{\dot{gen\_ah}} = 10 * (m_{\dot{w\_ah}} * (s_{w\_ah\_out} - s_{w\_ah\_in}) - Q_{\dot{load\_ah}} / (T_{amb} + 459.67))$  {btu/hr R}  
 $S_{\dot{gen\_pump\_pri}} = m_{\dot{w\_pump\_pri}} * (s_{pump\_pri\_out} - s_{pump\_pri\_in})$  {btu/hr R}  
 $S_{\dot{gen\_pump\_sec}} = m_{\dot{w\_pump\_sec}} * (s_{pump\_sec\_out} - s_{pump\_sec\_in})$  {btu/hr R}  
 $S_{\dot{gen\_mixing}} = m_{\dot{w\_pump\_pri}} * s_{pump\_pri\_in} - (m_{\dot{w\_bypass}} * s_{w\_bypass} + m_{\dot{w\_pump\_sec}} * s_{w\_sec})$  {btu/hr R}  
 $S_{\dot{gen\_evap}} = m_{\dot{w\_evap}} * (s_{w\_evap\_out} - s_{w\_evap\_in}) - (-Q_{\dot{evap}} / (T_{evap} + 459.67))$   
 $S_{\dot{gen\_cond}} = m_{\dot{w\_cond}} * (s_{w\_cond\_out} - s_{w\_cond\_in}) - (Q_{\dot{cond}} / (T_{cond} + 459.67))$   
 $S_{\dot{gen\_comp}} = (W_{\dot{comp}} - W_{\dot{carnot}}) / T_{amb}$  {btu/hr R}  
 $S_{\dot{gen\_tower}} = m_{\dot{w\_tow}} * (s_{w\_tow\_out} - s_{w\_tow\_in}) - (-Q_{\dot{tow}} / (T_{w\_tow\_ave} + 459.67))$   
 $S_{\dot{gen\_pump\_cond}} = m_{\dot{w\_cond}} * (s_{pump\_cond\_out} - s_{pump\_cond\_in})$  {btu/hr R}  
 $S_{\dot{gen\_loop\_pri}} = m_{\dot{w\_pump\_pri}} * (s_{pump\_sec\_in} - s_{w\_evap\_out})$  {btu/hr R}  
 $S_{\dot{gen\_loop\_sec}} = m_{\dot{w\_pump\_sec}} * (s_{w\_sec} - s_{w\_ah\_out} + s_{w\_ah\_in} - s_{pump\_sec\_out})$   
 $S_{\dot{gen\_loop\_cond}} = m_{\dot{w\_cond}} * (s_{pump\_cond\_in} - s_{w\_tow\_out} + s_{w\_tow\_in} - s_{w\_cond\_out})$   
 $S_{\dot{gen\_tot}} = S_{\dot{gen\_fan\_ah}} + S_{\dot{gen\_ah}} + S_{\dot{gen\_pump\_pri}} + S_{\dot{gen\_pump\_pri}} + S_{\dot{gen\_pump\_pri}} + S_{\dot{gen\_pump\_pri}} + S_{\dot{gen\_mixing}} + S_{\dot{gen\_evap}} + S_{\dot{gen\_cond}} + S_{\dot{gen\_comp}} + S_{\dot{gen\_tower}} + S_{\dot{gen\_pump\_cond}} + S_{\dot{gen\_loop\_pri}} + S_{\dot{gen\_loop\_sec}} + S_{\dot{gen\_loop\_cond}}$   
 $W_{\dot{lost}} = S_{\dot{gen\_tot}} * T_{amb}$  {btu/hr}

## {Section IV. Air handler model}

## {A. Air handler fan}

## {1. Fluid properties}

$T_{room} = 75$  {F}  
 $T_{a\_fan\_in} = \text{temperature}(\text{AIRH2O}, h = h_{a\_fan\_in}, P = P_{atm}, W = \text{HMRT}_{fan\_in})$  {F}  
 $T_{a\_fan\_out} = \text{temperature}(\text{AIRH2O}, h = h_{a\_fan\_out}, P = P_{atm} + \text{DELTA}P_{a\_ah}, W = \text{HMRT}_{fan\_in})$   
 $\text{HMRT}_{amb} = \text{humrat}(\text{AIRH2O}, T = T_{amb}, P = P_{atm}, B = \text{ODWB})$   
 $\text{HMRT}_{room} = \text{humrat}(\text{AIRH2O}, T = T_{room}, P = P_{atm}, R = R_{room})$   
 $\text{HMRT}_{fan\_in} = 0.85 * \text{HMRT}_{room} + 0.15 * \text{HMRT}_{amb}$   
 $R_{room} = .5549$   
 $h_{amb} = \text{enthalpy}(\text{AIRH2O}, T = T_{amb}, P = P_{atm}, B = \text{ODWB})$  {btu/lbm}  
 $h_{room} = \text{enthalpy}(\text{AIRH2O}, T = T_{room} + 5, P = P_{atm}, R = R_{room})$  {btu/lbm}  
 $h_{a\_fan\_in} = 0.85 * h_{room} + 0.15 * h_{amb}$  {btu/lbm}  
 $h_{a\_fan\_out\_rev} = \text{enthalpy}(\text{AIRH2O}, P = P_{atm} + \text{DELTA}P_{a\_ah}, T = T_{a\_fan\_out\_rev}, W = \text{HMRT}_{fan\_in})$   
 $s_{a\_fan\_in} = \text{entropy}(\text{AIRH2O}, T = T_{a\_fan\_in}, P = P_{atm}, W = \text{HMRT}_{fan\_in})$  {btu/lbm R}  
 $s_{a\_fan\_in} = \text{entropy}(\text{AIRH2O}, T = T_{a\_fan\_out\_rev}, P = P_{atm} + \text{DELTA}P_{a\_ah}, W = \text{HMRT}_{fan\_in})$   
 $s_{a\_fan\_out} = \text{entropy}(\text{AIRH2O}, T = T_{a\_fan\_out}, P = P_{atm} + \text{DELTA}P_{a\_ah}, W = \text{HMRT}_{fan\_in})$

## {2. Fan Calculations}

$\eta_{fan} = .65$   
 $\eta_{fan} = (h_{a\_fan\_in} - h_{a\_fan\_out\_rev}) / (h_{a\_fan\_in} - h_{a\_fan\_out})$   
 $W_{\dot{fan}} = -m_{\dot{a\_ah}} * (h_{a\_fan\_in} - h_{a\_fan\_out})$  {btu/hr}  
 $KW_{fan} = W_{\dot{fan}} * \text{convert}(\text{btu/hr}, \text{kW})$  {kW}

## {B. Inputs for Air Handler}

$h_{w\_ah\_in} = h_{pump\_sec\_out}$  {btu/lbm}  
 $h_{a\_fan\_out} = h_{a\_ah\_in}$  {btu/lbm}  
 $P_{w\_ah\_in} = P_{pump\_sec\_out} - (\text{Head}_{pipe\_sec} / 2 + \text{Elev}_{load} + \text{Head}_{valve}) * \rho_{w\_ah} * g * \text{convert}(\text{lbm/ft}^3 * \text{s}^2, \text{psia})$   
 $P_{a\_ah\_in} = P_{atm} + \text{DELTA}P_{a\_ah}$  {psia}  
 $\text{Head}_{valve} = 20 - \text{Head}_{coil}$  {ft}  
 $\text{HMRT}_{a\_ah\_in} = \text{HMRT}_{fan\_in}$

{C. Air Handler overall heat transfer coefficient calculation}

$$1/UA_{tot\_ah} = 1/(h_{i\_ah} * A_{i\_ah}) + \ln(D_{o\_ah}/D_{i\_ah}) / (2 * \pi * k_{pipe} * Length_{ah} * n_{row} * n_{column}) + 1/(h_{o\_ah} * A_{o\_ah} * \eta_{o\_ah}) \quad \text{{eqn 11.5 ref[3]}}$$

{D. Geometry}

$$\begin{aligned} Length_{ah} &= 7.555 && \text{{ft}} \\ Height_{ah} &= 5 && \text{{ft}} \\ Depth_{ah} &= 8.5 * \text{convert(in,ft)} && \text{{ft}} \\ fin\_pitch &= 12 / \text{convert(in,ft)} && \text{{1/ft}} \\ D_{o\_ah} &= .75 * \text{convert(in,ft)} && \text{{ft}} \\ D_{i\_ah} &= .666 * \text{convert(in,ft)} && \text{{ft}} \\ t_{fin} &= .006 * \text{convert(in,ft)} && \text{{ft}} \\ n_{row} &= 4 \\ n_{column} &= 40 \\ Elev\_load &= 0 && \text{{ft}} \end{aligned}$$

{E. Airside calculations}

{1. Air properties}

Call latentheat(T\_a\_ah\_in, T\_a\_ah\_out, T\_a\_ah\_ave, D\_a\_ah\_in, HMRT\_a\_ah\_in, P\_atm, P\_a\_ah\_in, h\_a\_ah\_in:HMRT\_a\_ah\_out, h\_a\_ah\_out, h\_a\_ah\_out\_eff, Cp\_eff)

$$HMRT_{a\_ah\_ave} = (HMRT_{a\_ah\_in} + HMRT_{a\_ah\_out}) / 2$$

$$k_{a\_ah} = \text{conductivity(AIRH2O, T=T_{a\_ah\_ave}, P=P_{a\_ah\_ave}, W=HMRT_{a\_ah\_ave})} \quad \text{{Btu/hr-ft-R}}$$

$$\mu_{a\_ah} = \text{viscosity(AIRH2O, T=T_{a\_ah\_ave}, P=P_{a\_ah\_ave}, W=HMRT_{a\_ah\_ave})} \quad \text{{lbm/ft-hr}}$$

$$\rho_{a\_ah} = \text{density(AIRH2O, T=T_{a\_ah\_ave}, P=P_{a\_ah\_ave}, W=HMRT_{a\_ah\_ave})} \quad \text{{lbm/ft^3}}$$

$$v_{m\_ah} = 1 / \rho_{a\_ah} \quad \text{{ft^3/lbm}}$$

$$Pr_{a\_ah} = Cp\_eff * \mu_{a\_ah} / k_{a\_ah}$$

{2. Air flow properties}

$$G_{a\_ah} = \dot{m}_{a\_ah} / (\sigma_{ah} * A_{fr\_ah}) \quad \text{{lbm/ft^2-hr}} \quad \text{{eqn 11.37 ref[3]}}$$

$$Re_{D_{o\_ah}} = G_{a\_ah} * D_{o\_ah} / \mu_{a\_ah} \quad \text{{eqn 14.37 ref[4]}}$$

$$Re_{L_{ah}} = G_{a\_ah} * b_{ah} / \mu_{a\_ah} \quad \text{{eqn ref[4]}}$$

{3. Airside geometry calculations}

$$a_{ah} = Height_{ah} / n_{column} \quad \text{{ft}}$$

$$b_{ah} = Depth_{ah} / n_{row} \quad \text{{ft}}$$

$$A_{fr\_ah} = Height_{ah} * Length_{ah} \quad \text{{ft^2}}$$

$$\sigma_{ah} = (a_{ah} - D_{o\_ah}) / a_{ah}$$

$$A_{f\_ah} = (2 * a_{ah} * b_{ah} - \pi * D_{o\_ah}^2 / 2) * fin\_pitch * Length_{ah} * n_{row} * n_{column} \quad \text{{ft^2}}$$

$$A_{t\_ah} = \pi * D_{o\_ah} * Length_{ah} * n_{row} * n_{column} \quad \text{{ft^2}}$$

$$A_{o\_ah} = A_{f\_ah} + A_{t\_ah} \quad \text{{ft^2}}$$

{4. Airside Heat Transfer Calculations}

$$h_{o\_ah} = (Cp\_eff * G_{a\_ah} * j_n / Pr_{a\_ah}^{(2/3)}) \quad \text{{Btu/ft^2-hr-R}} \quad \text{{eqn 14.36 ref[4]}}$$

$$j_4 = 0.2618 * JP + 0.0014 \quad \text{{eqn ref[4]}}$$

$$JP = Re_{D_{o\_ah}}^{(-0.4)} * (A_{o\_ah} / A_{t\_ah})^{(-0.15)} \quad \text{{eqn 14.46 ref[4]}}$$

$$j_n / j_4 = (1 - 1280 * n_{row} * Re_{L_{ah}}^{(-1.2)}) / (1 - 1280 * 4 * Re_{L_{ah}}^{(-1.2)}) \quad \text{{eqn 14.50 ref[4]}}$$

{5. Fin Calculations}

$$\eta_{o\_ah} = 1 - (A_{f\_ah} / A_{o\_ah}) * (1 - \eta_{fin}) \quad \text{{eqn 11.3 ref[3]}}$$

$$\eta_{fin} = .95$$

## {F. Waterside calculations}

## {1. Water properties}

$Cp\_w\_ah = \text{specheat}(\text{WATER}, T=T\_w\_ah\_ave, P=P\_atm)$  {Btu/lbm-R}  
 $k\_w\_ah = \text{conductivity}(\text{WATER}, T=T\_w\_ah\_ave, P=P\_atm)$  {Btu/hr-ft-R}  
 $\mu\_w\_ah = \text{viscosity}(\text{WATER}, T=T\_w\_ah\_ave, P=P\_atm)$  {lbm/ft-hr}  
 $\rho\_w\_ah = \text{density}(\text{WATER}, T=T\_w\_ah\_ave, P=P\_atm)$  {lbm/ft^3}  
 $Pr\_w\_ah = Cp\_w\_ah * \mu\_w\_ah / k\_w\_ah$

## {2. Flow properties}

$G\_w\_ah = m\_dot\_w\_ah / ((n\_column - 1) * \pi * D\_i\_ah^2 / 4)$  {lbm/ft^2-hr}  
 $Re\_D\_i\_ah = G\_w\_ah * D\_i\_ah / \mu\_w\_ah$  {eqn 11.10 ref[2]}

## {3. Waterside geometry calculations}

$A\_i\_ah = \pi * D\_i\_ah * Length\_ah * n\_row * n\_column$  {ft^2}

## {4. Waterside heat transfer calculations}

$h\_i\_ah = Nus\_ah * k\_w\_ah / D\_i\_ah$  {Btu/ft^2-hr-R} {eqn 3.66 ref[1]}  
 Call Regime(Re\_D\_i\_ah, Pr\_w\_ah, D\_i\_ah, epsilon\_pipe\_ah: Nus\_ah, f\_i\_ah)

## {G. Pipe and fin properties}

$k\_pipe = 401 * \text{convert}(\text{W/m}^*K, \text{Btu/hr}^*ft^*R)$  {Btu/hr-ft-R}  
 $k\_fin = 237 * \text{convert}(\text{W/m}^*K, \text{Btu/hr}^*ft^*R)$  {Btu/hr-ft-R}  
 $\epsilonpsilon\_pipe\_ah = .00015$  {ft}

## {H. Load conditions.}

Call loadprofile(T\_amb: Q\_ton\_ah)  
 CALL heat(C\_a\_ah, C\_w\_ah: C\_min\_ah, C\_max\_ah)  
 CALL Transfer(C\_a\_ah, C\_w\_ah, NTU\_ah, C\_r\_ah: epsilon\_ah)  
 $Q\_load\_ah = Q\_ton\_ah * \text{convert}(\text{ton}, \text{Btu/hr})$  {Btu/hr}  
 $"Q\_load\_ah = m\_dot\_w\_ah * (h\_w\_ah\_out - h\_w\_ah\_in)"$  {Btu/hr} {Blocked out for reset}"  
 $Q\_load\_ah = m\_dot\_a\_ah * Cp\_eff * \Delta T\_a\_ah$  {Btu/hr}  
 $Q\_max\_ah = C\_min\_ah * (T\_a\_ah\_in - T\_w\_ah\_in)$  {Btu/hr}  
 $C\_w\_ah = m\_dot\_w\_ah * cp\_w\_ah$  {Btu/hr R}  
 $C\_a\_ah = m\_dot\_a\_ah * Cp\_eff$  {Btu/hr R}  
 $C\_r\_ah = C\_min\_ah / C\_max\_ah$   
 $Q\_load\_ah = \epsilonpsilon\_ah * C\_min\_ah * (T\_a\_ah\_in - T\_w\_ah\_in)$  {Btu/hr}  
 $NTU\_ah = UA\_tot\_ah / C\_min\_ah$  {eqn 11.25 ref[3]}

## {I. Temperature}

$T\_w\_ah\_in = \text{temperature}(\text{WATER}, H=h\_w\_ah\_in, P=P\_w\_ah\_in)$  {F}  
 $T\_w\_ah\_out = \text{temperature}(\text{WATER}, H=h\_w\_ah\_out, P=P\_w\_ah\_out)$  {F}  
 $T\_w\_ah\_ave = (T\_w\_ah\_in + T\_w\_ah\_out) / \ln(T\_w\_ah\_in / T\_w\_ah\_out)$  {F}  
 $T\_a\_ah\_ave = (T\_a\_ah\_in + T\_a\_ah\_out) / \ln(T\_a\_ah\_in / T\_a\_ah\_out)$  {F}  
 $T\_a\_ah\_in = \text{temperature}(\text{AIRH2O}, h=h\_a\_ah\_in, P=P\_a\_ah\_in, W=HMRT\_a\_ah\_in)$  {F}  
 $T\_a\_ah\_out = 58$  {F}  
 $D\_a\_ah\_in = \text{dewpoint}(\text{AIRH2O}, T=T\_a\_ah\_in, P=P\_a\_ah\_in, W=HMRT\_a\_ah\_in)$  {F}  
 $\Delta T\_w\_ah = T\_w\_ah\_out - T\_w\_ah\_in$  {F}  
 $\Delta T\_a\_ah = T\_a\_ah\_in - T\_a\_ah\_out$  {F}

## {J. Entropy}

$s_{w\_ah\_in} = \text{entropy}(\text{WATER}, P=P_{w\_ah\_in}, T=T_{w\_ah\_in})$  {btu/lbm R}  
 $s_{w\_ah\_out} = \text{entropy}(\text{WATER}, P=P_{w\_ah\_out}, T=T_{w\_ah\_out})$  {btu/lbm R}

## {K. Flow rates}

## {1. Water flow}

$V_{w\_ah} = \text{FPS}_{w\_ah} * (n_{\text{column}} - 1) * \pi * D_{i\_ah}^2 / 4 * \text{convert}(1/\text{s}, 1/\text{min})$  {cfm}  
 $\text{GPM}_{w\_ah} = V_{w\_ah} * \text{convert}(\text{ft}^3, \text{gal})$  {gpm}  
 $m_{\text{dot}}_{w\_ah} = V_{w\_ah} * \rho_{w\_ah} * 60$  {lbm/hr}

## {2. Air flow}

$V_{a\_ah} = \text{FPM}_{a\_ah} * \text{Length}_{ah} * \text{Height}_{ah}$  {cfm}  
 $m_{\text{dot}}_{a\_ah} = V_{a\_ah} * \rho_{a\_ah} * 60$  {lbm/hr}  
 $\text{FPH}_{a\_ah} = \text{FPM}_{a\_ah} * \text{convert}(1/\text{min}, 1/\text{hr})$  {ft/hr}  
 $\text{FPS}_{a\_ah} = \text{FPM}_{a\_ah} * \text{convert}(1/\text{min}, 1/\text{s})$  {ft/s}

## {L. Pressure drop calculations}

## {1. Waterside pressure drop}

$\text{DELTA}P_{i\_ah} = \rho_{w\_ah} * g * \text{Head}_{\text{coil}} * \text{convert}(\text{lbm}/\text{ft}^2 * \text{s}^2, \text{psia})$  {psia}  
 $\text{DELTA}P_{\text{tube}_{ah}} = f_{i\_ah} * \text{Length}_{ah} * n_{\text{row}} / D_{i\_ah} * (\rho_{w\_ah} * \text{FPS}_{w\_ah}^2 / 2)$   
 $* \text{convert}(\text{lbm}/\text{s}^2 * \text{ft}, \text{psia})$  {psia} {eqn 3.27 ref[1]}  
 $\text{Head}_{\text{tube}_{ah}} = \text{DELTA}P_{\text{tube}_{ah}} / (\rho_{w\_ah} * g) * \text{convert}(\text{psia} * \text{ft}^2 * \text{s}^2 / \text{lbm}, \text{ft})$  {ft} {eqn 6.25 ref[6]}  
 $\text{Head}_{\text{bend}} = 5 * K * \text{FPS}_{w\_ah}^2 / (2 * g)$  {ft}  
 $\text{Head}_{\text{coil}} = \text{Head}_{\text{tube}_{ah}} + \text{Head}_{\text{bend}}$  {ft}  
 $P_{w\_ah\_out} = P_{w\_ah\_in} - \text{DELTA}P_{i\_ah}$  {psia}  
 $P_{w\_ah\_ave} = (P_{w\_ah\_in} + P_{w\_ah\_out}) / 2$  {psia}  
 $K = 4$

## {2. Airside pressure drop}

CALL Baretube(Re, D\_o\_ah: f\_tube\_ah)  
 $\text{DELTA}P_{a\_ah} = \text{delta}P_{o\_ah} * \text{convert}(\text{lbm}/\text{hr}^2 * \text{ft}, \text{psia})$  {psia}  
 $P_{a\_ah\_ave} = (P_{a\_ah\_in} + P_{\text{atm}}) / 2$  {psia}  
 $f_{f\_ah} = (\text{delta}P_{o\_ah} - \text{delta}P_{t\_ah}) / (v_{m\_ah} * G_{a\_ah}^2 / (2 * \sigma_{ah}))$  {eqn 7 ref[6]}  
 $f_{f\_ah} = 1.7 * \text{Re}_{L\_ah}^{-0.5}$  {eqn 9 ref[6]}  
 $a_{ah\_star} = a_{ah} / D_{o\_ah}$  {eqn 7.114 ref[1]}  
 $b_{ah\_star} = b_{ah} / D_{o\_ah}$  {eqn 7.114 ref[1]}  
 $\text{Chi}_{ah} = 1$  {Fig 7.13 ref[1]}  
 $\text{delta}P_{t\_ah} = n_{\text{row}} * f_{\text{tube}_{ah}} * \text{Chi}_{ah} * (\rho_{a\_ah} * (\text{FPH}_{a\_ah} / \sigma_{ah})^2 / 2)$  {lbm/hr^2 ft}  
{eqn 7.113 ref[1]}

## {Section V. Pump models}

## {A. Primary/Secondary Mixing Calculations}

CALL mixing(m\_dot\_w\_bypass, m\_dot\_w\_pump\_pri, m\_dot\_w\_pump\_sec, h\_w\_ah\_out, h\_w\_evap\_out:  
h\_w\_bypass, h\_pump\_pri\_in, h\_pump\_sec\_in)  
 $m_{\text{dot}}_{w\_bypass} = m_{\text{dot}}_{w\_pump\_pri} - m_{\text{dot}}_{w\_pump\_sec}$  {lbm/hr}

## {B. Pumping power calculations}

$\text{KW}_{\text{pump\_tot}} = \text{KW}_{\text{pump\_pri}} + \text{KW}_{\text{pump\_sec}}$  {kW}  
 $W_{\text{dot}}_{\text{pump\_tot}} = W_{\text{dot}}_{\text{pump\_pri}} + W_{\text{dot}}_{\text{pump\_sec}}$  {Btu/hr}

## {C. Primary pump model}

## {1. Inputs for primary pump model}

s\_w\_bypass=entropy(WATER,P=P\_min,h=h\_w\_bypass) {btu/lbm R}  
 s\_w\_sec=entropy(WATER,P=P\_min,h=h\_w\_ah\_out) {btu/lbm R}

## {2. Pressure calculations}

DELTA\_pump\_pri=rho\_w\_pump\_pri\*g\*Head\_loop\_pri\*convert(lbm/ft\*S^2,psia) {psia}  
 P\_pump\_pri\_out=P\_min+DELTA\_pump\_pri {psia}  
 P\_pump\_pri\_ave=P\_min+DELTA\_pump\_pri/2 {psia}  
 P\_min=125 {psia}

## {3. Pump efficiencies}

eta\_pump\_pri=.83  
 eta\_motor\_pri=.90  
 eta\_pump\_pri=(h\_pump\_pri\_out\_rev-h\_pump\_pri\_in)/(h\_pump\_pri\_out-h\_pump\_pri\_in)  
 W\_dot\_pump\_pri=m\_dot\_w\_pump\_pri\*(h\_pump\_pri\_out-h\_pump\_pri\_in)/eta\_motor\_pri {Btu/hr}  
 KW\_pump\_pri=W\_dot\_pump\_pri\*convert(Btu/hr,kW) {kW}

## {4. Head calculation}

Head\_pipe\_pri=f\_loop\_pri\*Length\_loop\_pri/D\_i\_pipe\_pri\*(FPS\_pump\_pri^2/2)/g {ft}  
 Head\_loop\_pri=Head\_pipe\_pri+Head\_evap {ft}  
 f\_loop\_pri=1/(-1.8\*log10(6.9/Re\_D\_i\_pump\_pri+(epsilon\_pipe\_pri/(D\_i\_pipe\_pri\*3.7))^1.11))^2

## {5. Pipe geometry}

D\_i\_pipe\_pri=10\*convert(in,ft) {ft}  
 Length\_loop\_pri=500 {ft}  
 epsilon\_pipe\_pri=.00015 {ft}

## {6. Flow properties}

GPM\_pump\_pri=2400 {gpm}  
 CFM\_pump\_pri=GPM\_pump\_pri\*convert(gpm,cfm) {ft^3/min}  
 FPM\_pump\_pri=CFM\_pump\_pri/(pi\*D\_i\_pipe\_pri^2/4)  
 {ft/min}  
 FPS\_pump\_pri=FPM\_pump\_pri\*convert(1/min,1/s) {ft/s}  
 FPH\_pump\_pri=FPM\_pump\_pri\*convert(1/min,1/hr) {ft/hr}  
 m\_dot\_w\_pump\_pri=rho\_w\_pump\_pri\*GPM\_pump\_pri\*convert(gpm,cfm)\*60 {lbm/hr}  
 Re\_D\_i\_pump\_pri=rho\_w\_pump\_pri\*FPH\_pump\_pri\*D\_i\_pipe\_pri/mu\_w\_pump\_pri

## {7. Fluid properties}

rho\_w\_pump\_pri=density(WATER,T=T\_pump\_pri\_ave,P=P\_pump\_pri\_ave) {lbm/ft^3}  
 mu\_w\_pump\_pri=viscosity(WATER,T=T\_pump\_pri\_ave,P=P\_pump\_pri\_ave) {lbm/ft hr}

## {8. Temperatures}

T\_pump\_pri\_in=temperature(WATER,h=h\_pump\_pri\_in,P=P\_min) {F}  
 T\_pump\_pri\_ave=(T\_pump\_pri\_out-T\_pump\_pri\_in)/ln((T\_pump\_pri\_out)/(T\_pump\_pri\_in)) {F}  
 T\_pump\_pri\_out\_rev=temperature(WATER,P=P\_pump\_pri\_out,s=s\_pump\_pri\_in) {F}  
 T\_pump\_pri\_out=temperature(WATER,P=P\_pump\_pri\_out,H=h\_pump\_pri\_out) {F}

## {9. Enthalpy and entropy}

h\_pump\_pri\_out\_rev=enthalpy(WATER,P=P\_pump\_pri\_out,T=T\_pump\_pri\_out\_rev) {Btu/lbm}  
 s\_pump\_pri\_in=entropy(WATER,P=P\_min,T=T\_pump\_pri\_in) {Btu/lbm R}  
 s\_pump\_pri\_out=entropy(WATER,P=P\_pump\_pri\_out,T=T\_pump\_pri\_out) {Btu/lbm R}

{D. Secondary pump model}

{1. Inputs for secondary pump model}

$P_{pump\_sec\_in} = P_{w\_evap\_out} - (\rho_w \cdot g \cdot \text{Head\_pipe\_pri} / 2) \cdot \text{convert}(\text{lbm/s}^2 \cdot \text{ft}, \text{psia})$   
 $m_{dot\_w\_pump\_sec} = 10 \cdot m_{dot\_w\_ah}$  {lbm/hr}

{2. Pressure calculations}

$\Delta P_{pump\_sec} = \rho_w \cdot g \cdot (\text{Head\_loop\_sec}) \cdot \text{convert}(\text{lbm/ft} \cdot \text{S}^2, \text{psia})$  {psia}  
 $P_{pump\_sec\_out} = P_{pump\_sec\_in} + \Delta P_{pump\_sec}$  {psia}  
 $P_{pump\_sec\_ave} = P_{pump\_sec\_in} + \Delta P_{pump\_sec} / 2$  {psia}

{3. Affinity Calculations}

$N_{pump\_act} = N_{pump\_design} \cdot (\text{GPM}_{pump\_sec} / \text{GPM}_{design})$  {rpm} {eqn 6.1 ref[7]}  
 $N_{pump\_act} = N_{pump\_design} \cdot (\text{Head\_loop\_sec} / \text{Head\_design})^{0.5}$  {rpm} {eqn 6.1 ref[7]}  
 $N_{pump\_design} = 1180$  {rpm} {ref[8]}

{4. Pump curves}

$\text{Head}_{design} = 71.39902 + 0.01539461 \cdot \text{GPM}_{design} - 0.00000846 \cdot \text{GPM}_{design}^2$   
 $\eta_{pump\_sec} = (0.03603715 + 0.00073264 \cdot \text{GPM}_{design} - 0.00000017 \cdot \text{GPM}_{design}^2) \cdot$   
 $(0.8158200 + 0.4025401 \cdot N_{pump\_act} / N_{pump\_design} - 0.2183601 \cdot (N_{pump\_act} / N_{pump\_design})^2)$   
 $\eta_{motor\_sec} = 0.0498386 + 1.846339 \cdot (N_{pump\_act} / N_{pump\_design}) -$   
 $1.029 \cdot (N_{pump\_act} / N_{pump\_design})^2$   
 $\eta_{pump\_sec} = (h_{pump\_sec\_out\_rev} - h_{pump\_sec\_in}) / (h_{pump\_sec\_out} - h_{pump\_sec\_in})$   
 $W_{dot\_pump\_sec} = m_{dot\_w\_pump\_sec} \cdot (h_{pump\_sec\_out} - h_{pump\_sec\_in}) / \eta_{motor\_sec}$  {Btu/hr}  
 $KW_{pump\_sec} = W_{dot\_pump\_sec} \cdot \text{convert}(\text{Btu/hr}, \text{kW})$  {kW}

{5. Head calculation}

$\text{Head\_pipe\_sec} = f_{loop\_sec} \cdot \text{Length\_loop\_sec} / D_{i\_pipe\_sec} \cdot (\text{FPS}_{pump\_sec}^2 / 2) / g$   
 {ft} {eqn 6.30 ref[5]}  
 $\text{Head\_loop\_sec} = \text{Head\_pipe\_sec} + \text{Head\_coil} + \text{Head\_valve}$  {ft}  
 $f_{loop\_sec} = 1 / (-1.8 \cdot \log_{10}(6.9 / \text{Re}_{D_{i\_pump\_sec}} + (\epsilon_{pipe\_sec} / (D_{i\_pipe\_sec} \cdot 3.7))^{\wedge} 1.11))^{\wedge} 2$   
 {eqn 6.64a ref[5]}

{6. Pipe geometry}

$D_{i\_pipe\_sec} = 10 \cdot \text{convert}(\text{in}, \text{ft})$  {ft}  
 $\text{Length\_loop\_sec} = 1500$  {ft}  
 $\epsilon_{pipe\_sec} = .00015$  {ft}

{7. Flow properties}

$\text{CFM}_{pump\_sec} = \text{GPM}_{pump\_sec} \cdot \text{convert}(\text{gpm}, \text{cfm})$  {ft<sup>3</sup>/min}  
 $\text{FPM}_{pump\_sec} = \text{CFM}_{pump\_sec} / (\pi \cdot D_{i\_pipe\_sec}^2 / 4)$  {ft/min}  
 $\text{FPS}_{pump\_sec} = \text{FPM}_{pump\_sec} \cdot \text{convert}(1/\text{min}, 1/\text{s})$  {ft/s}  
 $\text{FPH}_{pump\_sec} = \text{FPM}_{pump\_sec} \cdot \text{convert}(1/\text{min}, 1/\text{hr})$  {ft/hr}  
 $m_{dot\_w\_pump\_sec} = \rho_w \cdot g \cdot \text{GPM}_{pump\_sec} \cdot \text{convert}(\text{gpm}, \text{cfm}) \cdot 60$  {lbm/hr}  
 $\text{Re}_{D_{i\_pump\_sec}} = \rho_w \cdot g \cdot \text{FPH}_{pump\_sec} \cdot D_{i\_pipe\_sec} / \mu_{w\_pump\_sec}$

{8. Fluid properties}

$\rho_{w\_pump\_sec} = \text{density}(\text{WATER}, T = T_{pump\_sec\_ave}, P = P_{pump\_sec\_ave})$  {lbm/ft<sup>3</sup>}  
 $\mu_{w\_pump\_sec} = \text{viscosity}(\text{WATER}, T = T_{pump\_sec\_ave}, P = P_{pump\_sec\_ave})$  {lbm/ft hr}

{9. Temperatures}

$T_{pump\_sec\_in} = \text{temperature}(\text{WATER}, h = h_{pump\_sec\_in}, P = P_{pump\_sec\_in})$  {F}  
 $T_{pump\_sec\_ave} = (T_{pump\_sec\_out} + T_{pump\_sec\_in}) / \ln((T_{pump\_sec\_out}) / (T_{pump\_sec\_in}))$  {F}  
 $T_{pump\_sec\_out\_rev} = \text{temperature}(\text{WATER}, P = P_{pump\_sec\_out}, s = s_{pump\_sec\_in})$  {F}  
 $T_{pump\_sec\_out} = \text{temperature}(\text{WATER}, P = P_{pump\_sec\_out}, H = h_{pump\_sec\_out})$  {F}

## { 10. Enthalpy and entropy }

$h_{\text{pump\_sec\_out\_rev}} = \text{enthalpy}(\text{WATER}, P=P_{\text{pump\_sec\_out}}, T=T_{\text{pump\_sec\_out\_rev}})$  {Btu/lbm}  
 $s_{\text{pump\_sec\_in}} = \text{entropy}(\text{WATER}, P=P_{\text{pump\_sec\_in}}, T=T_{\text{pump\_sec\_in}})$  {Btu/lbm R}  
 $s_{\text{pump\_sec\_out}} = \text{entropy}(\text{WATER}, P=P_{\text{pump\_sec\_out}}, T=T_{\text{pump\_sec\_out}})$  {Btu/lbm R}

## { Section VI. Centrifugal chiller model }

## { A. Chiller inputs }

## { 1. Evaporator Side }

$P_{\text{w\_evap\_in}} = P_{\text{pump\_pri\_out}}$  {psia}  
 $h_{\text{w\_evap\_in}} = h_{\text{pump\_pri\_out}}$  {btu/lbm}  
 $m_{\text{dot\_w\_evap}} = m_{\text{dot\_w\_pump\_pri}}$  {lbm/hr}

## { 2. Condenser Side }

$P_{\text{w\_cond\_in}} = P_{\text{pump\_cond\_out}}$  {psia}  
 $h_{\text{w\_cond\_in}} = h_{\text{pump\_cond\_out}}$  {btu/lbm}

## { B. Compressor }

$W_{\text{dot\_carnot}} = Q_{\text{dot\_evap}} * ((T_{\text{cond}} + 459.67) / (T_{\text{evap}} + 459.67) - 1)$  {btu/hr}  
 $KW_{\text{comp}} = W_{\text{dot\_comp}} * \text{convert}(\text{Btu/hr}, \text{kW})$  {kW}  
 $W_{\text{dot\_comp}} = a + b * W_{\text{dot\_carnot}} + c * W_{\text{dot\_carnot}}^2$   
 $a = 3042.991 + 705.2175 * Q_{\text{ton\_evap}} + 0.9521675 * Q_{\text{ton\_evap}}^2$   
 $b = 1.228996 - 0.00438602 * Q_{\text{ton\_evap}} + 0.00000203 * Q_{\text{ton\_evap}}^2$   
 $c = 0.00000279 - 3.146E-09 * Q_{\text{ton\_evap}} + 1.310E-12 * Q_{\text{ton\_evap}}^2$

## { C. Evaporator }

## { 1. Evaporator heat transfer calculations }

Call

$\text{reset}(T_{\text{amb}}, Q_{\text{load\_ah}}, h_{\text{w\_ah\_in}}, h_{\text{w\_ah\_out}}, h_{\text{pump\_sec\_out}}, h_{\text{pump\_sec\_in}}, m_{\text{dot\_w\_ah}}, P_{\text{w\_eva}}$   
 $p_{\text{out}}: m_{\text{dot\_w\_pump\_sec}}, T_{\text{w\_evap\_out}})$   
 $Q_{\text{dot\_evap}} = Q_{\text{ton\_evap}} * \text{convert}(\text{ton}, \text{Btu/hr})$  {Btu/hr}  
 $Q_{\text{dot\_evap}} = m_{\text{dot\_w\_evap}} * (h_{\text{w\_evap\_in}} - h_{\text{w\_evap\_out}})$  {Btu/hr}  
 $Q_{\text{dot\_evap}} = \epsilon_{\text{evap}} * m_{\text{dot\_w\_evap}} * C_{\text{w\_evap}} * (T_{\text{w\_evap\_in}} - T_{\text{evap}})$  {Btu/hr}  
{eqn 11.19 ref[3]}  
 $\epsilon_{\text{evap}} = 1 - \exp(-NTU_{\text{evap}})$  {eqn 11.30a ref[3]}  
 $NTU_{\text{evap}} = UA_{\text{evap}} / (m_{\text{dot\_w\_evap}} * C_{\text{w\_evap}})$  {eqn 11.25 ref[3]}  
 $1/UA_{\text{evap}} = 1/(hA_{\text{i\_evap}}) + 1/(hA_{\text{o\_evap}})$   
 $hA_{\text{i\_evap}} = 6213 * (Re_{\text{D\_i\_evap}}^{0.5334881}) * Pr_{\text{w\_evap}}^{0.3}$   
 $hA_{\text{o\_evap}} = 180935.0 + 6243.157 * Q_{\text{ton\_evap}} - 1.474305 * Q_{\text{ton\_evap}}^2$

## { 2. Evaporator pressure drop calculations }

$f_{\text{i\_evap}} = 1 / (-1.8 * \log_{10}(6.9 / Re_{\text{D\_i\_evap}} + (\epsilon_{\text{pipe\_evap}} / (D_{\text{i\_evap}} * 3.7))^{1.11}))^2$  {eqn 6.64a ref[5]}  
 $\text{DELTA}P_{\text{evap}} = \text{Head}_{\text{evap}} * \rho_{\text{w\_evap}} * g * \text{convert}(\text{lbm/ft}^3, \text{psia})$  {psia}  
 $\text{Head}_{\text{evap}} = f_{\text{i\_evap}} * \text{Length}_{\text{evap}} * n_{\text{pass\_evap}} / D_{\text{i\_evap}} * (\text{FPS}_{\text{evap}}^2 / 2) / g$  {ft}  
{eqn 6.30 ref[5]}  
 $P_{\text{evap\_ave}} = P_{\text{min}} + \text{DELTA}P_{\text{evap}} / 2$  {psia}  
 $P_{\text{w\_evap\_out}} = P_{\text{w\_evap\_in}} - \text{DELTA}P_{\text{evap}}$  {psia}

## {3. Evaporator geometry}

$D_{i\_evap}=0.824*\text{convert}(\text{in},\text{ft})$  {ft}  
 $\text{Length}_{evap}=14.2$  {ft}  
 $n_{tubes\_evap}=215$   
 $n_{pass\_evap}=4$   
 $\text{epsilon}_{pipe\_evap}=0.00038731$  {ft}

## {4. Evaporator fluid properties}

$C_{w\_evap}=\text{specheat}(\text{WATER},T=T_{w\_evap\_ave},P=P_{evap\_ave})$  {Btu/lbm R}  
 $\rho_{w\_evap}=\text{density}(\text{WATER},T=T_{w\_evap\_ave},P=P_{evap\_ave})$  {lbm/ft<sup>3</sup>}  
 $\mu_{w\_evap}=\text{viscosity}(\text{WATER},T=T_{w\_evap\_ave},P=P_{evap\_ave})$  {lbm/ft hr}  
 $k_{w\_evap}=\text{conductivity}(\text{WATER},T=T_{w\_evap\_ave},P=P_{evap\_ave})$  {Btu/ft hr R}  
 $Pr_{w\_evap}=C_{w\_evap}*\mu_{w\_evap}/k_{w\_evap}$   
 $Re_{D_{i\_evap}}=\rho_{w\_evap}*FPH_{evap}*D_{i\_evap}/\mu_{w\_evap}$

## {5. Evaporator flow rate}

$V_{w\_evap}=\text{GPM}_{w\_evap}*\text{convert}(\text{gpm},\text{cfm})$  {cfm}  
 $V_{w\_evap}=(\pi*D_{i\_evap}^2/4)*FPM_{evap}*n_{tubes\_evap}$  {cfm}  
 $m_{dot\_w\_evap}=V_{w\_evap}*\rho_{w\_evap}*60$  {lbm/hr}  
 $FPS_{evap}=FPM_{evap}*\text{convert}(1/\text{min},1/\text{s})$  {ft/s}  
 $FPH_{evap}=FPM_{evap}*\text{convert}(1/\text{min},1/\text{hr})$  {ft/hr}

## {6. Evaporator Temperatures}

$T_{w\_evap\_out}=44$  {F} {Blocked out for reset}  
 $T_{w\_evap\_in}=\text{temperature}(\text{WATER},h=h_{w\_evap\_in},P=P_{w\_evap\_in})$  {F}  
 $T_{w\_evap\_ave}=(T_{w\_evap\_in}-T_{w\_evap\_out})/\ln(T_{w\_evap\_in}/T_{w\_evap\_out})$  {F}

## {7. Enthalpy and entropy}

$h_{w\_evap\_out}=\text{enthalpy}(\text{WATER},T=T_{w\_evap\_out},P=P_{w\_evap\_out})$  {btu/lbm}  
 $s_{w\_evap\_in}=\text{entropy}(\text{WATER},h=h_{w\_evap\_in},P=P_{w\_evap\_in})$  {btu/lbm R}  
 $s_{w\_evap\_out}=\text{entropy}(\text{WATER},h=h_{w\_evap\_out},P=P_{w\_evap\_out})$  {btu/lbm R}

## {D. Condenser}

## {1. Condenser UA calculation}

$Q_{dot\_cond}=\text{epsilon}_{cond}*m_{dot\_w\_cond}*C_{w\_cond}*(T_{cond}-T_{w\_cond\_in})$  {Btu/hr}  
 {eqn 1.23 ref[3]}  
 $Q_{dot\_cond}=m_{dot\_w\_cond}*(h_{w\_cond\_out}-h_{w\_cond\_in})$  {Btu/hr}  
 $Q_{dot\_cond}=Q_{dot\_evap}+W_{dot\_comp}$  {Btu/hr}  
 $Q_{ton\_cond}=Q_{dot\_cond}*\text{convert}(\text{btu}/\text{hr},\text{ton})$  {tons}  
 $\text{epsilon}_{cond}=1-\exp(-NTU_{cond})$  {eqn 1.30 ref[3]}  
 $NTU_{cond}=UA_{cond}/(m_{dot\_w\_cond}*C_{w\_cond})$   
 $UA_{cond\_1}=1845702 + 22792.36*T_{cond} - 96.24830*T_{cond}^2$   
 $UA_{cond\_2}=1.059937 - 0.00009226*Q_{ton\_cond} + 0.00000001*Q_{ton\_cond}^2$   
 $UA_{cond}=UA_{cond\_1}*UA_{cond\_2}$

## {2. Condenser fluid properties}

$\rho_{w\_cond}=\text{density}(\text{WATER},T=T_{w\_cond\_ave},P=P_{w\_cond\_ave})$  {lbm/ft<sup>3</sup>}  
 $C_{w\_cond}=\text{specheat}(\text{WATER},T=T_{w\_cond\_ave},P=P_{w\_cond\_ave})$  {Btu/lbm R}  
 $\mu_{w\_cond}=\text{viscosity}(\text{WATER},T=T_{w\_cond\_ave},P=P_{w\_cond\_ave})$  {lbm/ft hr}  
 $k_{w\_cond}=\text{conductivity}(\text{WATER},T=T_{w\_cond\_ave},P=P_{w\_cond\_ave})$  {Btu/hr ft R}

## {3. Condenser Temperatures}

$$T_{w\_cond\_ave} = (T_{w\_cond\_out} - T_{w\_cond\_in}) / \ln(T_{w\_cond\_out} / T_{w\_cond\_in}) \quad \{F\}$$

$$T_{w\_cond\_in} = \text{temperature}(\text{WATER}, h = h_{w\_cond\_in}, P = P_{w\_cond\_in}) \quad \{F\}$$

## {4. Enthalpy and entropy}

$$h_{w\_cond\_out} = \text{enthalpy}(\text{WATER}, T = T_{w\_cond\_out}, P = P_{w\_cond\_out}) \quad \{\text{btu/lbm}\}$$

$$s_{w\_cond\_in} = \text{entropy}(\text{WATER}, H = h_{w\_cond\_in}, P = P_{w\_cond\_in}) \quad \{\text{btu/lbm R}\}$$

$$s_{w\_cond\_out} = \text{entropy}(\text{WATER}, T = T_{w\_cond\_out}, P = P_{w\_cond\_out}) \quad \{\text{btu/lbm R}\}$$

## {5. Condenser pressures}

$$\text{HEAD}_{cond} = 60.63713 * T_{w\_cond\_ave}^{(-0.1908161)}$$

$$\text{DELTA}_{P}_{cond} = \rho_{w\_cond} * g * \text{HEAD}_{cond} * \text{convert}(\text{lbm/s}^2 * \text{ft}, \text{psia}) \quad \{\text{psia}\}$$

$$P_{w\_cond\_out} = P_{w\_cond\_in} - \text{DELTA}_{P}_{cond} \quad \{\text{psia}\}$$

$$P_{w\_cond\_ave} = (P_{w\_cond\_in} + P_{w\_cond\_out}) / 2 \quad \{\text{psia}\}$$

## {6. Condenser flow rate}

$$\text{GPM}_{w\_cond} = 3000 \quad \{\text{gpm}\}$$

$$m_{dot}_{w\_cond} = \rho_{w\_cond} * \text{GPM}_{w\_cond} * \text{convert}(\text{gpm}, \text{ft}^3/\text{hr}) \quad \{\text{lbm/hr}\}$$

## {Section VII. Condenser pump model}

## {A. Inputs for condenser pump}

$$h_{pump\_cond\_in} = h_{w\_tow\_out} \quad \{\text{btu/lbm}\}$$

$$P_{pump\_cond\_in} = P_{atm} - \text{Head}_{towtopump} * \rho_{w\_pump\_cond} * g * \text{convert}(\text{lbm/ft}^2 * \text{s}^2, \text{psia}) \quad \{\text{psia}\}$$

$$\text{Head}_{towtopump} = (\text{Head}_{pipe\_cond} / 2 - \text{Elev}_{tow}) \quad \{\text{ft}\}$$

$$m_{dot}_{w\_pump\_cond} = m_{dot}_{w\_cond} \quad \{\text{lbm/hr}\}$$

## {B. Condenser pump}

$$\eta_{pump\_cond} = .83$$

$$\eta_{motor\_cond} = .90$$

$$\eta_{pump\_cond} = (h_{pump\_cond\_out\_rev} - h_{pump\_cond\_in}) / (h_{pump\_cond\_out} - h_{pump\_cond\_in})$$

$$W_{dot}_{pump\_cond} = m_{dot}_{w\_pump\_cond} * (h_{pump\_cond\_out} - h_{pump\_cond\_in}) / \eta_{motor\_cond}$$

$$KW_{pump\_cond} = W_{dot}_{pump\_cond} * \text{convert}(\text{Btu/hr}, \text{kW}) \quad \{\text{kW}\}$$

## {C. Pressure calculation}

$$\text{DELTA}_{P}_{pump\_cond} = \rho_{w\_pump\_cond} * g * \text{HEAD}_{loop\_cond} * \text{convert}(\text{lbm/ft}^2 * \text{S}^2, \text{psia}) \quad \{\text{psia}\}$$

$$P_{pump\_cond\_out} = P_{pump\_cond\_in} + \text{DELTA}_{P}_{pump\_cond} \quad \{\text{psia}\}$$

$$P_{pump\_cond\_ave} = (P_{pump\_cond\_in} + \text{DELTA}_{P}_{pump\_cond}) / 2 \quad \{\text{psia}\}$$

$$\text{Head}_{pipe\_cond} = f_{loop\_cond} * \text{Length}_{loop\_cond} / D_{i\_pipe\_cond} * (\text{FPS}_{pump\_cond}^2 / 2) / g \quad \{\text{ft}\}$$

{eqn 6.30 ref[5]}

$$\text{Head}_{loop\_cond} = \text{Head}_{pipe\_cond} + \text{Head}_{cond} + \text{Head}_{strainer} \quad \{\text{ft}\}$$

$$\text{Head}_{strainer} = 30 \quad \{\text{ft}\}$$

$$f_{loop\_cond} = 1 / (-1.8 * \log_{10}(6.9 / \text{Re}_{D_{i\_pump\_cond}} + (\epsilon_{pipe\_cond} / (D_{i\_pipe\_cond} * 3.7))^{1.11}))^2$$

{eqn 6.64a ref[5]}

## {D. Pipe geometry}

$$D_{i\_pipe\_cond} = 12 * \text{convert}(\text{in}, \text{ft}) \quad \{\text{ft}\}$$

$$\text{Length}_{loop\_cond} = 500 \quad \{\text{ft}\}$$

$$\epsilon_{pipe\_cond} = .00015 \quad \{\text{ft}\}$$

$$\text{Elev}_{tow} = 200 \quad \{\text{ft}\}$$

## {E. Flow rates}

$GPM\_pump\_cond = m\_dot\_w\_pump\_cond / rho\_w\_pump\_cond * convert(ft^3/hr, gpm)$  {gpm}  
 $CFM\_pump\_cond = GPM\_pump\_cond * convert(gpm, cfm)$  {ft<sup>3</sup>/min}  
 $FPM\_pump\_cond = CFM\_pump\_cond / (pi * D\_i\_pipe\_cond^2 / 4)$  {ft/min}  
 $FPS\_pump\_cond = FPM\_pump\_cond * convert(1/min, 1/s)$  {ft/s}  
 $FPH\_pump\_cond = FPM\_pump\_cond * convert(1/min, 1/hr)$  {ft/hr}  
 $Re\_D\_i\_pump\_cond = rho\_w\_pump\_cond * FPH\_pump\_cond * D\_i\_pipe\_cond / mu\_w\_pump\_cond$

## {F. Fluid Properties}

$rho\_W\_pump\_cond = density(WATER, T=T\_pump\_cond\_ave, P=P\_pump\_cond\_ave)$  {lbm/ft<sup>3</sup>}  
 $mu\_W\_pump\_cond = viscosity(WATER, T=T\_pump\_cond\_ave, P=P\_pump\_cond\_ave)$  {lbm/ft hr}

## {G. Temperatures}

$T\_pump\_cond\_in = temperature(WATER, h=h\_pump\_cond\_in, P=P\_pump\_cond\_ave)$  {F}  
 $T\_pump\_cond\_ave = (T\_pump\_cond\_out - T\_pump\_cond\_in) / ln((T\_pump\_cond\_out) / (T\_pump\_cond\_in))$   
 $T\_pump\_cond\_out\_rev = temperature(WATER, P=P\_pump\_cond\_out, s=s\_pump\_cond\_in)$  {F}  
 $T\_pump\_cond\_out = temperature(WATER, P=P\_pump\_cond\_out, H=h\_pump\_cond\_out)$  {F}

## {H. Enthalpy and entropy}

$h\_pump\_cond\_out\_rev = enthalpy(WATER, P=P\_pump\_cond\_out, T=T\_pump\_cond\_out\_rev)$  {btu/lbm}  
 $s\_pump\_cond\_in = entropy(WATER, P=P\_pump\_cond\_in, T=T\_pump\_cond\_in)$  {btu/lbm R}  
 $s\_pump\_cond\_out = entropy(WATER, P=P\_pump\_cond\_out, T=T\_pump\_cond\_out)$  {btu/lbm R}

## {Section VIII. Cooling tower model}

## {A. Inputs for cooling tower}

$h\_w\_tow\_in = h\_w\_cond\_out$  {btu/lbm}  
 $m\_dot\_w\_tow = m\_dot\_w\_cond$  {lbm/hr}

## {B. Cooling tower calculations}

Call towerfan(Q\_dot\_tow, epsilon\_tow, m\_dot\_a\_tow, h\_s\_w\_tow\_in, h\_a\_tow\_in, T\_w\_tow\_out1:  
 fanduty, T\_w\_tow\_out)  
 $Q\_dot\_tow = 0.9 * fanduty * epsilon\_tow * m\_dot\_a\_tow * (h\_s\_w\_tow\_in - h\_a\_tow\_in) +$   
 $0.1 * epsilon\_tow * m\_dot\_a\_tow * (h\_s\_w\_tow\_in - h\_a\_tow\_in)$  {Btu/hr}  
 $Q\_dot\_tow = m\_dot\_w\_tow * (h\_w\_tow\_in - h\_w\_tow\_out)$  {btu/hr}  
 $epsilon\_tow = (1 - exp(-NTU\_tow * (1 - Cr\_tow))) / (1 - Cr\_tow * exp(-NTU\_tow * (1 - Cr\_tow)))$  {eqn 11.30a ref[3]}  
 $NTU\_tow = 1.3936 * (m\_dot\_w\_tow / m\_dot\_a\_tow)^{1.7044}$  {eqn II.17 ref[9]}  
 $Cr\_tow = (m\_dot\_a\_tow * Cs) / (m\_dot\_w\_tow * Cp\_w\_tow)$  {eqn II.12 ref[9]}  
 $Cs = (h\_s\_w\_tow\_in - h\_s\_w\_tow\_out) / (T\_w\_tow\_in - T\_w\_tow\_out)$  {btu/lbm R} {eqn II.13 ref[9]}

## {C. Water properties}

$rho\_w\_tow = density(WATER, T=T\_w\_tow\_ave, P=P\_atm)$  {lbm/ft<sup>3</sup>}  
 $Cp\_w\_tow = specheat(WATER, T=T\_w\_tow\_ave, P=P\_atm)$  {Btu/lbm R}  
 $h\_s\_w\_tow\_in = enthalpy(AIRH2O, R=1, T=T\_w\_tow\_in, P=P\_atm)$  {Btu/lbm}  
 $h\_s\_w\_tow\_out = enthalpy(AIRH2O, R=1, T=T\_w\_tow\_out, P=P\_atm)$  {Btu/lbm}

## {D. Air Properties}

$rho\_a\_tow = density(AIRH2O, B=ODWB, T=T\_a\_tow\_in, P=P\_atm)$  {lbm/ft<sup>3</sup>}  
 $Cp\_a\_tow = specheat(AIRH2O, B=ODWB, T=T\_a\_tow\_in, P=P\_atm)$  {Btu/lbm R}  
 $h\_a\_tow\_in = enthalpy(AIRH2O, B=ODWB, T=T\_a\_tow\_in, P=P\_atm)$  {Btu/lbm}

## {E. Temperatures}

$T_{a\_tow\_in}=T_{amb}$  {F}

$T_{w\_tow\_in}=temperature(WATER,h=h_{w\_tow\_in},P=P_{atm})$  {F}

$T_{w\_tow\_out1}=temperature(WATER,h=h_{w\_tow\_out},P=P_{atm})$  {F}

$T_{w\_tow\_ave}=(T_{w\_tow\_in}-T_{w\_tow\_out})/\ln((T_{w\_tow\_in})/(T_{w\_tow\_out}))$  {F}

## {F. Entropy}

$s_{w\_tow\_in}=entropy(WATER,h=h_{w\_tow\_in},P=P_{atm})$  {btu/lbm R}

$s_{w\_tow\_out}=entropy(WATER,h=h_{w\_tow\_out},P=P_{atm})$  {btu/lbm R}

## {G. Flow rates}

$m_{dot\_a\_tow}=\rho_{a\_tow}*cfm_{tow}*convert(1/min,1/hr)$  {lbm/hr}

$cfm_{tow}=250*1000$

## {H. Cooling tower fan model}

FHPCA=-2.3084 { Appendix A ref[10]}

FHPCB=6.3769 { Appendix A ref[10]}

$W_{dot\_fan\_tow}=(exp(FHPCA+((\ln(cfm_{tow})-10.5)/2)*FHPCB)/.9)*fanduty*convert(hp,btu/hr)$

{btu/hr} { Appendix A ref[10]}

$KW_{fan\_tow}=W_{dot\_fan\_tow}*convert(btu/hr,kW)$  {kW}

## {Section IX. Constants}

$P_{atm}=14.7$  {psia}

$g=32.2$  {ft/s<sup>2</sup>}

## {References:

[1] Bejan, Convection Heat Transfer, 2ed.

[2] Bejan, Advanced Engineering Thermodynamics, 2ed.

[3] Incropera and DeWitt, Introduction to Heat Transfer, 1ed.

[4] McQuiston, Faye and Parker, Jerald., Heating, Ventalating and Air Conditioning; Analysis and Design

[5] White, Fluid Mechanics, 2ed.

[6] Rich, Donald G., The effect of fin spacing on the heat transfer and friction performance of multirow smooth plate fin and tube heat exchangers, 1973.

[7] Rishel, James B., HVAC Pump Handbook, 1996.

[8] Goulds Pump Selection Software, 1995.

[9] Liu,Hubert H., Analysis and Performance Optimization of Commercial Chiller/Cooling Tower System.}

## References

- Air-Conditioning & Refrigeration Institute. "Standard 550/590." Air-Conditioning & Refrigeration Institute. 1998.
- American Society of Heating, Refrigerating and Air-Conditioning Engineers, Inc. Air-Conditioning Systems Design Manual. ASHRAE, Inc., 1993.
- Austin, Stephen B. "Optimal Chiller Loading." ASHRAE Journal. July 1991: 40-43.
- Avery, Gil. "Controlling Chillers in Variable Flow Systems." ASHRAE Journal. February 1998: 42-45.
- Bejan, Adrian. Advanced Engineering Thermodynamics. 2<sup>nd</sup> ed. New York: John Wiley & Sons, Inc., 1997.
- Bejan, Adrian. Convection Heat Transfer. 2<sup>nd</sup> ed. New York: John Wiley & Sons, Inc., 1995.
- Braun, J. E. "Methodologies for the Design and Control of Central Cooling Plants." Diss. University of Wisconsin-Madison, 1988.
- Coad, William J. "A Fundamental Perspective on Chilled Water Systems." Heating/Piping/AirConditioning. August 1988: 59-66.
- Colmac Coils MFG., Inc., "Bulletin 5050." Colmac Coils MFG., Inc. November 1993.
- Ecodyne Cooling Products Division. Weather Data Handbook for HVAC and Cooling Equipment Design.
- Eppelheimer, Donald M. "Variable Flow – The Quest for System Efficiency." ASHRAE Transactions. 1996: 673-678.
- Erth, Richard. "Chilled Water Reset: Variable Speed Solution." Heating/Piping/AirConditioning. May 1987: 79-81
- Hartman, Thomas B. "Design Issues of Variable Chilled-Water Flow Through Chillers." ASHRAE Transactions. 1996: 679-683.
- Incropera, Frank P., and DeWitt, David P., Introduction to Heat Transfer. New York: John Wiley & Sons, Inc. 1985.
- Joyce, Charles T. "Optimized Design of a Commercial Building Chiller/Cooling Tower System." Thesis. Georgia Institute of Technology, 1990.
- Kelley, David W., and Chan, Tumin. "Optimizing Chilled Water Plants." Heating/Piping/AirConditioning. January 1999: 145-147.
- Kirsner, Wayne. "The Demise of the Primary-Secondary Pumping Paradigm for Chilled Water Plant Design." Heating/Piping/AirConditioning. November 1996: 73-78.

- Kirsner, Wayne. "Rectifying the Primary-Secondary Paradigm for Chilled Water Plant Design to Deal with Low  $\Delta T$  Plant Syndrome." Heating/Piping/AirConditioning. January 1996: 129-131.
- Klein, S. A. and Alvarado, F. L., Engineer Equation Solver. Version 5.039, 1999.
- Lilly, Dana E. "Analysis and Performance of Gas-Electric Hybrid Chiller Systems." Thesis. Georgia Institute of Technology, 1998.
- Liu, Hubert H. "Analysis and Performance Optimization of Commercial Chiller/Cooling Tower System." Thesis. Georgia Institute of Technology, 1997.
- McQuiston, Faye C. "Finned Tube Heat Exchangers: State of the Art for the Air-Side." ASHRAE Transactions. 1981: 1077-1085.
- Oskarsson, S.P., Krakaw, K. I., and Lin, S. "Evaporator Models for Operation with Dry, Wet, and Frosted Finned Surfaces." ASHRAE Transactions. 1990:
- Redden, George H. "Effect of Variable Flow on Centrifugal Chiller Performance." ASHRAE Transactions. 1996: 684-687.
- Rich, Donald G. "The Effect of Fin Spacing on the Heat Transfer and Friction Performance of Multi-Row, Smooth Plate Fin-and-Tube Heat Exchangers." ASHRAE Transactions. 1973: 137-145.
- Rishel, James B. HVAC Pump Handbook. New York: McGraw-Hill, 1996.
- Sauer, John M. "Diagnosing Low Temperature Differential." ASHRAE Journal. June 1996: 32-36.
- Shabo, Daniel J. "Evaluation of Operating Parameters for Chiller, Cooling Towers and Air Handlers in a Large Commercial Building." Thesis. Georgia Institute of Technology, 1992.
- Weber, Eric D. "Modeling and Generalized Optimization of Commercial Building Chiller/Cooling Tower Systems." Thesis. Georgia Institute of Technology, 1988.
- White, Frank M. Fluid Mechanics. 2<sup>nd</sup> ed. New York: McGraw-Hill, 1986.